Table 1. Effects of the UTRs on h*CTR1* expression in yeast

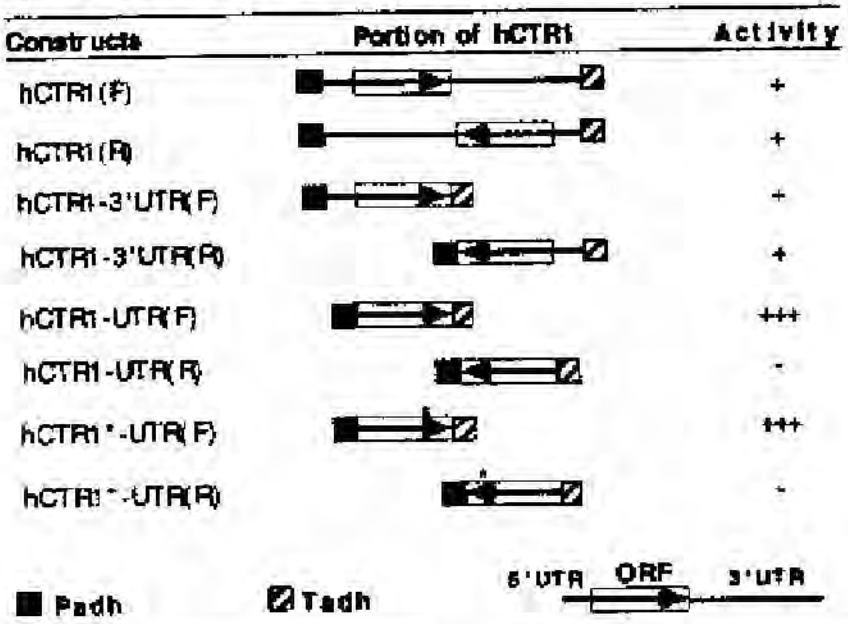

The box indicates the h*CTR1* ORF, and the arrow denotes the ORF orientation. 5′ and 3′ UTRs are shown as lines adjacent to the ORF. *, A stop codon introduced to the shorter reading frame in the antisense orientation of h*CTR1*. −, +, and +++, No, weak, and strong activity, respectively, of the constructs to complement *ctr1* defect of growth on YPG plates.

Figure A6.2(15)-1

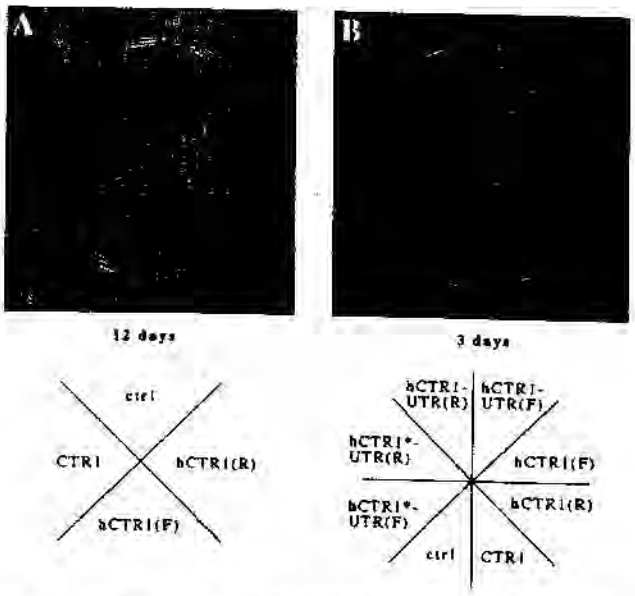

FIG. 1. Complementation of yeast *ctr1* growth on YPG medium with human h*CTR1* cDNA. (*A*) h*CTR1* expression complements *ctr1* growth defect on YPG medium. Both sense and antisense h*CTR1* cloned in vector pDB20 have the complementing ability. The plate was photographed after 12 days of growth at 30°C. The antisense complements slightly better, as shown by slightly larger colonies. (*B*) Growth of different h*CTR1* transformants on YPG medium compared with *ctr1* and *CTR1* strains. The photograph was taken after 3 days of growth. Notice that there is only minor growth for either hCTR1(F) or hCTR(R). The growth of hCTR1-UTR(F) transformant is nearly as robust as the wild-type *CTR1*. (See Table 1 for the nomenclature of constructs and the results.)

Figure A6.2(15)-2

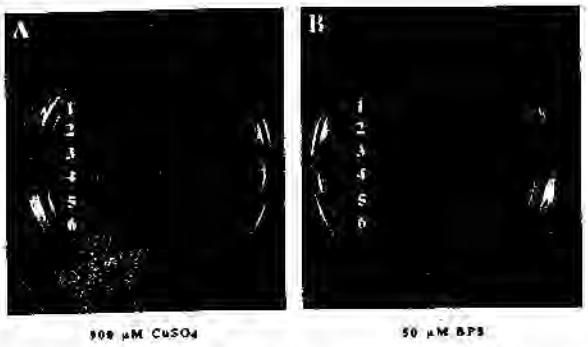

FIG. 3. Increased sensitivity to copper overload and rescue of high-affinity iron transport defect of *ctr1* strain by h*CTR1* expression. (*A*) h*CTR1* expression makes yeast more sensitive to the toxicity of copper overload. Rows: 1 and 4, hCTR1-UTR(R); 2 and 5, pDB20; 3 and 6, hCTR1-UTR(F). The transformed h*CTR1* strains and *ctr1* mutant strains are grown in rows 1–3 and 4–6, respectively. Spotted from left to right are 10-fold serially diluted yeast cultures. (*B*) h*CTR1* rescues iron transport defect of *ctr1* strain. *ctr1* yeast cannot grow in 50 μM bathophenanthrolinedisulfonic acid disodium salt, whereas h*CTR1* expression rescues this defect. Strains and plasmids in rows 1 to 6 are as in *A*.

Figure A6.2.14-3

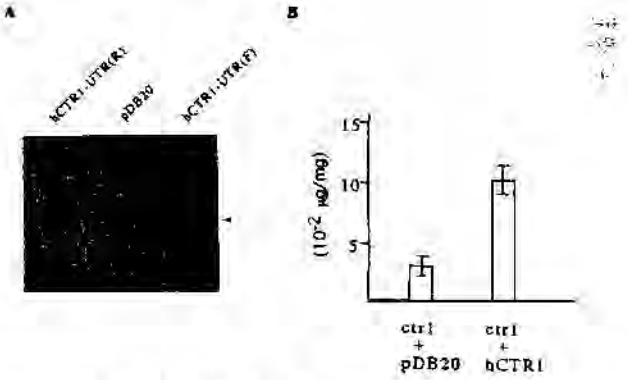

FIG. 4. Rescue of SOD1 defect and increase of cellular copper concentration in *ctr1* yeast by h*CTR1* expression. (*A*) SOD1 activity is observed in hCTR1 expression strain. The control strains with vector alone or antisense h*CTR1* have no detectable SOD1 activity. hCTR1-UTR(R), pDB20, and hCTR1-UTR(F) represent transformed *ctr1* yeast strains with antisense UTR-less h*CTR1*, vector alone, and sense UTR-less h*CTR1*, respectively. The arrowhead indicates the SOD1 activity band. (*B*) h*CTR1* expression in the *ctr1* strain increases its cellular copper concentration. The *y* axis denotes the copper amount per milligram of protein. The numbers are means of duplicate experiments. hCTR1-UTR(F) was used for h*CTR1* expression in *ctr1*.

Figure A6.2(15)-4

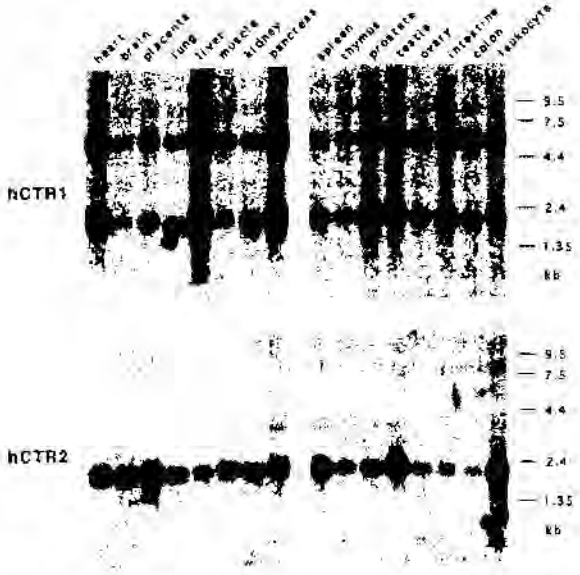

FIG. 5. Expression of h*CTR1* and h*CTR2* by Northern blot analysis. A pair of multiple-tissue Northern blots (CLONTECH) were probed with h*CTR1* and h*CTR2* coding regions. Approximately 2 (1.5–2.5) μg of mRNA was loaded in each lane.

			Official use only
		84 REFERENCE	
1.1	**Reference**	*Author(s), year, title, laboratory name, laboratory report number, report date (if published, list journal name, volume: pages) If necessary, copy field and enter other reference(s).* Gunshin, H., Mackenzie, B, Berger, U.V., Gunshin, Y., Romero, M.F., Boron, W.F., Nussberger, S., Gollan, J.L. & Hediger, M.A. (1997). Cloning and Characterisation of a Mammalian Proton-Coupled Metal-Ion transporter. Nature. **388**:482-488 (published).	
1.2	**Data protection**	No *(indicate if data protection is claimed)*	
1.2.1	Data owner	*Give name of company* Public domain	
1.2.2	Criteria for data protection	Choose one of the following criteria (see also TNsG on Product Evaluation) and delete the others: No data protection claimed	
		85 GUIDELINES AND QUALITY ASSURANCE	
85.1	**Guideline study**	No. This was a non-regulatory study to investigate the expression cloning, tissue distribution and initial characterisation of a divalent-cation transporter, DCT1. No guidelines are available to address this objective. *(If yes, give guidelines; if no, give justification, e.g. "no guidelines available" or "methods used comparable to guidelines xy")*	
85.2	**GLP**	No. This was a non-regulatory study. *(If no, give justification, e.g. state that GLP was not compulsory at the time the study was performed)*	
85.3	**Deviations**	Yes. Refer to section 5.3.2 for a general discussion of deviations and deficiencies. *(If yes, describe deviations from test guidelines or refer to respective field numbers where these are described, e.g. "see 3.x.y")*	
		86 MATERIALS AND METHODS *In some fields the values indicated in the EC or OECD test guidelines are given as default values. Adopt, change or delete these default values as appropriate.*	
86.1	**Test material**	Refer to section 3.3	
86.1.1	Lot/Batch number	Not applicable	
86.1.2	Specification	Deviating from specification given in section 2 as follows *(describe specification under separate subheadings, such as the following; additional subheadings may be appropriate):*	

86.1.2.1	Description	*If appropriate, give e.g. colour, physical form (e.g. powder, grain size, particle size/distribution)* Not applicable
86.1.2.2	Purity	*Give purity in % of active substance* [redacted]
86.1.2.3	Stability	*Describe stability of test material* Not applicable
86.1.2.4	Radiolabelling	*give structural location of radio labelling, give reason if not labelled* $^{55}FeCl_2$ (section 3.3.2) ^{32}P (section 3.3)
86.2	**Test Animals**	*Non*-entry *field*
86.2.1	Species	Rat
86.2.2	Strain	Not available
86.2.3	Source	Not available
86.2.4	Sex	Male
86.2.5	Age	Not available
86.3	**Procedures**	Non-entry field
86.3.1	Expression cloning	DCT1 cDNA was cloned from rats fed a low-iron diet for 3 – 4 weeks. RNA was extracted from duodenal mucosal scrapes from iron-deficient male rats and size-fractionated using preparative gel electrophoresis. A positive (approx. 4.5 kb) poly(A)$^+$ RNA fraction, which stimulated ^{55}Fe uptake in oocytes, was used to construct a directional cDNA library using a SuperScript cDNA synthesis system. cDNA was ligated into the pSPORT1 vector and ElecrtroMax DH10B cells were transformed. RNA synthesised *in vitro* from pools of approx. 200 clones was injected into oocytes. A positive pool was sequentially subdivided and analysed until a single clone (DCT1) was identified that was sequenced at the Yale University sequencing Facility.
86.3.2	Radiotracer uptake	Collagenase-treated *Xenopus* oocytes were injected with approx. 50 ng poly(A)$^+$ RNA or approx. 25 mg DCT1 RNA synthesised *in vitro*. Radiotracer uptake was determined (3d aferRNA injection) by incubating 6 – 10 oocytes for 1.0 or 1.5 hours in 750 il standard uptake medium together with 10 iM $^{55}FeCl_2$. Oocytes were solubilised using 10% SDS and the ^{55}Fe content was measured by liquid scintillation counting.
86.3.3	Northern analysis	Poly(A)$^+$ RNA (3ig each well) was separated on an 18% formaldehyde /1% agarose gel and blotted onto a nitrocellulose filter. The DCT1 insert was excised from pSPORT1 and labelled with ^{32}P using a T7 QuickPrime kit (Pharmacia). Hybridisation was for 16 hours at 42°C in 50% formaldehyde, and filters were washed in 5 x SSC/0.1% SDS at 50°C for 2 x 30 minutes, 0.1 x SSC/0.1% at 65°C for 3 x 20 minutes.
86.3.4	In situ hybridisation	Digoxigenin-labelled antisense and sense run-off transcripts were synthesised using a Genius kit (Boehringer-Mannheim) from a PCR fragment, which contained about 1.7 kb of DCT1 sequence, and which was flanked by promoter sites for SP6 and T7 RNA polymerase. Transcripts were alkali-hydrolysed to an average length of 200 – 400

base pairs. *In situ* hybridisation was performed on cryosections (12 im) of fresh-frozen tissue. The hybridisation buffer consisted of 50% formamide, 5 x SSC, 2% blocking reagent, 0.02% SDS, 0.1% N-laurylsarcosine; probe concentrations were approx. 200 ng ml^{-1}. Sections in slide mailers were immersed in hybridisation solution and hybridised at 70°C for 18 hours. Sections were then washed 3 times in 2 x SSC and for 2 x 30 min in 0.1 x SSC at 70°C. The hybridised labelled probes were visualised using anti-digoxigenin Fab fragments and BCIP/NBT substrate. Sections were developed in substrate solution for 42 hours, then rinsed in 10 mM Tris, 1mM EDTA, pH 8.0, and coverslipped with 50% PBS/glycerol.

86.3.5 Electrophysiology A two-microelectrode voltage clamp was used to measure steady-stare and presteady state currents in control oocytes and oocytes injected with approx. 25 ng of *in vitro* transcribed DCT1 RNA, 4 – 7 days after injection. Microelectrodes (resistance 0.5 – 5 MU) were filled with 3 M KCl. Oocytes were superfused at 23 - 24°C in a low-calcium medium with ascorbic acid (96 mM NaCl, 2mM KCl, 0.6 mN $CaCl_2$, 1 mM $MgCl_2$, 100 iM ascorbic acid, 2.5 mM HEPES, 2.5 mM MES, buffered between 5.5 and 7.5 with Tris) and clamped at a holding potential (V_h) of –50 mV. The current was low-pass filtered at 5 kHz and digitised at 5 kHz. Step-changes in membrane potential (V_m) were applied (from +50 mV to –150 mV for steady-state studies, and +90 mV to –110 mV for presteady-state analysis, in 20 mV increments), each for a duration of 200 ms, at pH 5.5 – 7.5 before and after the addition of the test substrate. Additionally, current was monitored continuously (sampling at 1 Hz) in oocytes clamped at –50 mV, but without step-changes in V_m. Test solutions were washed out by superfusing the oocyte with substrate-free medium at pH 7.5 for several minutes. Steady-state data (obtained by averaging the points over the final 11 ms at each V_m) were fitted to the following equation, for which I is the evoked current (that is, the difference in steady-state current measured in the presence and absence of substrate) $_{Imax}$ the derived current maximum, S the substrate (divalent cation or H^+) concentration, $_{KS0.5}$ the substrate concentration at which current was half-maximal, and n_H the Hill coefficient:

$$I = I_{max} S_{nH} / (K^S_{0.5})_{nH} + S^{nH}$$

86.3.6 Intracellular pH measurement

Changes in intracellular pH(pH_i) associated with DCT1-mediated transport in oocytes were measured using pH microelectrodes. Silanised borosilicate pipettes beack-filled with phosphate buffer at pH 7.0 were used, with the hydrogen ionophore I-cocktail B (Fluka). pH_i and current (filtered at 25 Hz) were measured simultaneously and digitised at 0.5Hz in voltage-clamped oocytes.

87 RESULTS AND DISCUSSION

Describe findings. If appropriate, include table. Sample tables are given below.

87.1 Results

Non-entry field.

87.1.1 Expression cloning By screening for iron uptake activity in oocytes, the DCT1 complementary DNA was isolated from a cDNA library prepared using duodenal messenger RNA from rats fed on a low-iron diet (Fe(-)D). *Xenopus* oocytes injected with Fe(-)D mRNA showed a 7-fold increase in ^{55}Fe uptake uptake compared with water-injected (control) oocytes (**Figure A6.2(16)-1**). Following size-fractionation, maximal ^{55}Fe

activity was induced by a 4.0 – 4.5 kilobase (kb) mRNA fraction, from which a single cDNA (DCT1) was isolated, which stimulated $^{55}Fe^{2+}$ uptake 200-fold. The 4409-base-pair (bp) DCT1 cDNA encodes a 561-amino-acid protein with 12 putative membrane-spanning domains (**Figure A6.2(16)-2**), predicted glycosylation sites in the fourth extracellular loop, and a consensus transport motif in the fourth intracellular loop.

87.1.2 Tissue distribution

High-stringency northern-blot analysis of DCT1 transcripts (**Figure A6.2(16)-3a**) revealed prominent bands of 4.5 kb from proximal intestine, kidney, thymus and brain, and fainter bands in testis, liver, colon, heart, spleen, skeletal muscle, lung, bone marrow and stomach. By loading an equal amount of each mRNA, it was found that DCT1 was expressed at a much higher level in proximal intestine than in kidney, and more so in kidney than in brain. Another strong band at ~3.5 kb was observed in kidney and thymus, indicating that a second isoform may exist in those tissues. In the intestine, DCT1 mRNA expression was highest in the duodenum and decreased toward the colon (**Figure A6.2(16)-3b, top row**). Following diet-induced iron deficiency, DCT1 mRNA expression was enhanced dramatically in duodenum (**Figure A6.2(16)-3b, bottom row**) and also, but to a lesser extent, in kidney, liver, brain, heart, lung and testis, suggesting that there is marked regulation of DCT1 mRNA by dietary iron and/or tissue iron concentration.

The cellular localisation of DCT1 mRNA in small intestine, kidney, testis, thymus and brain was investigates in frozen sections using non-radioactive *in-situ* hybridisation with a digoxigenin-labelled cRNA probe. High-stringency hybridisation yielded specific signals with antisense probe, but no labelling with sense probe (**Figure A6.2(16)-4**). In small intestine, DCT1 was highly expressed in enterocytes lining the villus, especially in the crypts and lower segments of the villi, but not at villar tips (**Figure A6.2(16)-4a**). Again, a proximal-to-distal gradient of expression was evident in the small intestine. This pattern of expression is consistent with the primary sites responsible for intestinal absorption of most divalent cations.

In kidney, DCT1 mRNA labelling was most prominent in S3 proximal tubule segments (**Figure A6.2(16)-4b**), suggesting that it is involved in the reabsorption of divalent cations. Staining was also significant over the entire length of the collecting ducts, suggesting that DCT1 may participate in the final reabsorption of these ions. In testis, DCT1 mRNA was expressed in the Sertoli cells of seminiferous tubules (**Figure A6.2(16)-4f**), and was more abundant in those tubules containing mature spermatocytes. In thymus, DCT1 labelling was positive in cortical, but not medullary, thymocytes (**Figure A6.2(16)-4d**).

In each region examined in brain, DCT1 mRNA was found in neurons but not glial or ependymal cells (**Figure A6.2(16)-4e**). A qualitative examination of saggital sections indicated that most neurons expressed DCT1 mRNA at low levels. More prominent labelling was present in densely packed cell groups, such as the hippocampal pyrimidal and granule cells (**Figure A6.2(16)-4g**), cerebellar granule cells, the preoptic nucleus and pyramidal cells of the piriform cortex. Moderate amounts of DCT1 mRNA were present in the substantia nigra (**Figure A6.2(16)- 4j**). One cell group, the ventral portion of the anterior olfactory nucleus (**Figure A6.2(16)-4i**), contained large amounts of DCT1 mRNA. DCT1 mRNA was also localised in epithelial cells of the choroid plexus.

87.1.3 Functional characterisation

The functional characteristics of DCT1 were investigated by using oocytes injected with DCT1 mRNA. Two-microelectrode voltage-clamp analysis indicated that the divalent cation transport mediated by DCT1 was rheogenic, with currents of up to –1000 nA (**Figure A6.2(16)-5**). Whereas Fe^{2+} evoked no appreciable current in control oocytes clamped at –50 mV (**Figure A6.2(16)-5a (1)**), in oocytes

	expressing DCT1 (**Figure A6.2(16)-5a (1)**), large inward currents were observed when 50 μM Fe^{2+} was superfused at pH 5.5. In DCT1-injected oocytes in the absence of substrate, switching extracellular pH from 7.5 to 5.5 caused a larger shift in the baseline (an inward current) than in control oocytes. In two oocytes expressing DCT1, this pH-dependent current was –24.0 nA and –23.5 nA (each the average of several replicates), compared with –5.7 ± 2.7 nA (mean ± SD) in control oocytes from the same batch. Ca^{2+} did not mimic the effect of Fe^{2+}; instead, 10 mM Ca^{2+} produced a small outward current at pH 5.5 and partially inhibited the current evoked by 50 μM Fe^{2+} (**Figure A6.2(16)-5a (2)**). Large inward currents were obtained by Zn^{2+}, Mn^{2+}, Cu^{2+} or Cd^{2+} applied at 50 μM; smaller currents were evoked by Ni^{2+} and Pb^{2+} (**Figure A6.2(16)-5b**). Following step-changes in membrane potential (Vm) of oocytes expressing DCT1, presteady-state and steady-state currents were observed at pH 5.5_o (**Figure A6.2(16)-5c**). These comprised a fast capacitive transient, which was also observed in control oocytes, and a transporter-mediated presteady-state current (half-time, τ = 30 – 70 ms), decaying to the steady-state value (**Figure A6.2(16)-5c**). DCT1-mediated presteady-state currents were abolished in the presence of divalent cations serving as substrates (**Figure A6.2(16)-5b**) or 10 mM Ca^{2+}, and were H^+-dependent, suggesting that H^+ may bind to the transporter. This was the first indication that DCT1-mediated metal-ion transport may be H^+-coupled. The possibility of H^+-coupling of metal ion transport was further investigated by simultaneously monitoring intracellular pH changes and Fe^{2+}-evoked currents (**Figure A6.2(16)-5f**). In an oocyte superfused with pH 7.5 medium at V_h = -90 mV, pH_i was ~7.35 and remained stable. The inward shift in baseline current after switching to pH_o 5.5 (in the absence of metal ion substrate) was associated with a significant decrease in pH_i that was not seen in control oocytes. Applying 50 μM Fe^{2+} at pH_o 5.5 induced a much larger and faster intracellular acidification, together with an inward current that peaked at about 200 nA. This procedure had no effect in control oocytes. It is therefore confirmed that DCT-1-mediated Fe^{2+} transport is H^+-coupled. Removal of Fe^{2+} halted the decline in pH_i and I^{Fe} returned to baseline.	X
87.2 Discussion	The data show that there is an active cellular uptake mechanism for divalent cations in mammalian cells. DCT1 accepts a broad range of metal ions, favouring the divalent cations Fe^{2+}, Cd^{2+}, Co^{2+}, Cu^{2+}, Ni^{2+}, Mn^{2+}, Pb^{2+} and Zn^{2+} among those tested. DCT1 mediates active transport that is proton-coupled and depends on the cell membrane potential. It is a 561 amino-acid protein with 12 putative membrane-spanning domains and is ubiquitously expressed, most notably in the proximal duodenum. DCT1 is upregulated by dietary iron deficiency, and is a member of the 'natural-resistance-associated macrophage protein (Nramp) family.	
	88 APPLICANT'S SUMMARY AND CONCLUSION	
88.1 Materials and methods	*Give concise description of method; give test guidelines no. and discuss relevant deviations from test guidelines* A study was carried out to investigate the expression cloning, tissue distribution and initial characterisation of a divalent-cation transporter, designated DCT1. The study was not designed to follow internationally	

accepted guidelines, and was not carried out or reported in compliance with GLP. The following techniques were used:

Expression cloning: DCT1 cDNA was cloned from male rats fed a low-iron diet for 3-4 weeks. RNA was extracted from duodenal mucosal scrapes and size-fractionated using gel electrophoresis. A positive poly(A)$^+$ RNA fraction, which stimulated ^{55}Fe uptake in oocytes, was used to construct a directional cDNA library. cDNA was ligated into the pSPORT1 vector and ElecrtroMax DH10B cells were transformed. RNA synthesised *in vitro* from pools of clones was injected into oocytes. A positive pool was sequentially subdivided and analysed until a single clone (DCT1) was identified. This was then sequenced.

Radiotracer uptake: Collagenase-treated *Xenopus* oocytes were injected with poly(A)$^+$ RNA or DCT1 RNA synthesised *in vitro*. Radiotracer uptake was determined 3days after RNA injection by incubating oocytes in standard uptake medium with 10 iM $^{55}FeCl_2$. Oocytes were solubilised using 10% SDS and the ^{55}Fe content measured by liquid scintillation counting.

Northern analysis: Poly(A)$^+$ RNA was separated on a formaldehyde/ agarose gel and blotted onto a nitrocellulose filter. The DCT1 insert was excised from pSPORT1 and labelled with ^{32}P using a T7 QuickPrime kit.

In situ hybridisation: Digoxigenin-labelled antisense and sense run-off transcripts were synthesised from a PCR fragment using a Genius kit and alkali-hydrolysed to an average length of 200-400 base pairs. *In situ* hybridisation was performed on frozen tissue sections. Sections were hybridised at 70°C for 18 hours and washed. Hybridised labelled probes were visualised using anti-digoxigenin Fab fragments and BCIP/NBT substrate. Sections were developed in substrate solution, rinsed and coverslipped.

Electrophysiology: A two-microelectrode voltage clamp was used to measure steady-state and presteady state currents in control oocytes and oocytes 4 – 7 days after injection with *in vitro* transcribed DCT1 RNA. Microelectrodes were filled with 3 M KCl. Oocytes were superfused in a low-calcium medium with ascorbic acid and clamped at a holding potential (V_h) of –50 mV. Step-changes in membrane potential (V_m) were applied, each for a duration of 200 ms, before and after addition of test substrate. Current was also monitored continuously in oocytes clamped at –50 mV without step-changes in V_m. Test solutions were washed out by superfusing the oocyte with substrate-free medium at pH 7.5. Steady-state data were fitted to the following equation, for which I is the evoked current, I_{max} the derived current maximum, S the substrate concentration, $K_{S0.5}$ the substrate concentration at which current was half-maximal, and n_H the Hill coefficient: $I = I_{max} S_{nH} / (K_{S0.5})_{nH} + S^{nH}$

Intracellular pH measurement: Changes in intracellular pH(pH_i) associated with DCT1-mediated transport in oocytes were measured using pH microelectrodes. Pipettes back-filled with phosphate buffer were used, with tips filled with hydrogen ionophore I-cocktail B. pH_i and current were measured simultaneously in voltage-clamped oocytes.

88.2 Results and discussion

Summarize relevant results; discuss dose-response relationship.

Expression cloning: DCT1 complementary DNA was isolated from a cDNA library prepared using duodenal messenger RNA from rats fed a low-iron diet (Fe(-)D). *Xenopus* oocytes injected with Fe(-)D mRNA showed a 7-fold increase in $^{55Fe2+}$ uptake uptake compared with control

	oocytes. Following size-fractionation, maximal ^{55}Fe activity was induced by a 4.5 kb mRNA fraction, from which a single cDNA was isolated, which stimulated $^{55}Fe^{2+}$ uptake 200-fold. The 4409 bp DCT1 cDNA encodes a 561-amino-acid protein with 12 membrane-spanning domains, predicted glycosylation sites in the fourth extracellular loop, and a consensus transport motif in the fourth intracellular loop.	
	Tissue distribution: Northern-blot analysis of DCT1 transcripts showed prominent bands of 4.5 kb from proximal intestine, kidney, thymus and brain, and fainter bands in testis, liver, colon, heart, spleen, skeletal muscle, lung, bone marrow and stomach. DCT1 expression was higher in proximal intestine than in kidney, and higher in kidney than in brain. A strong band at ~3.5 kb was observed in kidney and thymus, implying the existence of a second isoform. DCT1 mRNA expression in the intestine was highest in the duodenum, decreasing toward the colon.	
	Cellular localisation of DCT1 mRNA in small intestine, kidney, testis, thymus and brain was investigated in frozen sections using non-radioactive *in-situ* hybridisation with a digoxigenin-labelled cRNA probe. In small intestine, DCT1 was highly expressed in enterocytes lining the villus. Again, a proximal-to-distal gradient of expression was evident. In kidney, labelling was most prominent in S3 proximal tubule segments, suggesting involvement in reabsorption of divalent cations. Staining was also significant in collecting ducts, suggesting that DCT1 participates in final reabsorption of these ions. In testis, DCT1 mRNA was expressed in Sertoli cells, and was more abundant in seminiferous tubules containing mature spermatocytes. In thymus, labelling was positive in cortical thymocytes. In the brain, DCT1 mRNA was found in neurons throughout the brain, but not glial or ependymal cells.	X
	Functional characterisation: The functional characteristics of DCT1 were investigated by using oocytes injected with DCT1 mRNA. Two-microelectrode voltage-clamp analysis indicated that divalent cation transport mediated by DCT1 was rheogenic. Whereas Fe^{2+} evoked no appreciable current in control oocytes clamped at –50 mV, large inward currents were observed in oocytes expressing DCT1 when 50 µM Fe^{2+} was superfused at pH 5.5. In DCT1-injected oocytes in the absence of substrate, switching extracellular pH from 7.5 to 5.5 caused a larger shift in the baseline (an inward current) than in control oocytes. Large inward currents were also obtained by Zn^{2+}, Mn^{2+}, Cu^{2+} or Cd^{2+}; smaller currents were evoked by Ni^{2+} and Pb^{2+}.	X
	Following step-changes in membrane potential (Vm) of oocytes expressing DCT1, presteady-state and steady-state currents were observed at pH_o 5.5. These comprised a fast capacitive transient, which was also observed in control oocytes, and a transporter-mediated presteady-state current, decaying to the steady-state value. DCT1-mediated presteady-state currents were abolished in the presence of divalent cations serving as substrates, and were H^+-dependent, suggesting that H^+ may bind to the transporter. This finding indicates that DCT1-mediated metal-ion transport may be H^+-coupled.	
	The possibility of H^+-coupling of metal ion transport was further investigated by simultaneously monitoring intracellular pH changes and Fe^{2+}-evoked currents. In an oocyte superfused with pH 7.5 medium at V_h = -90 mV, pH_i was ~7.35 and remained stable. The inward shift in baseline current after switching to pH_o 5.5 was associated with a significant decrease in pH_i that was not seen in control oocytes. Applying 50 µM Fe^{2+} at pH_o 5.5 induced a much larger and faster	

	intracellular acidification, together with an inward current. This procedure had no effect in control oocytes. It is therefore confirmed that DCT-1-mediated Fe^{2+} transport is H^+-coupled.	
88.3 Conclusion	DCT1 accepts a broad range of metal ions, favouring the divalent cations Fe^{2+}, Cd^{2+}, Co^{2+}, Cu^{2+}, Ni^{2+}, Mn^{2+}, Pb^{2+} and Zn^{2+}. Active transport mediated by DCT1 is proton-coupled and depends on the cell membrane potential. DCT1 is a 561 amino-acid protein with 12 that is ubiquitously expressed, most notably in the proximal duodenum.	X
88.3.1 Reliability	*Based on the assessment of materials and methods include appropriate reliability indicator 0, 1, 2, 3, or 4* 2	
88.3.2 Deficiencies	Yes This study was not conducted and/or reported in strict compliance with the principles of GLP. However, this does not compromise the validity of the data generated, or the author's interpretation of that data, given that the study was not carried out for regulatory purposes. Furthermore, the research was published in a peer-reviewed journal, and has therefore been subject to the prior scrutiny of experts in the field. In addition this report has been included in a number of expert reviews of copper toxicokinetics. No internationally accepted guidelines are available that specifically address the objective of the research presented in this summary. Overall, this is a well-reported study, and its findings are considered to make a valuable contribution to the 'weight of evidence' approach that has been adopted for the purposes of the current review of copper toxicokinetics. A reliability indicator of 2 has been assigned on this basis. *(If yes, discuss the impact of deficiencies and implications on results. If relevant, justify acceptability of study.)*	

Evaluation by Competent Authorities

Use separate "evaluation boxes" to provide transparency as to the comments and views submitted

EVALUATION BY RAPPORTEUR MEMBER STATE

Date [redacted]

Materials and Methods [redacted]

Results and discussion [redacted]

Conclusion [redacted]

Section A6.2	**Metabolism in mammals**
Annex Point IIA6.2	*Specify section no., heading and species as appropriate*
IUCLID: 5.0/16	**A6.2(16), Cellular and molecular metabolism of copper**

Reliability	[redacted]
Acceptability	[redacted]
Remarks	[redacted]
	COMMENTS FROM ...
Date	*Give date of comments submitted*

Figure A6.2(16)-1

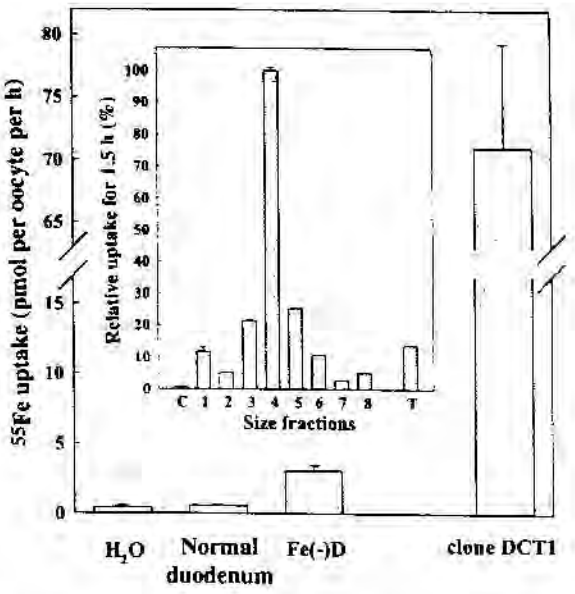

Figure 1 Uptake of 10 μM ^{55}Fe in *Xenopus* oocytes injected with poly(A)$^+$ RNA from normal or iron-deficient (Fe(−)D) rat duodenum or with RNA synthesized from DCT1 cDNA. Data are mean ± s.e.m. from 6–10 oocytes. Inset, relative ^{55}Fe uptake in oocytes injected with size-fractionated poly(A)$^+$ Fe(−)D RNA. C, Control water-injected oocytes; 1, 2.0–3.0 kb poly(A)$^+$ RNA; 2, 2.5–3.5 kb; 3, 3.3–4.0 kb; 4, 3.8–4.5 kb; 5, 4.4–5.7 kb; 6, 4.5–6.0 kb; 7, 4.8–6.4 kb; 8, 5.5–7.0 kb; and T, unfractionated poly(A)$^+$ Fe(−)D RNA.

Figure A6.2(16)-2

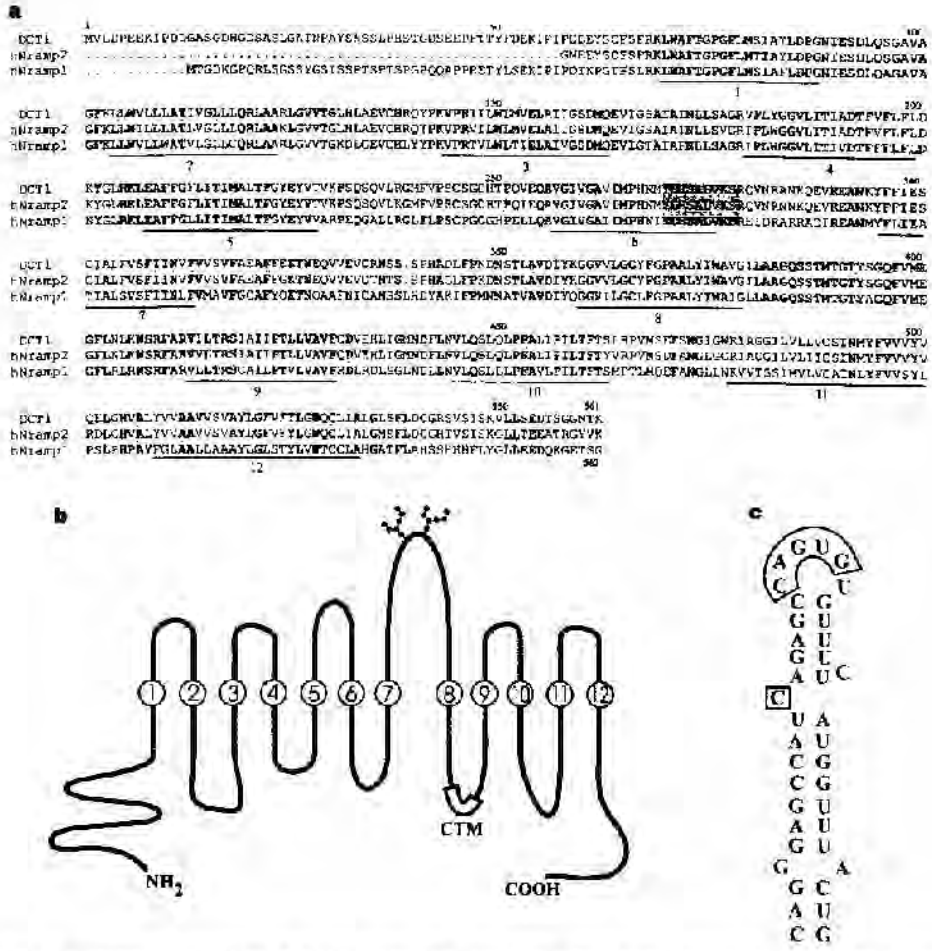

Figure 2 a, Sequence alignment of DCT1 and N(ramp)-related polypeptides. The sequences of rat DCT1, human Nramp1 and Nramp2 (GenBank accession numbers L32185 and L37347) were aligned using the GCG program, and identical residues are indicated by shading. The 12 putative transmembrane regions are underlined and numbered 1–12. b, Twelve-transmembrane-domain model of the DCT1 protein. Putative transmembrane domains 1 to 12 are indicated. The consensus transport motif is indicated (CTM), as the fourth intracellular loop and putative *N*-linked glycosylation sites are identified in the fourth extracellular loop. c, The putative iron-responsive regulatory stem–loop binding site (IRE) consensus sequence (CNNNNNCAGUG)[17], predicted to form a stem–loop.

Figure A6.2(16)-3

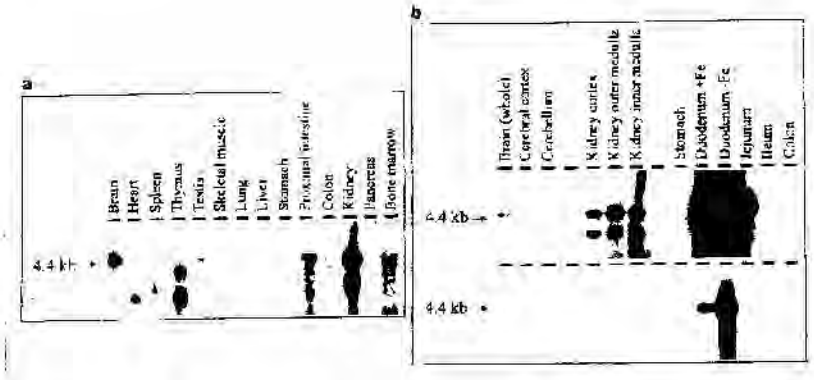

Figure 3 High-stringency northern blot analysis of RNA from all tissues probed with ^{32}P-labeled DCT1 cDNA. Each well was loaded with 3 μg poly(A)$^+$ RNA from a range of **a**, whole tissues or **b** (lower row), specific regions of brain, kidney and intestine, including duodenum from rats fed a low-iron diet (Fe−) or control (Fe+) diet (upper row). Duodenal samples after short exposure

Figure A6.2(16)-4

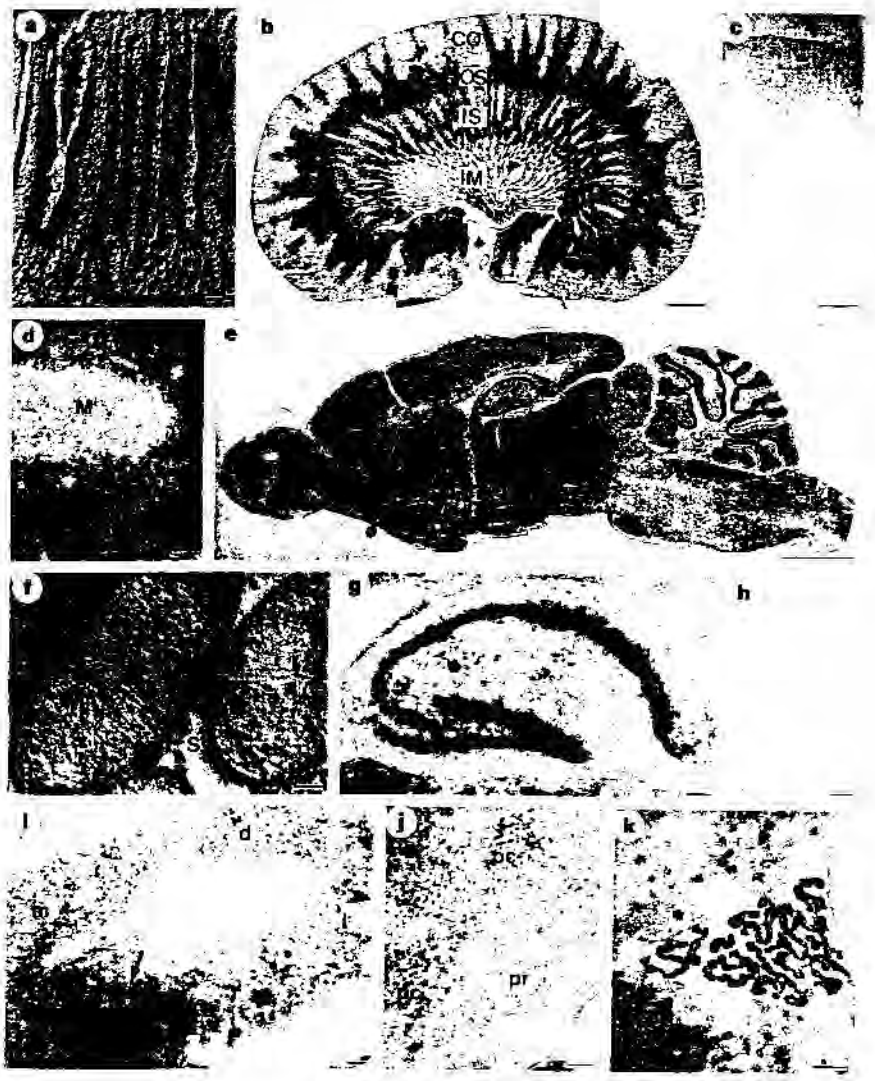

Figure 4 Tissue localization of rat DCT1 mRNA detected by *in situ* hybridization. Bright-field micrographs of cryosections hybridized to digoxigenin-labelled DCT1 antisense (or sense in **c**, **h**) cRNA probe. **a**, Duodenum (M, muscle layer; V, villi; L, lumen). **b**, Kidney (CO, cortex; OS, outer stripe of the medulla; IS, inner stripe; IM, inner medulla). **c**, Kidney hybridized with sense probe. **d**, Thymus (C, cortex; M, medulla). **e**, Sagittal section through brain; DCT1 mRNA was found in neurons throughout the brain. **f**, Testis (S, Sertoli cells; L, lumen). **g**, In hippocampus, positive labelling was prominent in the pyramidal and granule cells. No labelling was obtained with sense probe (**h**). **i**, Anterior olfactory nucleus (m, medial; d, dorsal; l, lateral; v, ventral). **j**, Substantia nigra (pr, pars reticulata; pc, pars compacta). **k**, Choroid plexus in the fourth ventricle. Scale bars: 100 μm in **a**, **d**, **f**, **i**, **k**; 1.5 mm in **b**, **c**; 3 mm in **e**; and 200 μm in **g**, **h**, **j**.

Figure A6.2(16)-5

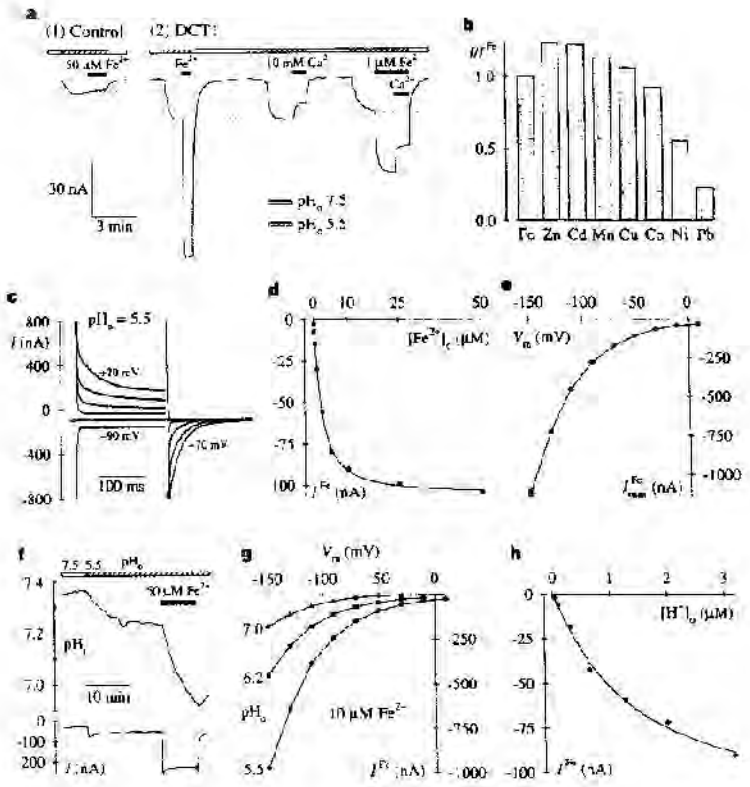

Figure 5 Currents associated with the divalent cation transporter DCT1 expressed in oocytes. **a** Current was continuously monitored in (1) a control oocyte and (2) a single oocyte expressing DCT1, each clamped at –60 mV and superfused for periods indicated by the boxes in the top panel, first at pH_o 7.5 (blank) then at pH 5.5 (diagonal hatch). Iron or additional calcium was applied for the periods shown by the solid bars, then washed out with substrate-free medium, pH 7.5. The dotted horizontal lines indicate the approximate baseline obtained in pH 5.5 medium before the addition of test substrates. **b** Substrate specificity of DCT1, applying test substrates at 50 μM (pH_o 5.5) in a single oocyte (V_m = –50 mV) evoked currents were normalized to the Fe^{2+}-evoked current (–98.5 nA). **c** An oocyte expressing DCT1 (superfused at pH_o 5.5), was held at V_h of –50 mV and V_m was stepped to between +80 mV and –110 mV (in 20-mV increments) for 200 ms. Currents are displayed from 3 ms after the voltage step (on and off); for clarity, only the currents obtained at V_m of +70, +50, +30, 10, –50 and –90 mV are shown. **d** Concentration-dependence of the Fe^{2+}-evoked currents (pH_o 5.5, V_m = –50 mV). The currents evoked by 0.1, 0.25, 0.5, 1, 2.5, 5, 10, 25 and 50 μM $FeCl_2$ were fitted to equation (1): I^{Fe}_{max} = –105 ± 1 nA, $K_{0.5}$ = 2.2 ± 0.1 μM and n_H = 1.2 ± 0.1 for iron. **e** Voltage-dependence of I^{Fe}_{max} (neither $K_{0.5}$ nor n_H varied with V_m). **f** Simultaneous recordings of intracellular pH (pH_i) changes and current in an oocyte expressing DCT1. The oocyte was clamped at V_h = –90 mV and superfused for the periods indicated by the boxes in the top panel, with pH 7.5 medium (blank), then with pH 5.5 medium (diagonal hatch). 50 μM $FeCl_2$ was added for the period shown by the solid bar. **g** Currents evoked by 10 μM Fe^{2+} as a function of extracellular pH (pH_o). **h** Proton activation of the currents evoked by 10 μM Fe^{2+} at V_m = –50 mV. Data were fitted to equation (1): I^{H}_{max} = –121 ± 21 nA (compare with I^{Fe}_{max}), $K_{0.5}$ = 1.3 ± 0.5 μM, n_H = 1.1 ± 0.2 for H^+ (I^{H}_{max} varied with V_m in a similar manner to I^{Fe}_{max}). All kinetic data presented (**d**, **e**, **g**, **h**) were obtained from the same oocyte; errors represent the error in the estimates of kinetic parameters (equation (1), see Methods).

Official use only

89 REFERENCE

1.1 Reference

Author(s), year, title, laboratory name, laboratory report number, report date (if published, list journal name, volume: pages)
If necessary, copy field and enter other reference(s).

McArdle, H.J., Gross, S.M. and Danks, D.M. (1988). Uptake of Copper by Mouse Hepatocytes. Journal of Cellular Physiology, **136**: 373-378 (published).

1.2 Data protection

No
(indicate if data protection is claimed)

1.2.1 Data owner

Give name of company

Public domain

1.2.2 Criteria for data protection

Choose one of the following criteria (see also TNsG on Product Evaluation) and delete the others: No data protection claimed

90 GUIDELINES AND QUALITY ASSURANCE

90.1 Guideline study

No. This was a non-regulatory study carried out to investigate the mechanism of copper uptake by mouse hepatocytes. No guidelines are available to address this objective.
(If yes, give guidelines; if no, give justification, e.g. "no guidelines available" or "methods used comparable to guidelines xy")

90.2 GLP

No. This was a non-regulatory study.
(If no, give justification, e.g. state that GLP was not compulsory at the time the study was performed)

90.3 Deviations

Yes. Refer to section 5.3.2 for a general discussion of deviations and deficiencies.

(If yes, describe deviations from test guidelines or refer to respective field numbers where these are described, e.g. "see 3.x.y")

91 MATERIALS AND METHODS

In some fields the values indicated in the EC or OECD test guidelines are given as default values. Adopt, change or delete these default values as appropriate.

91.1 Test material

^{64}Cu

91.1.1 Lot/Batch number Not available

91.1.2 Specification

Deviating from specification given in section 2 as follows
(describe specification under separate subheadings, such as the following; additional subheadings may be appropriate):

Section A6.2	**Metabolism in mammals**
Annex Point IIA6.2	*Specify section no., heading and species as appropriate*
IUCLID: 5.0/17	**A6.2(17), Cellular and molecular metabolism of copper**
91.1.2.1 Description	*If appropriate, give e.g. colour, physical form (e.g. powder, grain size, particle size/distribution)* Not available
91.1.2.2 Purity	*Give purity in % of active substance* [redacted]
91.1.2.3 Stability	*Describe stability of test material* Not applicable
91.1.2.4 Radiolabelling	*give structural location of radio labelling, give reason if not labelled* ^{64}Cu (specific activity of 160 mCi/mg; used within 3 days)
91.2 Test Animals	*Non-*entry *field*
91.2.1 Species	Mouse
91.2.2 Strain	ARC mice
91.2.3 Source	Not available
91.2.4 Sex	Female
91.2.5 Age	Adult
91.3 Procedures	Non-entry field
91.3.1 Hepatocyte isolation	The livers of test animals were perfused with 40 ml of 0.63 mM EGTA in perfusion buffer and then washed with 15 ml perfusion buffer followed by 60 ml collagenase solution. The cells were teased out of the capsule, only easily separated cells being taken, into 25 ml of Dulbecco's Minimal Medium (DMM) containing 1% Bovine Serum Albumin (BSA). The cells were centrifuged at 200 g for 1 minute, resuspended in the DMM with BSA, and re-centrifuged. The procedure was repeated with the cells finally being suspended in DMM containing 10% foetal calf serum, 1 ìM dexamethosone, and 0.2 U/ml insulin at a cell density of 1 x 10^6 cells/1.5 ml. The cells were tested for viability using tryptopan blue. If the cells were to be used in suspension, they would be taken at this stage at 1 x 10^6 cells/ml. Otherwise, 1 x 10^6 cells were plated onto 2.5 cm diameter culture dishes and kept at 37°C for 4 hours. The cells were then washed lightly to remove loosely attached debris and dead cells, and 1.5 ml of Ultroser G, a serum substitute in DMM was added per dish; the cells were incubated overnight and used the following day.
91.3.2 Experimental procedure	For the cells in suspension, the cells were incubated in the appropriate medium at 37°C in 1 ml final volume and at a cell density of 1 x 10^6 cells/ml. At appropriate times, 125 ìl aliquots were taken and layered onto 150 ìl of dinonyl:dibutyl phthalate (1:2). The cells were spun in a Beckman Microfuge for 10 seconds. The base of the tube containing the cell pellet was cut off and counted in a y-counter. For cells incubated overnight, the cells were washed three times in Hank's Balanced Salt Solution, prepared with Ultrapure chemicals to keep copper levels as low as possible, and the appropriate incubation medium was added. After incubation, the cells were washed three times in phosphate-buffered saline (PBS) to remove loosely-bound copper and 1 ml of 1mg/ml ice-cold pronase was added. The cells were incubated on ice for 30 minutes and aspirated using a Pasteur pipette. They were

transferred to Microfuge tubes, centrifuged at full speed in a Beckman Microfuge for 20 seconds, and the supernatant was removed and counted. Cu in the supernatant was regarded as representing the "surface-bound" (pronase-sensitive) compartment. The pellet was resuspended in 1 ml PBS and ultrasonicated; 100 il was removed for DNA analysis and the remainder was put into clean tubes and counted. Cu counted in the pellet was regarded as representing the "internalised" (pronase-resistant) compartment.

The cells were incubated in balanced salt solution containing 10% FCS. ^{64}Cu levels in the incubation media were measured using either flame or graphite furnace atomic absorption spectroscopy as appropriate, and ^{64}Cu specific activity calculated from these data and relevant standards. In experiments where ^{3}H-histidine was used, it was added, carrier free, to the incubation medium at a final concentration of 1 ìCi/ml. The cells were stored for 7 days to allow complete decay of the copper and counted on a Beckman â-counter. Standards and background blanks were routinely included.

91.3.3 DNA analysis

Aliquots of the sonicated cells (0.1 ml) were dried in an oven at 40°C overnight and resuspended in 100µl diaminobenzoic acid (0.4 mg/ml). The tubes were incubated at 50°C for 1 hour, and the reaction stopped by the addition of 1.5 ml 1M HCl. The tubes were read in a fluorometer at an excitation wavelength of 420 nm, and an emission wavelength of 510 nm.

92 RESULTS AND DISCUSSION

Describe findings. If appropriate, include table. Sample tables are given below.

92.1 Results

Cu uptake by hepatocytes was found to be approximately biphasic. There was an initial rapid rise in binding, followed by a slower increase, which remained linear over the time of the experiment (**Figure A6.2(17)-1a**). Pretreatment of the cells with proteolytic enzyme at 4°C decreased, but did not completely abolish Cu uptake (**Figure A6.2(17)- 1b**). Cu accumulation by the cells was almost completely absent at 4°C.

Histidine stimulated Cu uptake in the hepatocytes (**Figure A6.2(17)-2**). The results followed the same pattern whether or not albumin was present. The effect was concentration dependent (**Figure A6.2(17)-3**), and reached a maximum at a concentration of greater than 200 µM histidine at a Cu concentration of 2 µM. Albumin had little effect on Cu uptake by the cells up to a protein concentration of 20 µM, but thereafter uptake decreased to 100 µM (**Figure A6.2(17)-4**).

The concentration dependence of Cu uptake was found to be complex. At constant Cu:His ratios, uptake was linear, whereas the uptake showed saturation if the Cu:His ratio increased. In order to verify this finding, cells were allowed a period of time to recover from the isolation process. The following studies were therefore carried out on cells that had been cultured overnight. The cells were plated out at a density of 700,000 viable cells/2.5 cm plate. The plates were previously coated with rat-tail collagen. Binding of the radiolabelled complexes to the plates in the absence of cells was insignificant. Generally, the results in the monolayer culture followed a similar pattern for those in suspension. The results for a typical uptake experiment are shown in **Figure A6.2(17)-5**. Uptake was found to be temperature-dependent. The uptake pattern was found to be different from that of the cells in

suspension. Uptake was linear over the first 60 minutes, rather than biphasic. The uptake has been separated into Pronase-sensitive and Pronase-resistant compartments. As discussed in section 3.3.2, these data do not necessarily represent surface-bound and internalised Cu. However, the cells are not disrupted by the treatment, and it is considered reasonable to assume that the proportion of internalised Cu is increased in the pronase-resistant fraction.

Incorporation into the Pronase-resistant fraction was linear over the incubation period (**Figure A6.2(17)-5a**). At 4°C, uptake was much reduced. Incorporation into the pronase-sensitive compartment reached a plateau after about 20 minutes (**Figure A6.2(17)-5b**). At 37°C, in contrast, after 60 minutes the plateau had still not been reached. The amount of ^{64}Cu at 0 minutes in the pronase-resistant fraction was not measurable, whereas there were counts in the pronase-sensitive component supporting the idea that the treatment did at least partially differentiate between Cu that was taken up by the cell and that which was bound by the cell.

The specificity of the histidine effects was tested by incubating the cells with different amino acids. The concentrations chosen were those given as normal adult serum concentrations. The stimulatory effect was not specific for histidine, and other amino acids, notably cystine and theonine, also stimulated uptake (**Figure A6.2(17)-6**).

In contrast to the effect of histidine on Cu, increasing Cu concentrations had no consistent effect on histidine uptake on cells either in suspension or in petri dishes.

In order to investigate the metabolic requirements of the uptake process, cells were incubated with a variety of inhibitors including cyanide, sodium azide, and sodium fluoroacetate. The concentrations used significantly decreased the intracellular ATP concentration, generally to below detectable levels. None of them had any appreciable effect on untake, except N-ethyl maleimide (NEM), a sulphydryl group blocker, which inhibited uptake by greater than 50% at a concentration less than 10 µM. Together with NEM, ouabain and 2,4,dinitrophenyl were selected for closer examination. Whereas only NEM blocked uptake, ouabain and DNP had no effect and may even have increased uptake (**Figure A6.2(17)-7a**). In the same experiments, ^{3}H-histidine uptake was inhibited by both ouabain and DNP (**Figure A6.2(17)-7b**), providing further confirmation that the histidine and Cu uptake pathways are not the same.

The Cu uptake process appears to be saturable, since adding increasing amounts of either Cu or AlbCu results in a decrease in the amount of radioactive copper taken up by the cells (**Figure A6.2(17)-8**). Double reciprocal plots yield nonlinear curves, but Hill plots give a slope of 1, suggesting no cooperativity between binding or transport sites. From the Hill plot, apparent Ka values of 4.7 µM may be obtained. Since the equilibreum between the different Cu binding moieties is complex, the value of the estimated Ka is not clear.

92.2 Discussion

The pattern of Cu uptake by hepatocytes in suspension was qualitatively the same as that for the cells in culture. One difference was the shape of the uptake curve with time (**Figure A6.2(17)-1a** and **Figure A6.2(17)-5**). This may have been related to the fact that the cells in suspension were not washed prior to separation from the incubation medium, or ~~perhaps in the difference in spatial organisation of the~~ cells. On

balance, it was considered likely that the data obtained from cells that were given time to recover from the isolation procedure were more reliable. Furthermore, using cells on plates permitted separation of binding and uptake into pronase-sensitive and pronase-resistant compartments. This allowed a better estimate of the extent of intracellular uptake, as opposed to binding of the Cu.

Uptake was shown to follow first order kinetics and amino acids stimulated uptake. N-ethyl maleimide inhibited uptake.

The data supported the hypothesis that Cu was bound as a histidine-Cu complex, but that Cu is taken up separately from the amino acid. The process of Cu uptake was passive, since metabolic inhibitors had no effect on uptake even at concentrations where they caused considerable release of AST. A protein was involved, at least part of which must project out from the cell membrane, since treatment with pronase resulted in a decrease of Cu uptake. N-ethyl maleimide caused inhibition of uptake, suggesting that sulphydryl groups may be involved, either in maintaining the structural integrity of the protein, or in the actual translocation process.

Cu did not alter histidine uptake, and the metabolic dependence of the two processes, even when measured simultaneously, were different. Other amino acids could substitute for histidine, although not to the same extent. The degree to which the different amino acids could substitute for histidine did not seem to be related to their structural similarity. Furthermore, the effects appeared to be additive in that in the presence of all 15 amino acids, the effect was greater than for any individual.

The role of albumin in the uptake process was complex, but may be deduced from the Cu concentration curve. The fact that the reciprocal plots were nonlinear and no simple solution was given by the Eisenthal and Cornish-Bowden construct suggested that two processes may have been occurring, one that is rate limiting at low concentrations and another that is limiting at higher concentrations. It was suggested that, at low copper, the transfer of Cu from the albumin to histidine is rate limiting, whereas at higher concentrations of Cu, the transfer from histidine to the acceptor protein was the rate-limiting step.

93 APPLICANT'S SUMMARY AND CONCLUSION

93.1 Materials and methods

Give concise description of method; give test guidelines no. and discuss relevant deviations from test guidelines

A study was carried out to investigate the mechanism of copper uptake by mouse hepatocytes. The study was not designed to follow internationally accepted guidelines, and was not carried out or reported in compliance with GLP. The following techniques were used:

Hepatocyte isolation: The livers of test animals were perfused with 0.63 mM EGTA in perfusion buffer, washed with perfusion buffer and then collagenase solution. Cells were teased out of the capsule into Dulbecco's Minimal Medium (DMM) containing 1% BSA.

Cells were centrifuged at 200 g for 1 minute, resuspended in DMM with BSA, and recentrifuged. The procedure was repeated, with cells being suspended in DMM containing 10% foetal calf serum, 1 iM dexamethosone, and 0.2 U/ml insulin at a cell density of 1 x 10^6 cells/1.5 ml. The cells were tested for viability using tryptopan blue. If the cells were then to be used in suspension, they would be taken at this

stage at 1 x 10^6 cells/ml. Otherwise, 1 x 10^6 cells were plated onto culture dishes and kept at 37°C for 4 hours. Cells were then washed lightly and 1.5 ml of Ultroser G, a serum substitute, in DMM was added per dish. These cells were incubated overnight for use the next day.

Experimental procedure: Cells in suspension were incubated at 37°C at a cell density of 1 x 10^6 cells/ml in 1 ml medium. 125 il aliquots were taken and layered onto 150 il of dinonyl:dibutyl phthalate (1:2). The cells were spun in a Beckman Microfuge for 10 seconds. The base of the tube containing the cell pellet was cut off and counted in a y-counter.

Cells that were incubated overnight were washed 3 times in Hank's Balanced Salt Solution, and incubation medium was added. After incubation, cells were washed 3 times in PBS and 1 ml of 1mg/ml ice-cold pronase was added. Cells were incubated on ice for 30 minutes, and aspirated using a Pasteur pipette. They were centrifuged for 20 seconds and the supernatant removed and counted. Cu in the supernatant was regarded as representing the "surface-bound" (pronasesensitive) compartment. The pellet was resuspended in 1 ml PBS and ultrasonicated; 100 il was removed for DNA analysis and the remainder was put into clean tubes and counted. Cu counted in the pellet was regarded as representing the "internalised" (pronase-resistant) compartment.

Cells used in these experiments were incubated in balanced salt solution containing 10% FCS. Cu levels in the incubation media were measured using either flame or graphite furnace AAS, and ^{64}Cu-specific activity calculated from these data and relevant standards. When ^{3}H-histidine was used, it was added to the incubation medium at a concentration of 1 iCi/ml. Cells were stored for 7 days to allow complete decay of the Cu and counted on a Beckman â-counter. Standards and background blanks were routinely included.

DNA analysis: Aliquots of sonicated cells were dried in an oven at 40°C overnight and resuspended in diaminobenzoic acid (0.4 mg/ml). Tubes were incubated at 50°C for 1 hour, and the reaction stopped by addition of 1.5 ml 1M HCl. Tubes were read in a fluorometer at an excitation and emission wavelengths of 420 and 510 nm, respectively.

93.2 Results and discussion

Summarize relevant results; discuss dose-response relationship.

Cu uptake at 37°C by hepatocytes in suspension culture was approximately biphasic, with an initial rapid rise in binding, followed by a slower linear increase. Pretreatment of cells with proteolytic enzyme caused a reduction in the rate of Cu uptake. Cu accumulation by both treated and untreated cells was almost completely absent at 4°C.

Histidine stimulated Cu uptake, following the same pattern whether albumin was present or not. The effect was concentration dependent, reaching a maximum at a histidine concentration of > 200 µM and a Cu concentration of 2 µM. Albumin up to a concentration of 20 µM had little effect on Cu uptake by the cells, but uptake decreased thereafter.

The concentration dependence of Cu uptake was complex. At constant Cu:His ratios, uptake was linear, whereas it showed saturation if the Cu:His ratio increased. In order to investigate this finding, cells were allowed to recover from the isolation process. The following studies were therefore carried out on cells that had been cultured overnight:

Cells were plated out at a density of 7 x 10^5/plate (plates were previously coated with rat-tail collagen). The results seen in monolayer

culture followed a similar pattern to those seen in suspension, with temperature-dependent uptake. The *pattern* of uptake was different, however, being linear over the first 60 minutes, not biphasic. Uptake was divided into pronase-sensitive and pronase-resistant compartments. Incorporation into the pronase-resistant fraction was linear over the incubation period. Uptake was much reduced at 4°C. Incorporation into the pronase-sensitive compartment reached a plateau after about 20 minutes at 4°C. At 37°C, in contrast, after 60 minutes the plateau has still not been reached. The amount of ^{64}Cu at 0 minutes in the pronase-resistant fraction was not measurable, whereas there were counts in the pronase-sensitive component supporting the idea that the treatment did at least partially differentiate between copper that had been taken up by the cell and that which was bound.

The specificity of the histidine effects was tested by incubating cells with different amino acids at concentrations normally found in adult serum. The stimulatory effect was not specific to histidine, as other amino acids, notably cystine and theonine, also stimulated Cu uptake. In contrast to the effect of histidine on Cu, increasing Cu concentrations had no consistent effect on histidine uptake by cells either in suspension or in petri dishes.

To investigate the metabolic requirements of the uptake process, cells were incubated with a variety of inhibitors at concentrations that decreased intracellular ATP to undetectable levels. It was found that only N-ethyl maleimide (NEM), a sulphydryl group blocker, had any appreciable effect on untake of Cu (NEM at concentrations of less than 10 µM inhibited Cu uptake by more than 50%). ^{3}H-histidine uptake was, however, inhibited by both ouabain and DNP, thereby confirming that histidine and Cu uptake pathways are not the same.

The Cu uptake process appears to be saturable, since adding increasing amounts of either Cu or AlbCu results in a decrease in the amount of radioactive copper taken up by the cells.

93.3 Conclusion

Uptake of Cu showed saturation and appeared to follow first order kinetics. Histidine stimulated uptake in a concentration-dependent manner, as did some other amino acids, but Cu had little effect on histidine uptake. Cu uptake was shown not to be an energy dependent process, as metabolic inhibitors did not affect the process. Inhibitors did, however, block histidine uptake, indicating that copper and histidine are taken up by different pathways. Uptake of Cu was markedly reduced by N-ethyl maleimide, and pre-incubation of cells with pronase resulted in a decrease of uptake.

93.3.1 Reliability

Based on the assessment of materials and methods include appropriate reliability indicator 0, 1, 2, 3, or 4

2

93.3.2 Deficiencies

Yes

This study was not conducted and/or reported in strict compliance with the principles of GLP. However, this does not compromise the validity of the data generated, or the author's interpretation of that data, given that the study was not carried out for regulatory purposes. Furthermore, the research was published in a peer-reviewed journal, and has therefore been subject to the prior scrutiny of experts in the field. In addition this report has been included in a number of expert reviews of copper toxicokinetics.

Section A6.2	**Metabolism in mammals**
Annex Point IIA6.2	*Specify section no., heading and species as appropriate*
IUCLID: 5.0/17	**A6.2(17), Cellular and molecular metabolism of copper**

No internationally accepted guidelines are available that specifically address the objective of the research presented in this summary.

Overall, this is a well-reported study, and its findings are considered to make a valuable contribution to the 'weight of evidence' approach that has been adopted for the purposes of the current review of copper toxicokinetics. A reliability indicator of 2 has been assigned on this basis.

(If yes, discuss the impact of deficiencies and implications on results. If relevant, justify acceptability of study.)

Evaluation by Competent Authorities	
	Use separate "evaluation boxes" to provide transparency as to the comments and views submitted
	EVALUATION BY RAPPORTEUR MEMBER STATE
Date	[redacted]
Materials and Methods	[redacted]
Results and discussion	[redacted]
Conclusion	[redacted]
Reliability	[redacted]
Acceptability	[redacted]
Remarks	

	COMMENTS FROM ...
Date	*Give date of comments submitted*

Figure A6.2(17)-1

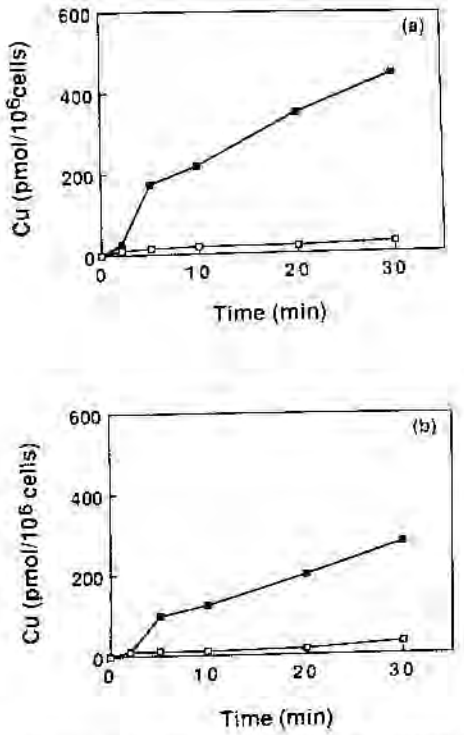

Fig. 1. **a.** Copper uptake by hepatocytes in suspension. Cells were incubated with ^{64}Cu (final concentration, 2 μM) in EBSS, 10% FCS as described in Materials and Methods at 4°C (□) and 37°C (■) for appropriate lengths of time before being counted as described. The results are the mean of three separate experiments. **b.** Copper uptake by hepatocytes in suspension after Pronase treatment. The cells were incubated for 30 minutes at 4°C in 1 mg/ml Pronase before being washed and incubated with radiolabeled Cu as described in Materials and Methods and (a) at 4°C (□) and at 37°C (■). The results are the mean of three separate experiments.

Figure A6.2(17)-2

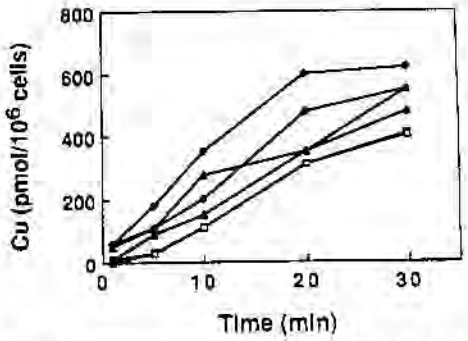

Fig. 2. Copper uptake in the presence of (□) 0 added histidine, (■) 5 μM, (▲) 10 μM, (△) 50 μM, (◆) 100 μM, and (◇) 200 μM added histidine. The basal level of histidine (0 added) was 7 μM. The cells were incubated in the presence of histidine and 2 μM ^{64}Cu for 30 minutes before being washed and treated as described in Materials and Methods. The results are the mean of three separate experiments.

Figure A6.2(17)-3

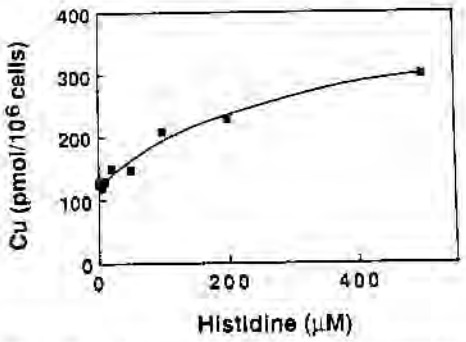

Fig 3. The effect of increasing histidine concentration on copper uptake by hepatocytes. The cells were incubated as described in the legend to Figure 2. This data presents a summary of that in Figure 2.

Figure A6.2(17)-4

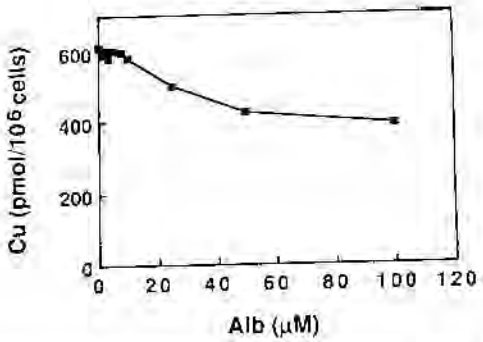

Fig 4. The effect of increasing albumin on copper uptake by mouse hepatocytes. The cells were incubated with increasing concentrations of albumin and 2 μM ^{64}Cu for 30 minutes, before being treated as described in Materials and Methods. It must be remembered that there is 10% FCS in the incubation medium, hence there is a very high background level of α-fetoprotein in the incubation medium. The results are the mean of four experiments.

Figure A6.2(17)-5

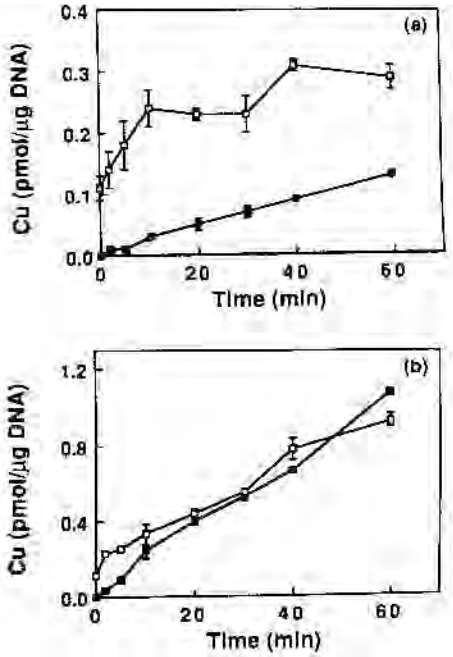

Fig. 5. Uptake of copper by hepatocytes cultured overnight. Following overnight culture, the cells were washed and incubated with ^{64}Cu as described in Materials and Methods. After 30 minutes of incubation at either 4°C (a) or 37°C (b), the cells were washed and removed from the plates by incubating for 30 minutes at 4°C in 1 mg/ml Pronase. The results are presented as Pronase-sensitive (□) and Pronase-resistant (■). For more detail, see Materials and Methods and Results. The results are the mean ± SEM of six plates in three experiments.

Figure A6.2(17)-6

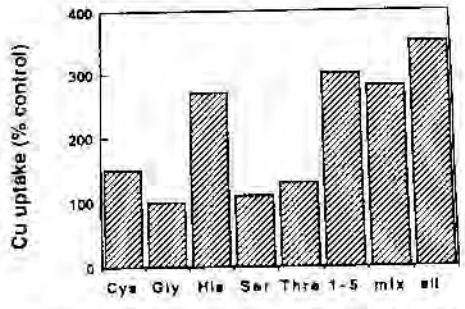

Fig. 6. The effect of amino acids on copper uptake by hepatocytes. The cells were incubated for 30 minutes in the presence of ^{64}Cu with the addition of amino acids at the concentrations given below. These concentrations are close to those measured in human adult serum. Cys, cystine, 50 μM; Gly, glycine, 200 μM; His, histidine, 100 μM; Ser, serine, 100 μM; Thre, threonine, 130 μM; 1–5, a mixture of the above five amino acids, each at the given concentration. Mix, a mixture of arginine, glutamine, isoleucine, leucine, lysine, methionine, phenylalinine, tryptophan, tyrosine and valine, all at serum concentrations (see Table 1). All, a mixture of all the above amino acids at serum concentrations. The results are expressed as % of control, with the control being 2.3 ± 0.3 pmol/μg DNA/30 minutes and are the mean ± SEM of six observations.

Figure A6.2(17)-7

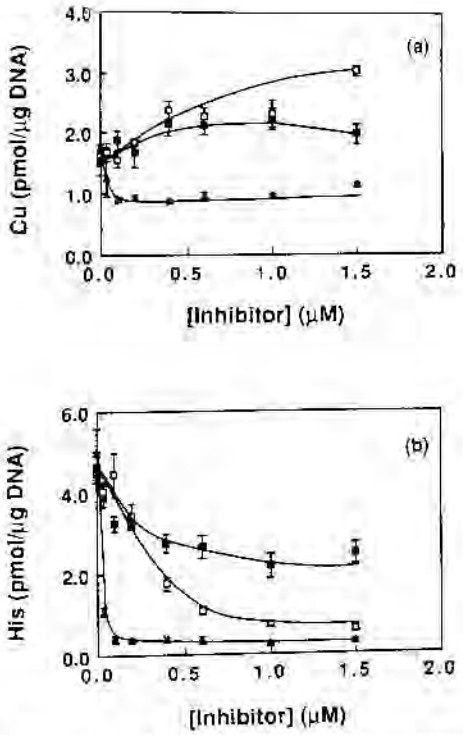

Fig. 7. **a.** The effect of ouabain (□), 2,4, dinitrophenol (■) and N-ethyl maleimide (▲) on copper uptake by hepatocytes. The cells were incubated with the inhibitor at the given concentrations and ^{64}Cu for 30 minutes prior to washing and treatment as described in Materials and Methods. The results are the mean ± SEM of six observations. **b.** The effect of ouabain (□), 2,4, dinitrophenol (■), and N-ethyl maleimide (▲) on histidine uptake by hepatocytes. The cells were incubated with the inhibitor at the given concentrations and ^{3}His at 1 μCi/ml for 30 minutes prior to washing and treatment as described in Materials and Methods. The results are the mean ± SEM of six observations.

Figure A6.2(17)-8

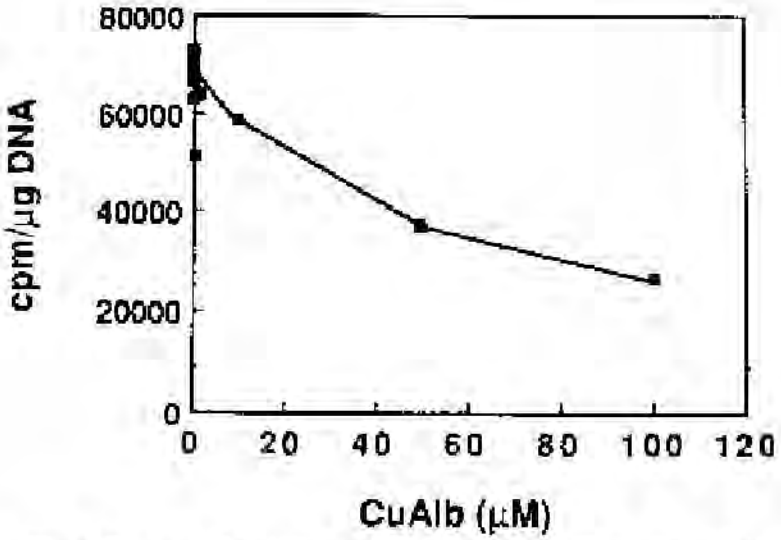

Fig. 8. The effect of the increasing concentration of CuAlb on ^{64}Cu uptake by hepatocytes. The cells were incubated with the medium and ^{64}Cu at 2 μM and unlabeled CuAlb at increasing concentrations for 30 minutes before being washed and counted as described in Materials and Methods. The results are from one experiment and show the mean of duplicate observations.

Official use only

94 REFERENCE

1.1 Reference

Author(s), year, title, laboratory name, laboratory report number, report date (if published, list journal name, volume: pages)
If necessary, copy field and enter other reference(s).
*Darwish, H.M., Cheney, J.C., Schmitt, R.C. and Ettinger, M.J. (1984). Mobilisation of copper (II) from plasma components and mechanism of hepatic copper transport. Am. J. Physiol., **246 (9)**:G72-G79 (published).*

1.2 Data protection

No
(indicate if data protection is claimed)

1.2.1 Data owner

Give name of company

Public domain

1.2.2 Criteria for data protection

Choose one of the following criteria (see also TNsG on Product Evaluation) and delete the others: No data protection claimed

95 GUIDELINES AND QUALITY ASSURANCE

95.1 Guideline study

No. This was a non-regulatory study carried out to investigate the mechanism of copper uptake by rat hepatocytes. No guidelines are available to address this objective.
(If yes, give guidelines; if no, give justification, e.g. "no guidelines available" or "methods used comparable to guidelines xy")

95.2 GLP

No. This was a non-regulatory study.

(If no, give justification, e.g. state that GLP was not compulsory at the time the study was performed)

95.3 Deviations

Yes. Refer to section 5.3.2 for a general discussion of deviations and deficiencies.

(If yes, describe deviations from test guidelines or refer to respective field numbers where these are described, e.g. "see 3.x.y")

96 MATERIALS AND METHODS

In some fields the values indicated in the EC or OECD test guidelines are given as default values. Adopt, change or delete these default values as appropriate.

96.1 Test material

^{64}Cu(II) as the free ion or as ^{64}Cu(II).albumin.

L-[^{3}H]histidine

96.1.1 Lot/Batch number Not available

96.1.2 Specification

Deviating from specification given in section 2 as follows
(describe specification under separate subheadings, such as the following; additional subheadings may be appropriate):

Section A6.2	**Metabolism in mammals**
Annex Point IIA6.2	*Specify section no., heading and species as appropriate*
IUCLID: 5.0/18	**A6.2(18), Cellular and molecular metabolism of copper**
96.1.2.1 Description	*If appropriate, give e.g. colour, physical form (e.g. powder, grain size, particle size/distribution)* Not available
96.1.2.2 Purity	*Give purity in % of active substance* [redacted]
96.1.2.3 Stability	*Describe stability of test material* Not applicable
96.1.2.4 Radiolabelling	*give structural location of radio labelling, give reason if not labelled* ^{64}Cu(II) L-[^{3}H]histidine (specific activity 42 Ci/mmol).
96.2 Test Animals	Non-entry field
96.2.1 Species	Rat
96.2.2 Strain	Sprague-Dawley
96.2.3 Source	Not available
96.2.4 Sex	Male
96.2.5 Age, weight	150 g – 250 g
96.3 Procedures	Non-entry field
96.3.1 Cell isolation and characterisation	The livers of test animals were perfused with 40 ml of 0.63 mM EGTA in perfusion buffer and then washed with 15 ml perfusion buffer followed by 60 ml collagenase solution. The cells were teased out of the capsule, only easily separated cells being taken, into 25 ml of Dulbecco's Minimal Medium (DMM) containing 1% BSA. The cells were centrifuged at 200 g for 1 minute, resuspended in the DMM with BSA, and centrifuged. The procedure was repeated with the cells finally being suspended in DMM containing 10% foetal calf serum, 1 ìM dexamethosone, and 0.2 U/ml insulin at a cell density of 1 x 10^{6} cells/1.5 ml. The cells were tested for viability using tryptopan blue. If the cells were to be used in suspension, they would be taken at this stage at 1 x 10^{6} cells/ml. Otherwise, 1 x 10^{6} cells were plated onto 2.5 cm diameter culture dishes and kept at 37°C for 4 hours. The cells were then washed lightly to remove loosely attached debris and dead cells, and 1.5 ml of Ultroser G, a serum substitute in DMM was added per dish; the cells were incubated overnight and used the following day.
96.3.2 Cell incubation and copper uptake determinations	Isolated hepatocytes were incubated in a modified Earle's salts buffer at 20°C under 95% O_2 – 5% CO_2 in a Dubnoff metabolic shaking water bath set at 100 cycles/min for 5 – 15 min. ^{64}Cu(II), at equilibrium with copper ligands when present, was then added to the shaking cell suspension. Samples were removed at intervals for copper uptake determinations. In order to remove all surface-bound Cu(II), the samples were immediately transferred to 5 ml of 10 mM EDTA-0.9% NaCl at 0°C and centrifuged at 0 – 4°C for 2.5 minutes. The pellet was then washed once with 3 ml of 10 mM EDTA-0.9% NaCl and recentrifuged. 1 ml of 0.1% sodium dodecyl sulphate in H_2O was added to the pellet, and 0.8 ml was removed for gamma counting and protein determination. Samples were counted in a gamma scintillation counter with 20% gain and 5.16% efficiency. Results were corrected for isotope decay by a laboratory computer program. Protein concentrations were

	determined using bovine serum albumin as the standard.	
96.3.3 Effects of albumin on ^{64}Cu(II) uptake.	^{64}Cu(II) was added to the cells as the free ion or in the form of ^{64}Cu(II).albumin at molar ratios of 5:1, 2:1 or 1:1 Cu(II) to albumin. Duplicate samples (1 ml) were removed at the appropriate times for 0 – 40 minutes to determine net ^{64}Cu(II) uptake. To examine the effect of albumin on the kinetic parameters for uptake, initial rates (0.5 min) were measured at ^{64}Cu(II) concentrations from 2 to 25 µM with and without 2 µM albumin, and duplicate samples were evaluated for ^{64}Cu(II) uptake.	
96.3.4 Effect of histidine on coppper uptake in presence of albumin.	Equilibrium mixtures of ^{64}Cu(II), albumin, and L-histidine were prepared before addition to cells. Net uptake was determined at 5 and 10 µM copper plus 20 µM albumin with or without 10 or 50 µM histidine. Duplicate samples (1 ml) were removed at appropriate times.	
96.3.5 Effects of various other amino acids on copper uptake.	Net uptake of ^{64}Cu(II) (20 µM) was measured in the presence of 20 µM albumin and 50 µM of each amino acid shown in **Table A6.2(18)-1**, individually or in combination with 50 µM histidine. Selected amino acids were also tested similarly in the absence of albumin (**TableA6.2(18)-6**). Copper uptake per hour was determined for 6 replicates with each condition.	
96.3.6 Effects of Gly-His-Lys on copper transport.	^{64}Cu(II) transport was measured in the presence of Gly-His-Lys with and without albumin and histidine at the concentrations and combinations shown in **Table A6.2(18)-2. Net** uptake was measured in quadruplicate samples after 60 minutes incubation. The effect of GlyHis-Lys on ^{64}Cu(II) uptake kinetics was determined as described for albumin **(section 3.3.2)** using 2 µM Gly-His-Lys and copper concentrations of 2-25 µM. Quadruplicates were obtained at each copper concentration.	X
96.3.7 Fractionation of rat plasma.	Freshly isolated rat plasma (2 ml) was applied to a 1.5 x 30 cm column of Sephadex G-25 equilibrated with 0.25 M Tris-HCl at pH 8.0. The column was eluted with the same buffer at 4°C, collecting 2 ml fractions. Protein absorbances at 280 and 220 nm were monitored, as was conductivity. A low molecular weight fraction (≤5000) was tested for its effect on copper uptake after readjusting the pH to 7.4. The concentration of histidine in this fraction was estimated from the conductivity-derived dilution factor and the known histidine concentration in plasma of 70 µM.	
96.3.8 Cu(II) transport rates from albumin-containing and albumin-free dialysis fractions.	Albumin (20 µM) and ^{64}Cu(II) (10 µM) in Earle's buffer were dialysed against histidine-free buffer or buffer containing 20 and 50 µM L-histidine at 4°C for 20 hours. Initial rates of ^{64}Cu uptake (0.5 min) were determined with the albumin-containing and albumin-free fractions at equilibrium.	
96.3.9 Transport kinetics of ^{64}Cu(II) from $His_2Cu(II)$ complex.	Initial rates (0.5 min) were measured at ^{64}Cu(II) concentrations from 1 to 25 µM as free ^{64}Cu(II) or a His_2 ^{64}Cu(II) at the same concentrations. Uptake was determined for quadruplicate samples, and the results are shown as means ± SD. Kinetic parameters were determined from least-squares fits to reciprocal data without weighting and nonlinear least-squares fits to the *v* vs. [Cu} data.	
96.3.10 Assessing possible transport of copper with histidine in histidine.Cu(II) complexes.	Initial rates of (0.5 min) of ^{64}Cu(II) uptake at 10 µM ^{64}Cu(II) were measured in Na^+-containing and chlorine-substituted Earle's buffer since histidine transport is known to be Na^+ dependent. L-[^{3}H]histidine with specific activity of 42 Ci/mmol was used in experiments testing for possible transport of both [^{3}H]-histidine and ^{64}Cu(II) from	

Cu(II).histidine complexes. The labelled histidine was added (50 nCi/ml in the final mixture), and the initial rates of histidine uptake were determined at 10 and 20 µM histidine in Na^+- and choline-containing buffers in the presence or absence of 10 µm ^{64}Cu(II). The samples were processed identically to those for copper uptake determinations and counted with a scintillation counter in addition to the gamma counting. Quenching of the tritium label was minimal. Six samples were assayed with each set, and the results are expressed as means ± SD in nM per minute per mg protein of and/or [^{3}H]histidine. X

97 RESULTS AND DISCUSSION

Describe findings. If appropriate, include table. Sample tables are given below.

97.1 Results

Non-entry field

97.1.1 Effects of albumin on ^{64}Cu(II) uptake

At equimolar Cu(II) and albumin, albumin markedly inhibited uptake of ^{64}Cu(II) by hepatocytes, and significant inhibition was detected at up to a 10:1 molar excess of Cu(II) (**Figures A6.2(18)-1 and A6.2(18)-2**). Both initial rates and the rate of attaining a steady state were affected in that, at Cu (II) to albumin molar ratios of 1:1 (**Figure A6.2(18)-1**) or less (**Figure A6.2(18)-3**), net uptake continued after 40 minutes, whereas when copper is in excess, significant net uptake is apparently minimal after 40 minutes (**Figure A6.2(18)-1**).

The effect of albumin on initial rates of ^{64}Cu(II) uptake was examined further to determine the mechanism of inhibition. At relatively high concentrations of copper, the initial rates of uptake with albumin approached the rates observed without albumin (**Figure A6.2(18)-2**). Thus the apparent Vmax and Km parameters converge toward the values obtained with free copper. In the presence of albumin, reciprocal plots were non-linear, i.e. the slope increased dramatically with decreasing total copper concentration (**Figure A6.2(18)-2**). This is the type of kinetic profile that is observed with enzyme inhibitors that act by decreasing the concentration of the reacting substrate.

97.1.2 Effect of histidine and other amino acids on albumin-inhibited copper uptake.

The effect of histidine on albumin-inhibited copper uptake was examined to determine whether histidine facilitates copper transport. The copper concentrations used correspond to about 0.5 and 1.0 K_m for copper transport in the absence of albumin; albumin was at 4:1 and 2:1 molar excesses of copper, respectively. Histidine equimolar to the total copper increased the rate of copper uptake by hepatocytes under these conditions, and the stimulatory effect increased with increasing histidine (**Figure A6.2(18)-3**). However, under all conditions tested, the rates of copper uptake never exceeded the rates observed with free ^{64}Cu(II) at the same total concentration. The approach to steady state also remained slow, reflecting the relatively low concentrations of copper.histidine complexes under the conditions used. Thus, at 10 µM Cu(II), 10 µM albumin, and 50 µM histidine, the total ^{64}Cu accumulated at 60 minutes was 0.60 times that for free copper but 1.35 times that obtained with albumin in the absence of histidine (**Table A6.2(18)-2**).

The relative specificity of histidine was assessed by testing other amino acids that have been isolated from plasma in binary and/or ternary complexes with copper and selected non-complexing amino acids as controls. Within single amino acid.copper complexes, cystine was the only amino acid other than histidine to exert any facilitation effect (**Table A6.2(18)-1**). Moreover, the total facilitation effect of 50 µM

	threonine, glutamine, or serine plus 50 µM histidine was identical to the effect of 50 µM histidine alone (**Table A6.2(18)-1**).	
97.1.3 Effects of Gly-His-Lys on copper uptake.	The effect of Gly-His-Lys on ^{64}Cu(II) uptake by hepatocytes was very similar to the effect of albumin. Gly-His-Lys markedly inhibited copper uptake at low Cu(II)-to-Gly-His-Lys ratios, but with increasing copper the initial rates of copper uptake approached the rates for free ^{64}Cu(II) transport (**Figure A6.2(18)-4**). Thus, Gly-His-Lys also apparently inhibits copper transport by decreasing the concentration of free Cu(II) in solution. The inhibitory effects of albumin and Gly-His-Lys are additive, i.e., at equivalent concentrations albumin decreased Gly-His-Lys-inhibited copper uptake by the same factor as it decreased the rate of free Cu(II) uptake (**Table A6.2(18)-2**). Moreover, the facilitation effect of histidine on albumin-inhibited ^{64}Cu(II) uptake was decreased by the inhibitory effect of Gly-His-Lys when transport was measured in the presence of all three copper ligands (**Table A6.2(18)-2**). Histidine facilitated Gly-His-Lys-inhibited ^{64}Cu(II) uptake by approx. the same factor as its effect on albumin-inhibited uptake (**Table A6.2(18)-2**).	
97.1.4 Effect of low-molecular weight plasma fraction on albumin-inhibited copper uptake	As a more inclusive test for possible facilitators (or inhibitors) of hepatic copper transport in plasma, a low molecular weight fraction of rat plasma was added to an incubation medium that contained 20 µM albumin and 10 µM ^{64}Cu. These are the same concentrations used in the experiments illustrated in **Figure A6.2(18)-3** for assessing the effects of histidine. The facilitation effect of the plasma fraction was equivalent to the effect of 10 µM histidine (**Table A6.2(18)-3**). The estimated histidine concentration in the fraction added to the cells was 8 µM. Possible additional strong inhibitors of copper transport were also not detected since the low molecular weight plasma fect on copper uptake at 10 µM Cu(II) in the absence of albumin (**Table A6.2(18)-3**).	X
97.1.5 Cu(II).histidine vs. Cu(II).histidine. albumin as active species.	To determine whether copper is delivered to hepatocytes complexed to histidine, albumin, or within the copper.histidine.albumin chelate, albumin, ^{64}Cu(II) and histidine mixtures were dialysed until equilibrium was attained and the rates of Cu(II) uptake from the albumin-containing and albumin-free fractions were compared. In each case, the initial uptake rates (0.5 min) of fractions containing only free Cu plus excess histidine were the same as those of fractions containing 20µM albumin.	X
97.1.6 Kinetics of copper uptake from His2Cu(II).	The kinetic parameters of histidine.copper complexes were compared with those of free copper. The active species in all experiments reported here in which histidine was in excess of nonalbumin-bound copper was the $His_2Cu(II)$ complex, since this is the predominant species at pH 7.4 at 2:1 and higher molar excesses of histidine. The reciprocal velocity versus reciprocal [$His_2Cu(II)$] plot was linear; V_{max} was identical, while Km (15 ± 0.7 µM) was slightly higher for the ternary complex than for free Cu(II) (**Figure A6.2(18)-5**).	
97.1.7 $His_2Cu(II)$ vs. free ionic copper as transported species.	Transport of [^{3}H]histidine and ^{64}Cu(II) was monitored concurrently to determine whether histidine is transported with copper from Cu(II).histidine complexes by the putative hepatic copper transport system. Since histidine transport by hepatocytes occurs in part by Na^+-dependent mechanisms, experiments were done in Na^+ and choline media. Hepatocyte copper uptake in the presence of free Cu(II), histidine.Cu(II), or $His_2Cu(II)$ was identical in Na^+ and choline media (**Table A6.2(18)-5**). This confirmed that copper transport *per se* is not Na^+ dependent. In the absence of copper, uptake of [^{3}H]histidine was negligible in both Na^+ and choline media (**Table A6.2(18)-5**). No	

additional transport of [^{3}H]histidine was detected during ^{64}Cu(II) uptake. At 10 µM ^{64}Cu(II).[^{3}H]histidine (1:1), the nanomoles ^{64}Cu per minute per mg protein transported were an order of magnitude higher than the amount of [^{3}H]-histidine transported, and [^{3}H]histidine uptake was unaffected by copper in either Na+- or choline-containing media (**Table A6.2(18)-5**). The only detectable effect of copper on histidine transport was a small inhibitory effect of the $His_2Cu(II)$ complex relative to the equivalent concentration of free histidine (**Table A6.2(18)-5**).

97.2 Discussion

The unavailability of albumin-bound Cu(II) for uptake by hepatocytes during the initial velocity period of 0.5 min was illustrated directly by the dialysis experiments involving the histidine + Cu(II) fractions in equilibrium with albumin-bound Cu(II). Both the rate of copper uptake in the absence of histidine and the facilitation effect of histidine were found to be determined largely by the concentrations of the non-albumin species. Although the differences in observed copper uptakes between the corresponding sets of albumin-containing and albumin-free dialysis fractions were insignificant by t-test criteria, copper uptake was consistently slightly (~10%) higher from the albumin-containing fractions (**Table A6.2(18)-4**). This small apparent effect of albumin is attributed to a shift in the Cu(II).albumin equilibrium toward free copper. The kinetic results suggest that albumin's principal effect on copper transport is simply to remove Cu(II) from access to the transport system. There was no evidence for involvement of a direct functional interaction between Cu(II).albumin or His.Cu(II).albumin with hepatocytes. Moreover, Cu(II) does not appear to be rapidly released from albumin due to albumin-hepatic membrane interactions.

That histidine is the principal plasma component involved in mobilising copper from albumin is indicated by 1) the lack of effect of most other amino acids on albumin-inhibited Cu(II) uptake and 2) the facilitating effect of the low molecular weight plasma fraction was largely accounted for by its histidine concentration.

The transport kinetic data for the $His_2Cu(II)$ complex relative to that for free Cu(II) are most consistent with $His_2Cu(II)$ interaction with the putative transport protein. The data do not preclude dissociation of the Cu(II) prior to transport, provided the dissociation rate constant is higher than the rate constant of the rate-limiting step in transport. However, this is considered to be unlikely, given the high stability constant of the $His_2Cu(II)$ complex. Also, the reciprocal velocity-reciprocal [$His_2Cu(II)$] plot would be non-linear if the binding species were free Cu(II) and the dissociation rate was smaller than the transport rate. The relatively small difference between the K_m for the $His_2Cu(II)$ complex and free Cu(II) further implies that the contributions of histidine to specific interactions with the Cu(II) transport protein are minimal.

The experiments involving [^{3}H]histidine and ^{64}Cu(II) indicate that ^{64}Cu(II) from the $His_2Cu(II)$ complex is transported as the free ion, since concurrent transport of the labelled histidine did not occur. The fact that V_{max} is identical for uptake of free Cu(II) and $His_2Cu(II)$ is consistent with transport of the free ion in each case. Thus, a ligand-displacement reaction apparently occurs between $His_2Cu(II)$ and the hepatic transport protein prior to actual transport. The identical $_{Vmax}$ value for the free Cu(II) form indicates that the rate-limiting step occurs after the ligand displacement reaction.

The data indicate that Gly-His-Lys will inhibit Cu(II) uptake by

hepatocytes under conditions in which Gly-His-Lys, histidine and albumin are all in excess of the Cu(II). Since the estimated concentration of Gly-His-Lys in human plasma is ~1.7 µM, these are the conditions that prevail *in vivo*.

These results show that, at physiological concentrations, albumin inhibits copper uptake. Histidine facilitates hepatic copper uptake from plasma by effectively competing with albumin for copper. Although Cu(II) uptake rates from the $His_2Cu(II)$ complex are slightly less than for free Cu(II), copper is available for transport in this form.

98 APPLICANT'S SUMMARY AND CONCLUSION

98.1 Materials and methods

Give concise description of method; give test guidelines no. and discuss relevant deviations from test guidelines.

A study was carried out to investigate the mechanism of copper uptake by rat hepatocytes. Hepatocytes isolated from the livers of male Sprague-Dawley rats weighing 150 g were used. The study was not designed to follow internationally accepted guidelines, and was not carried out or reported in compliance with GLP. The following techniques were used:

Cell isolation and characterisation: Livers of test animals were perfused with 0.63 mM EGTA in perfusion buffer and washed, first with perfusion buffer, and then with collagenase solution. Cells were then teased out of the capsule into Dulbecco's Minimal Medium (DMM) containing 1% Bovine Serum Albumin (BSA), centrifuged at 200 g for 1 minute, resuspended in DMM with BSA, and re-centrifuged. This procedure was repeated, with the cells finally being suspended in DMM containing 10% foetal calf serum, 1 iM dexamethosone, and 0.2 U/ml insulin at a cell density of 1×10^6 cells/1.5 ml. Cells were tested for viability using tryptopan blue. Cells to be used in suspension were taken at this stage at 1×10^6 cells/ml. Otherwise, 1×10^6 cells were plated out and kept at 37°C for 4 hours. They were then washed lightly and 1.5 ml of Ultroser G (a serum substitute in DMM) was added per dish; cells were incubated overnight and used the following day.

Cell incubation and copper uptake determinations: Isolated hepatocytes were incubated in a modified Earle's salts buffer at 20°C under 95% O_2 and 5% CO_2 in a shaking water bath for 5–15 min. $^{64}Cu(II)$ was then added to the cell suspension. Samples were removed at intervals for copper uptake determinations. To remove surface-bound Cu(II), samples were transferred to 10 mM EDTA-0.9% NaCl at 0°C and centrifuged at 0–4°C for 2.5 minutes. The pellet was washed with 10 mM EDTA-0.9% NaCl and recentrifuged. 0.1% sodium dodecyl sulphate in H_2O was added to the pellet, and an aliquot was removed for gamma counting and protein determination. Samples were counted in a gamma scintillation counter, and results were corrected for isotope decay. Protein concentrations were determined using BSA as standard.

Effects of albumin on $^{64}Cu(II)$ uptake: $^{64}Cu(II)$ was added to the cells as the free ion or in the form of $^{64}Cu(II)$.albumin at molar ratios of 5:1, 2:1 or 1:1 Cu(II) to albumin. Duplicate samples were removed at intervals for up to 40 minutes to determine $^{64}Cu(II)$ uptake. To examine the effect of albumin on uptake, initial rates (0.5 min) were measured at $^{64}Cu(II)$ concentrations from 2 to 25 µM with and without 2 µM albumin. Duplicate samples were evaluated for $^{64}Cu(II)$ uptake.

Effect of histidine on coppper uptake in presence of albumin:

Equilibrium mixtures of ^{64}Cu(II), albumin, and L-histidine were prepared before addition to cells. Net uptake was determined at 5 and 10 µM copper plus 20 µM albumin with or without 10 or 50 µM histidine. Duplicate samples were removed at appropriate times.

Effects of various other amino acids on copper uptake: Net uptake of ^{64}Cu(II) was measured in the presence of 20 µM albumin and 50 µM of various amino acids, individually or combined with 50 µM histidine. Selected amino acids were also tested in the absence of albumin. Cu uptake per hour was determined for 6 replicates with each condition.

Effects of Gly-His-Lys on copper transport: ^{64}Cu(II) transport was measured in the presence of Gly-His-Lys with and without albumin and histidine. Net uptake was measured in quadruplicate samples after 60 minutes incubation. The effect of Gly-His-Lys on ^{64}Cu(II) uptake kinetics was also determined (as previously described for albumin) using 2 µM Gly-His-Lys and copper concentrations of 2-25 µM. Quadruplicates were obtained at each copper concentration.

Fractionation of rat plasma: Rat plasma was applied to a column of Sephadex G-25 equilabrated with 0.25 M Tris-HCl at pH 8.0. The column was eluted with the same buffer at 4°C. Protein absorbances at 280 and 220 nm were monitored, as was conductivity. A low molecular weight fraction (≤5000) was tested for its effect on copper uptake after readjusting the pH to 7.4. The concentration of histidine in this fraction was estimated from the conductivity-derived dilution factor and the histidine concentration in plasma of 70 µM.

Cu(II) transport rates from albumin-containing and albumin-free dialysis fractions: Albumin (20 µM) and ^{64}Cu(II) (10 µM) in Earle's buffer were dialysed against histidine-free buffer or buffer containing 20 and 50 µM L-histidine at 4°C for 20 hours. Initial rates of ^{64}Cu uptake (0.5 min) were determined with the albumin-containing and albuminfree fractions at equilibrium.

Transport kinetics of ^{64}Cu(II) from His$_2$Cu(II) complex: Initial rates (0.5 min) were measured at ^{64}Cu(II) concentrations of 1 - 25 µM as free ^{64}Cu(II) or as His$_2$^{64}Cu(II) at the same concentrations. Uptake was determined for quadruplicate samples, the results were shown as means ± SD. Kinetic parameters were determined from least-squares fits to reciprocal data without weighting and nonlinear least-squares fits to the *v* vs. [Cu] data.

Assessing possible transport of copper with histidine in histidine.Cu(II) complexes: Initial rates (0.5 min) of ^{64}Cu(II) uptake at 10 µM ^{64}Cu(II) were measured in Na^+-containing and chlorine-substituted Earle's buffer (histidine transport is known to be Na^+ dependent). L-[^{3}H]histidine with specific activity of 42 Ci/mmol was used in experiments testing for possible transport of both [^{3}H]-histidine and ^{64}Cu(II) from Cu(II).histidine complexes. The labelled histidine was added (50 nCi/ml in the final mixture), and initial rates of histidine uptake were determined at 10 and 20 µM histidine in Na^+- and choline-containing buffers in the presence or absence of 10 µm ^{64}Cu(II). Samples were processed identically to those for copper uptake determinations and counted by scintillation counting and gamma counting. Six samples were assayed with each set, and the results were expressed as means ± SD in nM/minute/mg protein of ^{64}Cu(II) and/or [^{3}H]histidine.

98.2 Results and discussion

Summarize relevant results; discuss dose-response relationship.

Effects of albumin on ^{64}Cu(II) uptake: At equimolar Cu(II) and

albumin, albumin markedly inhibited ^{64}Cu(II) uptake by hepatocytes, and significant inhibition was detected at up to a 10:1 molar excess of Cu(II). Both initial rates and the rate of attaining a steady state were affected in that, at Cu (II):albumin molar ratios of 1:1 or less, net uptake continued after 40 minutes, whereas when copper was in excess, significant net uptake was minimal after 40 minutes.

The effect of albumin on initial rates of ^{64}Cu(II) uptake was examined to determine the mechanism of inhibition. At relatively high Cu concentrations, uptake rates with albumin approached those observed without it. Thus the apparent $_{V_{max}}$ and K_m parameters converged toward values obtained with free Cu. In the presence of albumin, the slope increased dramatically with decreasing total Cu concentration. This type of profile is observed with enzyme inhibitors that act by decreasing the concentration of the reacting substrate. The kinetic results suggest that albumin's principal effect on copper transport is simply to remove Cu(II) from access to the transport system.

Effect of histidine and other amino acids on albumin-inhibited copper uptake: The effect of histidine on albumin-inhibited Cu uptake was examined to determine whether histidine facilitates Cu transport. The Cu concentrations used corresponded to about 0.5 and 1.0 K_m for Cu transport in the absence of albumin; albumin was at 4:1 and 2:1 molar excesses of Cu, respectively. Histidine equimolar to the total Cu increased the rate of Cu uptake; an effect that increased with increasing histidine. However, under all conditions tested, the rates of Cu uptake never exceeded the rates observed with free ^{64}Cu(II) at the same total concentration. The approach to steady state also remained slow, reflecting the relatively low concentrations of Cu.histidine complexes. Thus, at 10 µM Cu(II), 10 µM albumin, and 50 µM histidine, the total ^{64}Cu accumulated at 60 minutes was 0.60 times that for free copper but 1.35 times that obtained with albumin in the absence of histidine.

The relative specificity of histidine was assessed by testing other amino acids that have been isolated from plasma in binary and/or ternary complexes with Cu. Cystine was the only amino acid other than histidine to exert a substantial facilitation effect.

It was concluded that histidine ie the principal plasma component involved in mobilising Cu from albumin.

Effects of Gly-His-Lys on copper uptake: The effect of Gly-His-Lys on ^{64}Cu(II) uptake was similar to that of albumin. Gly-His-Lys markedly inhibited Cu uptake at low Cu(II):Gly-His-Lys ratios, but with increasing Cu the initial uptake rates approached those for free ^{64}Cu(II). Thus, Gly-His-Lys also inhibits Cu transport by decreasing free Cu(II) in solution. The inhibitory effects of albumin and Gly-His-Lys are additive. i.e., at equivalent concentrations, albumin decreased Gly-HisLys-inhibited Cu uptake by the same factor as it decreased the rate of free Cu(II) uptake. Moreover, the facilitation effect of histidine on albumin-inhibited ^{64}Cu(II) uptake was decreased by the inhibitory effect of Gly-His-Lys when transport was measured in the presence of all 3 Cu ligands. Histidine facilitated Gly-His-Lys-inhibited ^{64}Cu(II) uptake by about the same factor as its effect on albumin-inhibited uptake.

It was concluded that Gly-His-Lys inhibit Cu(II) uptake by hepatocytes under conditions in which Gly-His-Lys, histidine and albumin are all in excess of the Cu(II). As the estimated concentration of Gly-His-Lys in human plasma is ~1.7 µM, these are the conditions that prevail *in vivo*.

Effect of low-molecular weight plasma fraction on albumin-inhibited copper uptake: As a more inclusive test for possible facilitators (or inhibitors) of hepatic copper transport in plasma, a low molecular weight fraction of rat plasma was added to an incubation medium that contained 20 μM albumin and 10 μM ^{64}Cu. These are the same concentrations as those used in experiments for assessing the effects of histidine. The facilitation effect of the plasma fraction was equivalent to that of 10 μM histidine. The estimated histidine concentration in the fraction added to the cells was 8 μM. Addition of the the low molecular weight plasma fraction in the absence of albumin resulted in a Cu uptake rate that was the same as that obtained for 10 μM Cu(II) alone.

The results of this experiment confirmed (1) that the facilitating effect of the low molecular weight plasma fraction was largely accounted for by its histidine concentration and (2) the absence of previously undetected strong inhibitors of Cu uptake..

Cu(II).histidine vs. Cu(II).histidine. albumin as active species: An experiment was carried out to determine whether Cu is delivered to hepatocytes complexed to histidine, albumin or within the Cu.histidine.albumin chelate. Albumin, ^{64}Cu(II) and histidine mixtures were dialysed until equilibrium was attained and rates of Cu(II) uptake from albumin-containing and albumin-free fractions were compared. In each case, the initial uptake rates (0.5 min) of fractions containing only free Cu plus excess histidine were the same as those of fractions containing 20μM albumin.

There was, therefore, no evidence for involvement of a direct functional interaction between Cu(II).albumin or His.Cu(II).albumin with hepatocytes. Moreover, Cu(II) does not appear to be rapidly released from albumin due to albumin-hepatic membrane interactions.

Kinetics of copper uptake from $His_2Cu(II)$: The kinetic parameters of histidine.copper complexes were compared with those of free copper. The active species in all experiments in which histidine was in excess of nonalbumin-bound copper was the $His_2Cu(II)$ complex, since this is the predominant species at pH 7.4 at 2:1 and higher molar excesses of histidine. The reciprocal velocity versus reciprocal [$His_2Cu(II)$] plot was linear; v_{max} was identical, while Km (15 ± 0.7 μM) was slightly higher for the ternary complex than for free Cu(II).

It was concluded that the transport kinetic data for the $His_2Cu(II)$ complex relative to that for free Cu(II) are most consistent with $His_2Cu(II)$ interaction with the putative transport protein. However, the relatively small difference between the K_m for the $His_2Cu(II)$ complex and free Cu(II) indicate that specific interactions of histidine with the Cu(II) transport protein are minimal. The fact that V_{max} is identical for uptake of free Cu(II) and $His_2Cu(II)$ is consistent with transport of the free ion in each case, with a ligand-displacement reaction apparently occurring between $His_2Cu(II)$ and the hepatic transport protein prior to actual transport. The identical V_{max} value for the free Cu(II) form also indicates that the rate-limiting step occurs after the ligand displacement reaction.

$His_2Cu(II)$ vs. free ionic copper as transported species: Transport of [^{3}H]histidine and ^{64}Cu(II) was monitored concurrently to determine whether histidine is transported with copper from Cu(II).histidine complexes. Since histidine transport by hepatocytes occurs in part by Na^+-dependent mechanisms, experiments were done in Na^+ and choline media. Cu uptake from free Cu(II), histidine.Cu(II), or $His_2Cu(II)$ was

	identical in Na^+ and choline media, confirming that Cu transport is not Na^+ dependent. In the absence of Cu, uptake of [^{3}H]histidine was negligible in both Na^+ and choline media. No additional transport of [^{3}H]histidine was detected during ^{64}Cu(II) uptake. At 10 µM ^{64}Cu(II).[^{3}H]histidine (1:1), the nanomoles ^{64}Cu per minute per mg protein transported were an order of magnitude higher than the amount of [^{3}H]-histidine transported, and [^{3}H]histidine uptake was unaffected by copper in either Na^+- or choline-containing media. The only detectable effect of copper on histidine transport was a small inhibitory effect of the $His_2Cu(II)$ complex relative to the equivalent concentration of free histidine. These experiments confirm that ^{64}Cu(II) from the $His_2Cu(II)$ complex is transported as the free ion, as concurrent transport of the labelled histidine did not occur.
98.3 Conclusion	These results are consitent with histidine mobilising Cu(II) from albumin by competing for Cu(II), interaction of the $His_2Cu(II)$ complex with the hepatic copper transport protein, and transport of copper as free ionic copper.
98.3.1 Reliability	*Based on the assessment of materials and methods include appropriate reliability indicator 0, 1, 2, 3, or 4* 2
98.3.2 Deficiencies	Yes This study was not conducted and/or reported in strict compliance with the principles of GLP. However, this does not compromise the validity of the data generated, or the author's interpretation of that data, given that the study was not carried out for regulatory purposes. Furthermore, the research was published in a peer-reviewed journal, and has therefore been subject to the prior scrutiny of experts in the field. In addition this report has been included in a number of expert reviews of copper toxicokinetics. No internationally accepted guidelines are available that specifically address the objective of the research presented in this summary. Overall, this is a well-reported study, and its findings are considered to make a valuable contribution to the 'weight of evidence' approach that has been adopted for the purposes of the current review of copper toxicokinetics. A reliability indicator of 2 has been assigned on this basis. *(If yes, discuss the impact of deficiencies and implications on results. If relevant, justify acceptability of study.)*

Evaluation by Competent Authorities

Section A6.2	**Metabolism in mammals**
Annex Point IIA6.2	*Specify section no., heading and species as appropriate*
IUCLID: 5.0/18	**A6.2(18), Cellular and molecular metabolism of copper**

	Use separate "evaluation boxes" to provide transparency as to the comments and views submitted
	EVALUATION BY RAPPORTEUR MEMBER STATE
Date	[redacted]
Materials and Methods	[redacted]
Results and discussion	[redacted]
Conclusion	[redacted]
Reliability	[redacted]
Acceptability	[redacted]
Remarks	[redacted]

	COMMENTS FROM ...
Date	*Give date of comments submitted*

TABLE A6.2(18) – 1 effects of amino acids on albumin-inhibited copper uptake

Condition	Relative Uptake
20 iM Albumin alone	1.00± 0.04
+50 iM Glycine	0.83± 0.06
+50 iM Alanine	0.96± 0.18
+50 iM Lysine	0.91± 0.14
+50 iM Arginine	1.13± 0.18
+50 iM Aspartic Acid	0.96± 0.16
+50 iM Threonine	1.04± 0.10
+50 iM Glutamine	1.04± 0.10
+50 iM Serine	1.00± 0.10
+50 iM Cystine	1.43± 0.14
+50 iM Histidine	2.04± 0.19
+50 iM Histidine + 50 iM threonine	2.13± 0.24
+50 iM Histidine +50iM glutamine	2.09± 0.16
+50 iM Histidine +50iM serine	1.91± 0.27

Relative uptake values (±SD) of 6 replicates were calculated by comparing uptake under each condition (nmol Cu • h^{-1} • mg prot $^{-1}$) to uptake in the presence of 20 iM albumin alone. Hepatocytes were incubated with 20 iM ^{64} Cu (II) plus the indicated potential ligands.

Table A6.2(18)-2. Effects of Gly-His-Lys on copper uptake in presence of albumin and histidine.

Condition	Relative Uptake
10 M Cu(II) alone	1.00± 0.10
+10 iM Albumin	0.44± 0.05
+10 iM Gly-His-Lys	0.54± 0.03
+10 iM Albumin + 5 iM Gly-His-Lys	0.35± 0.04
+10 iM Albumin + 10 iM Gly-His-Lys	0.27± 0.03
+10 iM Albumin + 50 iM Histidine	0.60± 0.08
+10 iM Albumin + 10 iM Gly-His-Lys + 50 iM Histidine	0.45± 0.05
+10 iM Gly-His-Lys + 50 iM Histidine	0.61± 0.03

Relative uptake values (±SD) of 4 replicates were calculated by comparing uptake under each condition (nmol Cu•h^{-1}•mg $prot^{-1}$) to uptake in the presence of 10 iM Cu (II) alone.

Table A6.2(18)-3. Effect of a low-molecular-weight plasma fraction on ^{64}Cu (II) uptake.

Condition	Relative Uptake
10 ìM ^{64}Cu (II) alone	1.00 ± 0.05
+ 20 ìM Albumin	0.13 ± 0.02
+ 20 ìM Albumin + 10 ìM Histidine	0.19 ± 0.02
+ 20 ìM Albumin + 50 ìM Histidine	0.25 ± 0.02
+ 20 ìM Albumin + ≤5,000 fraction	0.18 ± 0.01
10 ìM ^{64}Cu + ≤5,000 fraction	1.09 ± 0.08

Relative uptake value (±SD) of 6 replicated were calculated by comparing uptake under each condition (nmol) Cu·h^{-1} ·mg prot $^{-1}$) with uptake in the presence of 10 µM Cu (II) alone. Low-molecular-weight plasma fraction was isolated by gel-exclusion chromatography of fresh rat plasma as described in MATERIALS AND METHODS.

Table A6.2(18) – 4. Cu(II) transport from an albumin-free dialysis fraction in equilibrium with albumin, copper and histidine.

Condition	Albumin Fraction, nmol Cu·min^{-1}·mg prot^{-1} (x 10^3)	Albumin-Free Fraction, nmol Cu·min^{-1}·mg prot^{-1} (x 10^3)
No histidine	6.4 ± 10	5.7 ± 0.3
+ 20 ìM Histidine	8.5 ± 0.4	7.8 ± 0.2
+50 ìM Histidine	9.8 ± 0.4	9.0 ± 0.3

Values shown are means ± SD of 3 determinations. Ten micromolar ^{64} Cu(II) in Earle's buffer containing 20 ìM albumin was dialyzed at 4°C for 20 h against 10 vol of buffer or buffer containing 20 or 50 ìM histidine. Isolated hepatocytes were then incubated with the albumin-containing and albumin-free fractions to determine the initial rates of ^{64}Cu uptake.

Table A6.2(18) – 5. Effects of Copper on histidine transport.

Species Present	Na^+, nmol ^{64}Cu·min^{-1}· mg prot^{-1}	Choline, nmol ^{4}Cu·min^{-1}· mg prot^{-1}	Na^+, nmol (^{3}H) His· min^{-1}· mg prot^{-1}	Choline nmol (^{3}H) His· min^{-1}· mg prot^{-1}
Cu (II) 10 ìM	0.58 ± 0.06	0.54 ± 0.004		
Histidine, 10 ìM			0.041 ± 0.006	0.038 ± 0.002
Histidine, 20 ìM			0.092 ± 0.010	0.093 ± 0.002
His·Cu(II), 10 ìM	0.51 ± 0.05	0.54 ± 0.02	0.04 ± 0.002	0.035 ± 0.002
His_2·Cu(II), 10 ìM	0.30 ± 0.02	0.30 ± 0.01	0.068 ± 0.002	0.074 ± 0.004

Initial rates of copper uptake represent means ± SD for 6 determinations. Hepatocytes were incubated with the indicated species in both Na^+-containing and choline-substituted Earle's salts buffer.

Table A6.2(18) – 6.

TABLE 6. *Effects of glutamine, threonine, and asparagine on copper uptake*

Additions	Relative Uptake
10 μM Cu(II) alone	1.00 ± 0.10
+20 μM His	0.64 ± 0.08
+20 μM Gln	0.69 ± 0.08
+20 μM Thr	0.73 ± 0.09
+20 μM Asn	0.91 ± 0.11
+10 μM His + 10 μM Gln	0.87 ± 0.11
+10 μM His + 10 μM Thr	0.85 ± 0.11
+10 μM His + 10 μM Asn	0.87 ± 0.12
+10 μM His + 10 μM cystine	1.10 ± 0.08

Relative uptake values (±SD) of 6 replicates were calculated by comparing uptake under each condition (nmol $Cu \cdot h^{-1} \cdot mg\ prot^{-1}$) with uptake in the presence of 20 μM Cu(II) alone. Hepatocytes were incubated with the indicated copper ligands.

Figure A6.2(18)-1

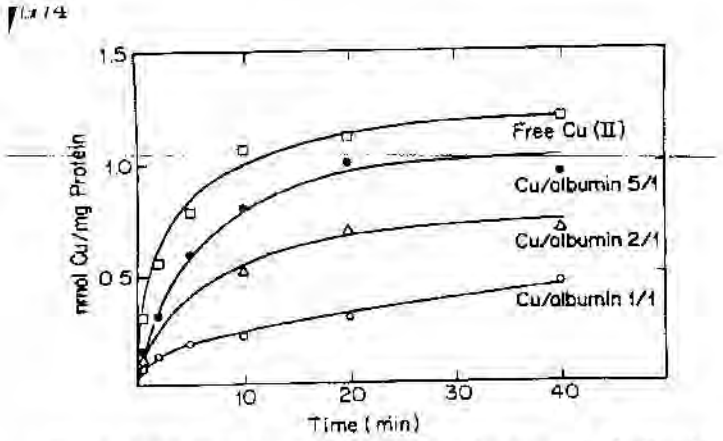

FIG. 1. Time dependence of ^{64}Cu uptake in presence of albumin. Isolated rat hepatocytes were incubated at 20°C with 10 μM $^{64}Cu(II)$ in presence of albumin at a copper-to-albumin ratio of 1:0 (□), 5:1 (●), 2:1 (△), and 1:1 (○). Each *point* represents mean of duplicate determinations.

Figure A6.2(18)-2

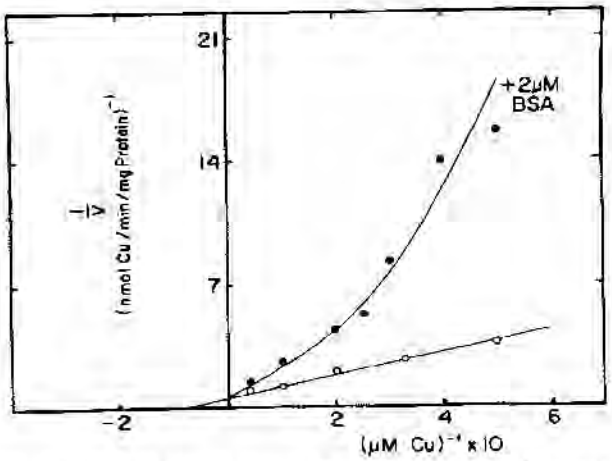

FIG. 2. Effect of bovine serum albumin (BSA) on ^{64}Cu uptake kinetics. Initial rates (1 min) of $^{64}Cu(II)$ uptake by isolated rat hepatocytes were measured at indicated $^{64}Cu(II)$ concentrations in absence (○) and presence (●) of 2 μM albumin. Each *point* represents mean of duplicate determinations.

Figure A6.2(18)-3

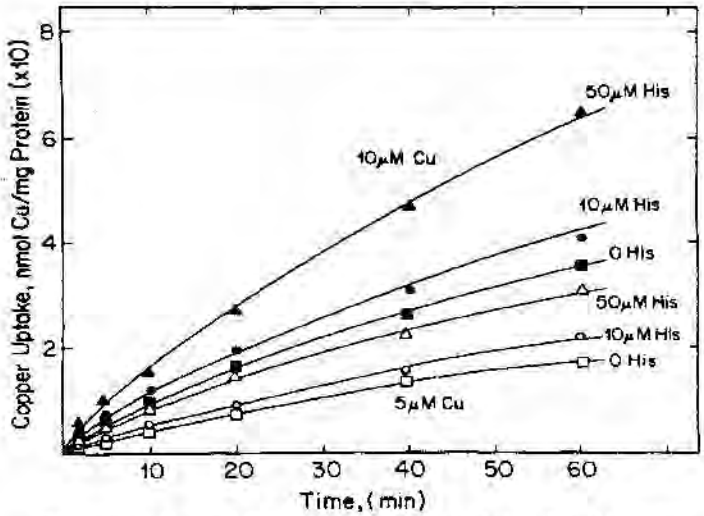

FIG. 3. Effect of histidine on albumin-inhibited ^{64}Cu(II) uptake. Cells were incubated at 20°C with 5 μM (*open symbols*) and 10 μM (*closed symbols*) ^{64}Cu. Albumin was added at 20 μM to incubation buffer. Uptake of ^{64}Cu was measured in presence of 0 histidine (*squares*), 10 μM histidine (*circles*), and 50 μM histidine (*triangles*). Each *point* represents mean of duplicate determinations.

Figure A6.2(18)-4

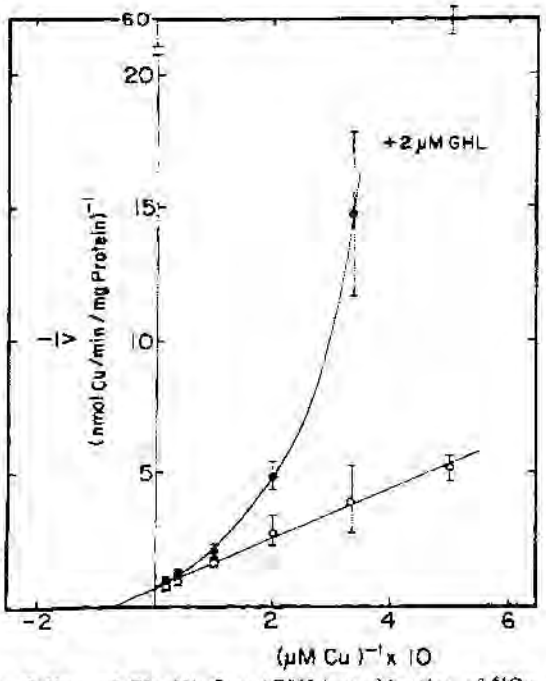

FIG. 4. Effect of Gly-His-Lys (GHL) on kinetics of ^{64}Cu uptake. Initial rates of ^{64}Cu(II) uptake by hepatocytes were measured in absence (○) and presence (●) of 2 μM Gly-His-Lys. Each *point* represents mean ± SD of 6 determinations.

Figure A6.2(18)-5

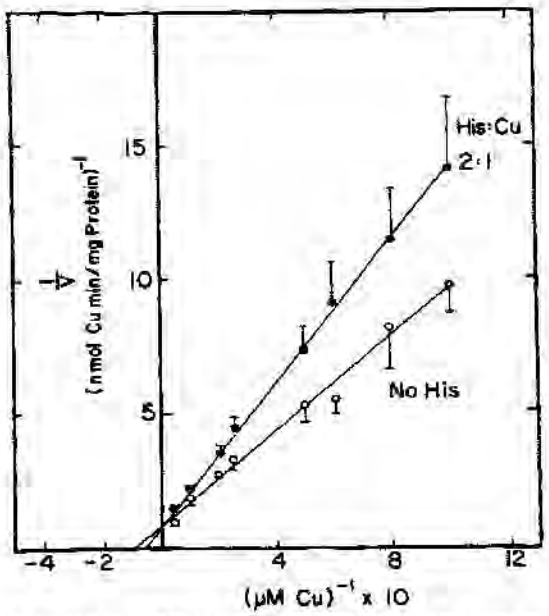

FIG. 5. Kinetics of ^{64}Cu(II) uptake from $His_2Cu(II)$ complex. Initial rates (0.5 min) of ^{64}Cu(II) uptake by hepatocytes were measured from free ^{64}Cu(II) (○) and $His_2Cu(II)$ complex (●) at indicated copper concentrations. Each *point* represents mean ± SD of 4 determinations.

Official use only

99 REFERENCE

1.1 Reference

Author(s), year, title, laboratory name, laboratory report number, report date (if published, list journal name, volume: pages)
If necessary, copy field and enter other reference(s).

McArdle, H.J., Gross S.M., Danks D.M. & Wedd, A.G. (1990). Role of Albumin's Copper Binding Site in Copper Uptake by Mouse Hepatocytes. Am. J. Physiol. **258 (Gastrointest. Liver Physiol. 21)**: 988-991 (published).

1.2 Data protection

No
(indicate if data protection is claimed)

1.2.1 Data owner

Give name of company

Public domain

1.2.2 Criteria for data protection

Choose one of the following criteria (see also TNsG on Product Evaluation) and delete the others: No data protection claimed

100 GUIDELINES AND QUALITY ASSURANCE

100.1 Guideline study

No. This was a non-regulatory study carried out to investigate the molecular mechanism responsible for the high-affinity cellular uptake of copper in mouse hepatocytes. No guidelines are available to address this objective.
(If yes, give guidelines; if no, give justification, e.g. "no guidelines available" or "methods used comparable to guidelines xy")

100.2 GLP

No. This was a non-regulatory study.
(If no, give justification, e.g. state that GLP was not compulsory at the time the study was performed)

100.3 Deviations

Yes. Refer to section 5.3.2 for a general discussion of deviations and deficiencies.

(If yes, describe deviations from test guidelines or refer to respective field numbers where these are described, e.g. "see 3.x.y")

101 MATERIALS AND METHODS

In some fields the values indicated in the EC or OECD test guidelines are given as default values. Adopt, change or delete these default values as appropriate.

101.1 Test material

^{64}Cu

101.1.1 Lot/Batch number

Not available

101.1.2 Specification

Deviating from specification given in section 2 as follows
(describe specification under separate subheadings, such as the following; additional subheadings may be appropriate):

101.1.2.1	Description	*If appropriate, give e.g. colour, physical form (e.g. powder, grain size, particle size/distribution)* Not available
101.1.2.2	Purity	*Give purity in % of active substance* [redacted]
101.1.2.3	Stability	*Describe stability of test material* Not applicable
101.1.2.4	Radiolabelling	*give structural location of radio labelling, give reason if not labelled* ^{64}Cu (obtained from the Australian Nuclear Science and Technology Organisation; initial specific activity 160 mCi/mg).
101.2 Test Animals		*Non-entry field*
101.2.1 Species		Mouse
101.2.2 Strain		ARC mice
101.2.3 Source		Animal Resource Center, Perth, Western Australia
101.2.4 Sex		Female
101.2.5 Age		Adult
101.3 Procedures		Non-entry field
101.3.1 Hepatocyte isolation		The livers of adult female ARC mice were perfused with a washing solution and then with a collagenase-containing buffer. The cells were teased out of the capsule, only easily separated cells being taken. The isolated cells were washed with Dulbecco's minimal medium with 1% bovine serum albumin and allowed to settle on collagen-coated dishes for 4 hours. Loosely attached and dead cells were then washed off, and the cells were incubated overnight and used the next day.
101.3.2 Experimental		The cells were washed three times in Hank's balances salt solution (HBSS), prepared with Ultrapure chemicals to keep copper levels as low as possible, and the appropriate incubation medium was added. After incubation, the cells were washed three times in phosphate-buffered saline (PBS) to remove loosely bound copper, and 1 ml of 1 mg/ml ice-cold Pronase was added. The cells were incubated on ice for 30 minutes and aspirated using a Pasteur pipette. They were transferred to Microfuge tubes, centrifuged at full speed in a Beckman Microfuge for 20 seconds, and the supernatant was removed and counted. The pellet was resuspended in 1 ml PBS, transferred to clean tubes, and ultrasonicated. A 100 µl portion was removed for DNA analysis, and the remainder was counted together with the supernatant. The counts from the supernatant and pellets were combined to give the total radioactivity associated with the cell. The incubation medium (Earle's balanced salt solution containing 10% foetal bovine serum with either 2 or 200 µM BSA added, as appropriate) was adjusted to the appropriate pH using HCl. ^{64}Cu was added to give a starting concentration of 1 µCi/ml (total Cu concentration range between 1.2 and 2.3 µM, measured by atomic absorption spectrophotometry), and the medium was then taken to pH 7.4 as soon as possible using NaOH. In the experiments with dog protein, dog albumin was added instead of BSA. Therefore, in the low concentration, there would still be an excess of bovine protein in the

culture medium.

For electron spin resonance (ESR), 1 mM solutions of human or bovine serum albumin were mixed with equimolar amounts of copper added at the appropriate pH as described above, and the spectra were measured within 30 minutes.

101.3.3 Analytical

Copper levels in media and tissues were assayed using either flame or graphite furnace atomic absorption spectrophotometry (AAS) as appropriate in a Perkin-Elmer (PE 5000) spectrophotometer. Gamma counting was performed on a Packard gamma-counter with automatic decay correction and background subtraction.

The DNA assay was carried out as follows: Aliquots of the sonicated cells (0.1 ml) were dried in an oven at 40°C overnight and resuspended in 100 µl diaminobenzoic acid (0.4 mg/ml). The tubes were incubated at 50°C for 1 hour, and the reaction stopped by the addition of 1.5 ml 1M HCl. The tubes were read in a fluorometer at an excitation wavelength of 420 nm, and an emission wavelength of 510 nm.

ESR spectra were recorded at 77K on a Varian E-9 spectrometer operating at X-band with 100 kHz modulation. The spectra were calibrated with diphenylpicrylhydrazyl.

102 RESULTS AND DISCUSSION

Describe findings. If appropriate, include table. Sample tables are given below.

102.1 Results

Figure A6.2(19)-1 shows ESR spectra for copper-albumin (CuAlb) where equimolar copper was added to albumin that had previously been taken to pH 5.5 and then raised to 7.4. CuAlb labelled at pH 5.5 and then raised to 7.4 showed a single class of site, whereas the spectrum of CuAlb labelled at 7.4 showed at least two binding sites. The second class was evidenced by the peaks at 2,780 and 2,980 G and the smoothing of the large peak at 3,100 G. From the areas under the curves, it was estimated that the non-specific fraction was ~10% of total copper bound. Similar data was obtained at ratios as low as 0.5:1. It was assumed that the albumin labelled at pH 5.5 represented only specifically bound copper, and that labelled at pH 7.4 represented a mixture of specifically bound and non-specifically bound copper.

Figure A6.2(19)-2 shows the effect of incubating hepatocytes with pH 5.5 or 7.4 labelled albumin. Uptake was higher from the pH 5.5 labelled albumin than from the 7.4 labelled protein (**Figure A6.2(19)-2A**). The effect was insignificant when the protein-to-metal ratio became much higher (**Figure A6.2(19)-2B**). This was attributed to the fact that at these higher ratios, more of the copper would have been bound by the specific site. It is considered possible that, given sufficient time, the ^{64}Cu added at pH 7.4 would also equilibrate to the specific site. To test whether this was the case, ^{64}Cu was incubated with albumin at pH 7.4 overnight before adding to the hepatocytes.

Measuring ^{64}Cu uptake within 0.5 hour after adding the ^{64}Cu to the albumin at pH 5.5 gave levels of 4.36 ± 0.21 pmol. µg DNA^{-1}. 40 min^{-1} (n = 3), whereas uptake from pH 7.4 labelled CuAlb was 1.8 ± 0.07 pmol. µg DNA^{-1}. 40 min^{-1} ($P < 0.001$). After overnight incubation, uptake from the pH 7.4 CuAlb increased to 2.3 ± 0.15 pmol. µg DNA^{-1}. 40 min^{-1}, whereas uptake from the pH 5.5 labelled protein was 3.12 ± 0.13 pmol. µg DNA^{-1}. 40 min^{-1}. These results were still significantly

different ($P < 0.005$) but were closer together than the first set, suggesting that an equilibrium was being approached.

The effect of histidine on uptake of copper located on albumin's specific binding site was investigated. **Figure A6.2(19)-3** shows that histidine increased uptake by the cells and that the degree of difference between pH 7.4 and 5.5 labelled protein remained similar at all concentrations. When the experiment was performed with a high-protein concentration, the difference decreased and became non-significant.

The effect of labelling pH on the uptake of copper from dog albumin was studied (dog albumin lacks the specific binding site). Dog albumin was added to the incubation medium containing the 10% fœtal calf serum (FCS), and the pH was altered as described above. The ^{64}Cu was then added, and the pH was altered as appropriate. At 2 μM dog albumin, at low-histidine concentrations, there may be some stimulation of uptake. This may be related to the high ratio of FCS to dog protein. The difference disappeared at 200 μM albumin (**Figure A6.2(19)-4**).

Most exchangable copper in serum is likely to be in the form of a ternary complex with histidine and albumin. Because histidine further stimulates uptake of ^{64}Cu, it is considered feasible that the ternary complex forms the preliminary association with the cell.

Experiments were carried out with mouse hepatocytes using varying concentrations of ^{64}Cu copper, ^{125}I-labelled albumin and [^{3}H] histidine at 4°C. It was not possible to demonstrate any specificity of binding of either albumin or [^{3}H] histidine, as it related to copper binding.

102.2 Discussion

Albumin was shown to have a specific binding site for copper as far back as the 1950s. It is postulated that this may act as a recognition site for the liver membrane copper transport protein. It is possible in vitro to label albumin with copper either exclusively on the specific binding site or partly on the specific site and also on other sites by altering the pH at which the two ligands are mixed.

It was found that, when all the copper is bound to the specific site, by adjusting the pH to 5.5, uptake is increased over that occurring at pH 7.4. The difference between the two pH treatments was found to decrease as the protein-to-metal ratio increased. This was because of an increase in the amount of copper on the specific binding site as the amount of protein increased. Furthermore, overnight as opposed to short-term incubation of the copper and albumin at pH 7.4, which resulted in more copper being attached to the specific site, also resulted in an increase in uptake. These results strongly support the hypothesis that copper in serum is attached to the specific binding site on albumin.

Additional histidine was found to stimulate uptake of copper, irrespective of the copper binding site on albumin. This effect is considered to be related to the histidine on position 3 of the albumin, as it is not seen when dog albumin is labelled under the same conditions.

The data suggest that cells recognise and bind copper-albumin (CuAlb) complex, but may preferentially recognise the ternary complex formed by Cu Alb and histidine. It is suggested that, *in vivo*, copper is bound mainly as the ternary complex and that the structure formed, similar to that formed by a copper-histidine complex, is what is recognised by the cell. After binding, the albumin and histidine are released and copper is transported across the membrane. If the copper cannot be transported (as occurs when cells are incubated at 4°C), then further binding of the ternary complex is blocked.

103 APPLICANT'S SUMMARY AND CONCLUSION

103.1 Materials and methods

Give concise description of method; give test guidelines no. and discuss relevant deviations from test guidelines.

A study was carried out to investigate the molecular mechanism responsible for the high-affinity cellular uptake of copper in mouse hepatocytes. The study was not designed to follow internationally accepted guidelines, and was not carried out or reported in compliance with GLP. The following techniques were used:

Hepatocyte isolation: Livers of adult female ARC mice were perfused with a washing solution and then with a collagenase-containing buffer. After isolation, cells were washed with Dulbecco's minimal medium with 1% BSA and allowed to settle on collagen-coated dishes for 4 hours. Loosely attached and dead cells were washed off, and the cells were incubated overnight for use the next day.

Experimental: Cells were washed 3 times in Hank's balanced salt solution (HBSS), and the appropriate incubation medium was added. After incubation, cells were washed 3 times in PBS to remove loosely bound copper, and 1 ml of 1 mg/ml ice-cold Pronase was added. Cells were incubated on ice for 30 minutes and aspirated using a Pasteur pipette. They were then centrifuged at full speed in a Beckman Microfuge for 20 seconds and the supernatant was removed and counted. The pellet was resuspended in 1 ml PBS and ultrasonicated. A portion was removed for DNA analysis, and the remainder was counted together with the supernatant. Counts from the supernatant and pellets were combined to give total radioactivity associated with the cell.

The incubation medium (Earle's balanced salt solution containing 10% foetal bovine serum with either 2 or 200 µM BSA added) was adjusted to the appropriate pH using HCl. ^{64}Cu was added to give a starting concentration of 1 µCi/ml, and the medium was then taken to pH 7.4 using NaOH. In experiments with dog protein, dog albumin was added instead of BSA. In the low concentration, there would still be an excess of bovine protein in the culture medium.

For electron spin resonance (ESR), 1 mM solutions of human or bovine serum albumin were mixed with equimolar amounts of Cu added at the appropriate pH. Spectra were measured within 30 minutes.

Analytical Copper levels in media and tissues were assayed using either flame or graphite furnace AAS. Gamma counting was performed on a counter with automatic decay correction and background subtraction.

The DNA assay was carried out as follows: Aliquots of sonicated cells were dried in an oven at 40°C overnight and resuspended in diaminobenzoic acid (0.4 mg/ml). Tubes were incubated at 50°C for 1 hour, and the reaction stopped by the addition of 1M HCl. Tubes were read in a fluorometer at an excitation wavelength of 420 nm, and an emission wavelength of 510 nm.

ESR spectra were recorded at 77K on a Varian E-9 spectrometer operating at X-band with 100 kHz modulation. The spectra were calibrated with diphenylpicrylhydrazyl.

103.2 Results and discussion

Summarize relevant results; discuss dose-response relationship.

ESR spectra for Cu-albumin (CuAlb) where equimolar Cu was added to albumin that had previously been taken to pH 5.5 and then raised to 7.4 showed a single class of site, whereas the spectrum of CuAlb labelled at

	7.4 showed at least two binding sites. From the areas under the curves, it was estimated that the non-specific fraction was ~10% of total Cu bound. Similar data were obtained at ratios as low as 0.5:1. It was assumed that the albumin labelled at pH 5.5 represented only specifically bound copper, and that labelled at pH 7.4 represents a mixture of specifically bound and non-specifically bound copper. Effects of incubating hepatocytes with pH 5.5 or 7.4 labelled albumin were investigated. Uptake was higher from the pH 5.5 labelled albumin than from pH 7.4 labelled protein. The effect was insignificant when the protein-to-metal ratio became much higher. This was attributed to the fact that at these higher ratios, more of the copper would have been bound by the specific site. It was considered that, given sufficient time, ^{64}Cu added at pH 7.4 would also equilibrate to the specific site. To test whether this was the case, ^{64}Cu was incubated with albumin at pH 7.4 overnight before adding to hepatocytes. Measuring ^{64}Cu uptake within 0.5 hour after adding ^{64}Cu to albumin at pH 5.5 gave levels of 4.36 ± 0.21 pmol. µg DNA^{-1}. 40 min^{-1}, whereas uptake from pH 7.4 labelled CuAlb was 1.8 ± 0.07 pmol. µg DNA^{-1}. 40 min^{-1}. After overnight incubation, uptake from the pH 7.4 CuAlb increased to 2.3 ± 0.15 pmol. µg DNA^{-1}. 40 min^{-1}, whereas uptake from the pH 5.5 labelled protein was 3.12 ± 0.13 pmol. µg DNA^{-1}. 40 min^{-1}. These results suggested that an equilibrium was being approached, with more copper being attached to the specific binding site on albumin. The effect of histidine on uptake of copper located on albumin's specific binding site was investigated. It was found that histidine increased uptake by cells and that the degree of difference between pH 7.4 and 5.5 labelled protein remained similar at all concentrations. When the experiment was performed with a high-protein concentrations, the difference decreased and became non-significant. The effect of labelling pH on the uptake of Cu from dog albumin was studied (dog albumin lacks the specific Cu-binding site). Dog albumin was added to the incubation medium containing the 10% foetal calf serum (FCS), and the pH was altered as described above. ^{64}Cu was then added, and the pH was altered as appropriate. At 2 µM dog albumin and low-histidine concentrations, there may have been some stimulation of uptake. This may have been related to the high ratio of FCS to dog protein. The difference disappeared at 200 µM albumin. Experiments were carried out with mouse hepatocytes using varying concentrations of ^{64}Cu copper, ^{125}I-labelled albumin and [^{3}H]-histidine at 4°C. It was not possible to demonstrate any specificity of binding of either albumin or [^{3}H] histidine, as it related to copper binding. The data suggest that cells recognise and bind copper-albumin (CuAlb) complex, but may preferentially recognise the ternary complex formed by Cu Alb and histidine. It is suggested that, *in vivo*, copper is bound mainly as the ternary complex and that the structure formed is what is recognised by the cell. After binding, the albumin and histidine are released and copper is transported across the membrane; it was not possible to detect concomitant binding of either histidine or albumin, probably because the turnover on cell receptor sites is very rapid and the sites cannot bind the complex once the copper has been released. If the copper cannot be transported (as occurs when cells are incubated at 4°C), then further binding of the ternary complex is blocked.
103.3 Conclusion	It is suggested that, *in vivo*, hepatocytes recognised and bind copper

	mainly as part of a ternary complex with albumin and histidine. After binding, the albumin and histidine are released and the copper is transported across the membrane.
103.3.1 Reliability	*Based on the assessment of materials and methods include appropriate reliability indicator 0, 1, 2, 3, or 4* 2
103.3.2 Deficiencies	Yes This study was not conducted and/or reported in strict compliance with the principles of GLP, and experimental details have been omitted on a number of occasions. However, this does not necessarily compromise the validity of the data presented, or the author's interpretation of those data, given that the study was not carried out for regulatory purposes. Furthermore, the research was published in a peer-reviewed journal, and has therefore been subject to the prior scrutiny of experts in the field. In addition, this report has been included in a number of expert reviews of copper toxicokinetics. No internationally accepted guidelines are available that specifically address the objective of the research presented in this summary. Overall, this is an adequately-presented study, and its findings are considered to make a valuable contribution to the 'weight of evidence' approach that has been adopted for the purposes of the current review of copper toxicokinetics. A reliability indicator of 2 has been assigned on this basis. *(If yes, discuss the impact of deficiencies and implications on results. If relevant, justify acceptability of study.)*

Evaluation by Competent Authorities	
Use separate "evaluation boxes" to provide transparency as to the comments and views submitted	
EVALUATION BY RAPPORTEUR MEMBER STATE	
Date	[redacted]
Materials and Methods	[redacted]
Results and discussion	[redacted]
Conclusion	[redacted]
Reliability	[redacted]
Acceptability	[redacted]
Remarks	

COMMENTS FROM ...	
Date	*Give date of comments submitted*

Figure A6.2(19)-1

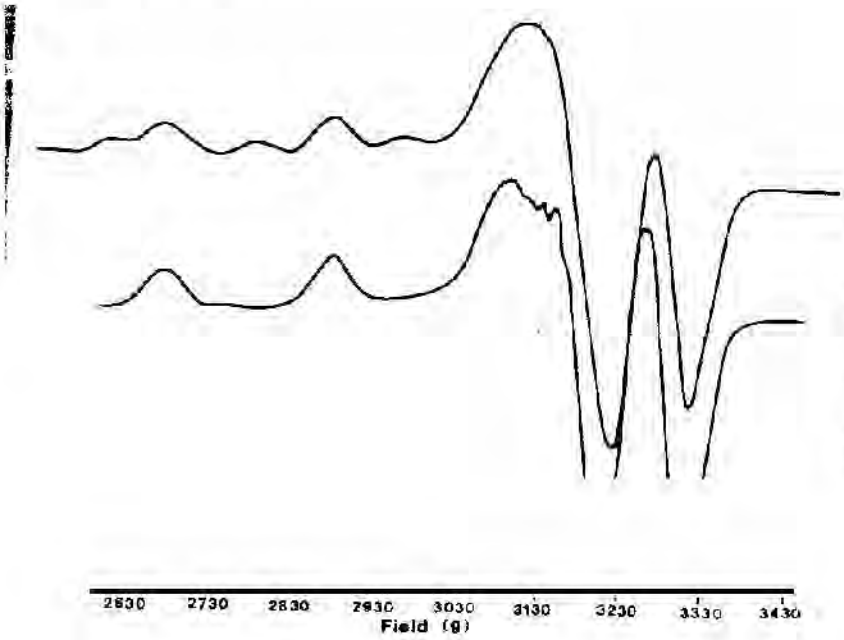

FIG. 1. *Top trace*: ESR spectrum of 1 mM copper bovine serum albumin (CuBSA) in phosphate-buffered saline (PBS). Metal and protein were mixed at pH 7.4 and frozen in liquid nitrogen. pH was measured before and after measurement and was found not to have altered significantly. Modulation amplitude was 10 G, and microwave power was 1 mW. *Bottom trace*: ESR spectrum of 1 mM BSA in PBS. Metal and protein were mixed at pH 5.5, and pH was adjusted to 7.4 before freezing. Modulation amplitude was 10 G and microwave power was 1 mW.

Figure A6.2(19)-2

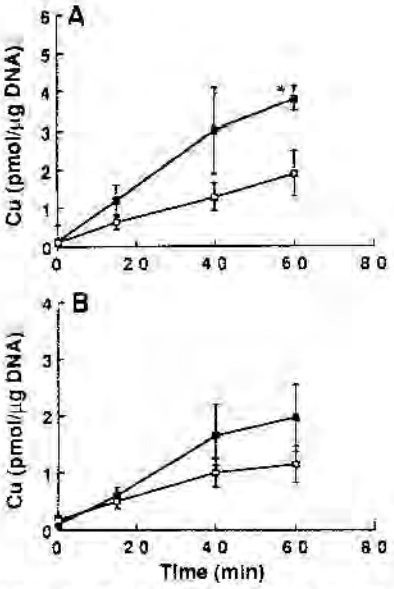

FIG. 2. *A*: Effect of pH of labeling of 2 μM added albumin (final concentration ~62 μM) on ^{64}Cu (~2 μM) uptake by hepatocytes. * $P < 0.01$ (Student's t test). *B*: effect of pH of labeling of 200 μM added albumin (final concentration ~260 μM) on ^{64}Cu (~2 μM) uptake by hepatocytes. There was no significant difference between the 2 conditions as measured by Student's t test. For both *A* and *B*: incubation media were treated as described in MATERIALS AND METHODS. ■, Uptake from albumin labeled initially at 5.5; □, data obtained from protein labeled at pH 7.4. Each point is mean ± SE of 5 plates.

Figure A6.2(19)-3

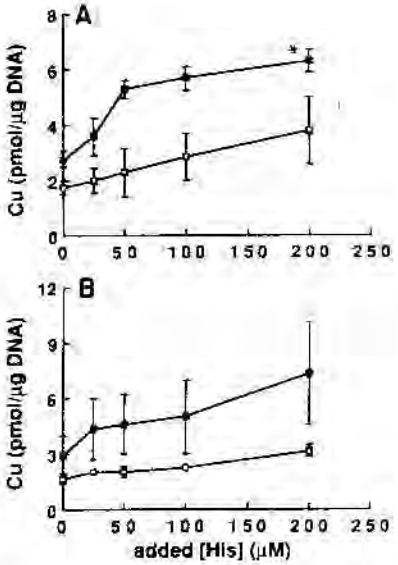

FIG. 3. Effect of added histidine on ^{64}Cu (~2 μM) uptake from 62 μM (*A*) and 260 μM (*B*) ^{64}Cu-labeled albumin labeled at either pH 5.5 (■) or pH 7.4 (□). Cells were incubated for 30 min before being washed and treated as described in MATERIALS AND METHODS. Results are means ± SE of 6 plates. * $P < 0.02$ (Student's *t* test).

Figure A6.2(19)-4

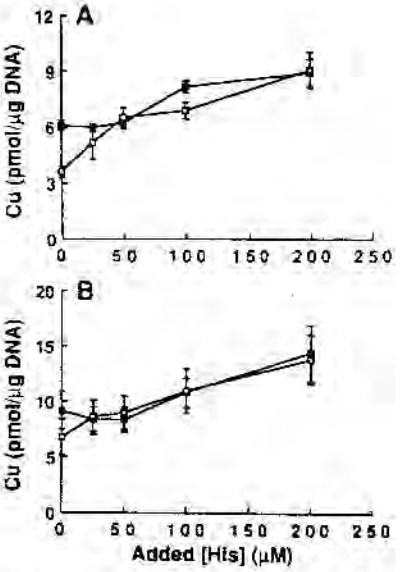

FIG. 4. Effect of added histidine on ^{64}Cu (~2 μM) uptake from 2 μM (*A*) or 200 μM (*B*) dog albumin in 60 μM ^{64}Cu-labeled BSA at either pH 5.5 (■) or pH 7.4 (□). Cells were incubated for 30 min before being washed and treated as described in MATERIALS AND METHODS. Results are means ± SE of 5 plates in 2 separate experiments.

Official use only

104 REFERENCE

1.1 Reference

Author(s), year, title, laboratory name, laboratory report number, report date (if published, list journal name, volume: pages) If necessary, copy field and enter other reference(s).

Whitaker, P. & McArdle, H.J. (1997). Iron Inhibits Copper Uptake by Rat Hepatocytes by Down-Regulating the Plasma Membrane NADH Oxidase. In. Fisher, P.W., L'Abbe, M.R., Cockell, K.A. et al. (Eds). Trace Elements in Man and Animals. (TEMA9). NRC Research Press, Ottowa, pp 237-239 (published).

1.2 Data protection

No
(indicate if data protection is claimed)

1.2.1 Data owner

Give name of company

Public domain

1.2.2 Criteria for data protection

Choose one of the following criteria (see also TNsG on Product Evaluation) and delete the others: No data protection claimed

105 GUIDELINES AND QUALITY ASSURANCE

105.1 Guideline study

No. This was a non-regulatory study carried out to test the hypothesis that increased iron inhibits copper uptake into the hepatocyte. No guidelines are available to address this objective.
(If yes, give guidelines; if no, give justification, e.g. "no guidelines available" or "methods used comparable to guidelines xy")

105.2 GLP

No. This was a non-regulatory study.
(If no, give justification, e.g. state that GLP was not compulsory at the time the study was performed)

105.3 Deviations

Yes. Refer to section 5.3.2 for a general discussion of deviations and deficiencies.

(If yes, describe deviations from test guidelines or refer to respective field numbers where these are described, e.g. "see 3.x.y")

106 MATERIALS AND METHODS

In some fields the values indicated in the EC or OECD test guidelines are given as default values. Adopt, change or delete these default values as appropriate.

106.1 Test material

Refer to section 3.3

106.1.1 Lot/Batch number

Not applicable

106.1.2 Specification

Deviating from specification given in section 2 as follows
(describe specification under separate subheadings, such as the following; additional subheadings may be appropriate):

106.1.2.1	Description	*If appropriate, give e.g. colour, physical form (e.g. powder, grain size, particle size/distribution)* Not applicable
106.1.2.2	Purity	*Give purity in % of active substance* [redacted]
106.1.2.3	Stability	*Describe stability of test material* Not applicable
106.1.2.4	Radiolabelling	*give structural location of radio labelling, give reason if not labelled* Not appropriate to the current study.
106.2 Test Animals		*Non-*entry *field*
106.2.1 Species		Rat
106.2.2 Strain		Not available
106.2.3 Source		Not available
106.2.4 Sex		Male
106.2.5 Weight		250 – 400 g
106.3 Procedures		Non-entry field.
106.3.1 Hepatocyte isolation		Hepatocytes were isolated from male hooded rats as follows : The livers of test animals were perfused with 40 ml of 0.63 mM EGTA in perfusion buffer and then washed with 15 ml perfusion buffer followed by 60 ml collagenase solution. The cells were teased out of the capsule, only easily separated cells being taken, into 25 ml of Dulbecco's Minimal Medium (DMM) containing 1% Bovine Serum Albumin (BSA). The cells were centrifuged at 200 g for 1 minute, re-suspended in the DMM with BSA, and re-centrifuged. The procedure was repeated with the cells finally being suspended in DMM containing 10% foetal calf serum, 1 iM dexamethosone, and 0.2 U/ml insulin at a cell density of 1 x 10^6 cells/1.5 ml. The cells were tested for viability using tryptopan blue. If the cells were to be used in suspension, they would be taken at this stage at 1 x 10^6 cells/ml. Otherwise, 1 x 10^6 cells were plated onto 2.5 cm diameter culture dishes and kept at 37°C for 4 hours. The cells were then washed lightly to remove loosely attached debris and dead cells, and 1.5 ml of Ultroser G, a serum substitute in DMM was added per dish; the cells were incubated overnight and used the following day.
106.3.2 Experimental procedure		Cells were loaded with iron by incubating overnight with iron saturated transferrin (FeTf). Cells incubated overnight were washed three times in Hank's Balanced Salt Solution and the appropriate incubation medium was added. After incubation, the cells were washed three times in phosphate-buffered saline (PBS) to remove loosely-bound copper and 1 ml of 1mg/ml ice-cold pronase was added. The cells were incubated on ice for 30 minutes and aspirated using a Pasteur pipette. They were transferred to Microfuge tubes, centrifuged at full speed in a Beckman Microfuge for 20 seconds, and the supernatant was removed and counted. Cu in the supernatant was regarded as representing the "surface-bound" (pronase-sensitive) compartment. The pellet was re-suspended in 1 ml PBS and ultrasonicated; 100 il was removed for

DNA analysis and the remainder was put into clean tubes and counted. Cu counted in the pellet was regarded as representing the "internalised" (pronase-resistant) compartment.

The cells used in this study were incubated in balanced salt solution containing 10% FCS. Cu levels in the incubation media were measured using either flame or graphite furnace atomic absorption spectroscopy.

106.3.3 DNA analysis

0.1 ml aliquots of sonicated cells were dried overnight in an oven at 40°C and re-suspended in 100µl diaminobenzoic acid (0.4 mg/ml). Tubes were incubated at 50°C for 1 hour, and the reaction stopped with 1.5 ml 1M HCl. The tubes were read in a fluorometer at an excitation wavelength of 420 nm, and an emission wavelength of 510 nm.

106.3.4 NADH oxidase activity

Cell surface NADH oxidase activity was measured by adding 0.15 mmol/L NADH in BSS containing 1 mmol/L KCN to the washed cells. The rate of oxidation was calculated using an absorption co-efficient of 6.21×10^{-3} cm^{-1} mM^{-1}.

107 RESULTS AND DISCUSSION

Describe findings. If appropriate, include table. Sample tables are given below.

107.1 Results

Loading the cells with iron decreased the rate of Cu uptake by the hepatocytes, while levels of Cu associated with the cell surface increased. Increasing iron resulted in an increase in K_m, the apparent affinity for uptake (**Figure A6.2(20)-1a**) ($p < 0.05$), and a minor decrease in $_{Vmax}$ (**Figure A6.2(20)-1b**). In contrast, iron caused an increase in $_{Bmax}$ (**Figure A6.2(20)-1c**), the maximum surface binding value for Cu, without any change in the $_{K0.5}$. The data suggested that copper was binding to its transporter, but that, in the presence of iron, a condition necessary for uptake was not being fulfilled. It was considered that this condition was the reduction of Cu(II) to Cu(I) by the plasma membrane NADH oxidase. **Figure A6.2(20)-2** shows that loading of cells with iron dramatically decreases NADH oxidase activity. The effect cannot be reversed by adding NADH, which indicates that there is no competition for the active site of the enzyme.

107.2 Discussion

The results of this study indicate the importance of NADH oxidase enzyme in the transport of copper across the hepatocyte membrane. It is proposed that oxidation of NADH provides the electron necessary for reduction of Cu(II) on CuHis2 to Cu(I), which results in the release of Cu from its complex and uptake by the hepatocyte. The fact that changes in NADH oxidase activity are mirrored by changes in copper uptake is considered to demonstrate strong support for this proposal. The second conclusion is that copper uptake by the hepatocyte is regulated by iron levels within the cell.

108 APPLICANT'S SUMMARY AND CONCLUSION

108.1 Materials and methods

Give concise description of method; give test guidelines no. and discuss relevant deviations from test guidelines

A study was carried out to test the hypothesis that increased iron inhibits copper uptake into the hepatocyte. The study was not designed to follow internationally accepted guidelines, and was not carried out or reported in compliance with GLP. The following techniques were used:

Hepatocyte isolation: Hepatocytes were isolated from male hooded rats

(250 – 400 g) as follows: Livers of test animals were perfused with 0.63 mM EGTA in perfusion buffer, and washed with perfusion buffer and then collagenase solution. Cells were teased out of the capsule into Dulbecco's Minimal Medium (DMM) containing 1% BSA.

Cells were centrifuged at 200 g for 1 minute, re-suspended in DMM with BSA, and re-centrifuged. The procedure was repeated, with cells finally being suspended in DMM containing 10% foetal calf serum, 1 iM dexamethosone, and 0.2 U/ml insulin at a density of 1 x 10^6 cells/1.5 ml. Cells were tested for viability using tryptopan blue. 1 x 10^6 cells were plated out and kept at 37°C for 4 hours. Cells were then washed lightly and 1.5 ml of Ultroser G, a serum substitute, in DMM was added per dish. These cells were incubated overnight for use the next day.

Experimental procedure: Cells were loaded with iron by incubating overnight with iron-saturated transferrin (FeTf). Cells were then washed 3 times in Hank's Balanced Salt Solution, and the incubation medium was added (balanced salt solution containing 10% FCS). After incubation, cells were washed 3 times in PBS and 1 ml of 1mg/ml ice-cold pronase was added. They were then incubated on ice for 30 minutes, centrifuged, and the supernatant removed and counted. Cu in the supernatant represented the "surface-bound" (pronase-sensitive) compartment. The pellet was re-suspended in 1 ml PBS and ultrasonicated; 100 il was removed for DNA analysis and the remainder was put into clean tubes and counted. Cu counted in the pellet represented the "internalised" (pronase-resistant) compartment. Cu levels in the incubation media were measured using either flame or graphite furnace atomic absorption spectroscopy, as appropriate.

DNA analysis: Aliquots of sonicated cells were dried in an oven at 40°C overnight and re-suspended in diaminobenzoic acid (0.4 mg/ml). Tubes were incubated at 50°C for 1 hour, and the reaction stopped by addition of 1M HCl. Tubes were read in a fluorometer at an excitation and emission wavelengths of 420 and 510 nm, respectively.

NADH oxidase activity: Cell surface NADH oxidase activity was measured by adding 0.15 mmol/L NADH in BSS containing 1 mmol/L KCN to the washed cells. The rate of oxidation was calculated using an absorption co-efficient of 6.21 x 10^{-3} cm^{-1} mM^{-1}.

108.2 Results and discussion

Summarize relevant results; discuss dose-response relationship.

Loading hepatocytes with iron decreased the rate of Cu uptake, but increased the levels of Cu associated with the cell surface. Increasing iron resulted in an increase in K_m (the apparent affinity for Cu uptake) and a minor decrease in V_{max}. In contrast, iron caused an increase in B_{max} (the maximum surface binding value for Cu), without any change in the $K_{0.5}$. The data suggested that copper was binding to its transporter, but that, in the presence of iron, a condition necessary for uptake was not being fulfilled. It was considered that this condition was the reduction of Cu(II) to Cu(I) by the plasma membrane NADH oxidase. Loading of cells with iron dramatically decreased NADH oxidase activity. The effect could not be reversed by adding NADH, indicating that there was no competition for the enzyme's active site.

108.3 Conclusion

The importance of NADH oxidase enzyme in the transport of copper across the hepatocyte membrane was demonstrated. It was concluded that oxidation of NADH provides the electron necessary for reduction of Cu(II) on CuHis2 to Cu(I), resulting in the release of Cu from its

	complex and uptake by the hepatocyte. Copper uptake by the hepatocyte is regulated by iron within the cell, which dramatically decreases NADH oxidase activity.
108.3.1 Reliability	*Based on the assessment of materials and methods include appropriate reliability indicator 0, 1, 2, 3, or 4* 2
108.3.2 Deficiencies	Yes. This study was not conducted and/or reported in strict compliance with the principles of GLP. In particular, experimental detail was omitted in a number of places within the report and results were presented only in the form of graphs. However, this does not compromise the validity of the data generated, or the author's interpretation of that data, given that the study was not carried out for regulatory purposes. Furthermore, the research was published in a peer-reviewed publication, and has been subject to the prior scrutiny of experts in the field. In addition this report has been included in a number of expert reviews of Cu toxicokinetics. No internationally accepted guidelines are available that specifically address the objective of the research presented in this summary. The findings of this study are considered to make a valuable contribution to the 'weight of evidence' approach that has been adopted for the purposes of the current review of copper toxicokinetics. A reliability indicator of 2 has been assigned on this basis. *(If yes, discuss the impact of deficiencies and implications on results. If relevant, justify acceptability of study.)*

Evaluation by Competent Authorities	
	Use separate "evaluation boxes" to provide transparency as to the comments and views submitted
	EVALUATION BY RAPPORTEUR MEMBER STATE
Date	[redacted]
Materials and Methods	[redacted]
Results and discussion	[redacted]
Conclusion	[redacted]
Reliability	[redacted]
Acceptability	[redacted]
Remarks	
	COMMENTS FROM ...
Date	*Give date of comments submitted*

Figure A6.2(20)-1 & 2

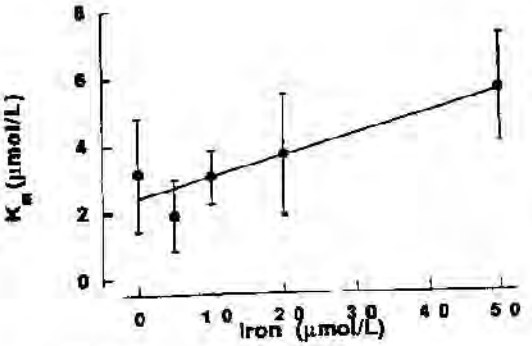

Figure 1a.

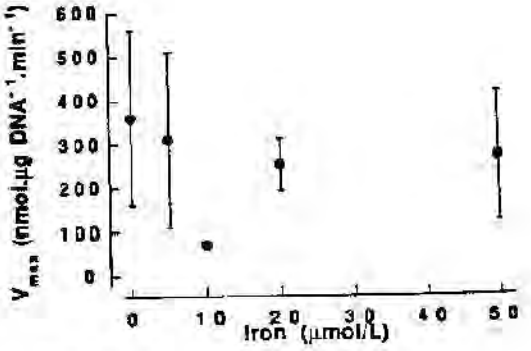

Figure 1b.

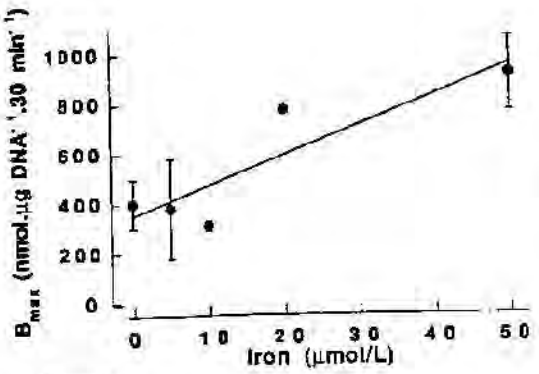

Figure 1c.

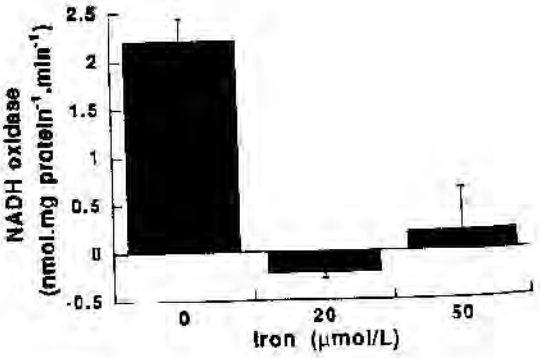

Figure 2.

Official use only

109 REFERENCE

1.1 Reference

Author(s), year, title, laboratory name, laboratory report number, report date (if published, list journal name, volume: pages) If necessary, copy field and enter other reference(s).

Klomp, L.W.J., Lin, S.J., Yuan, D.S., Klausner, R.D., Culotta, V.C. and Gitlin, J.D. (1997). Identification and Functional Expression of HAH1, a Novel Human Gene Involved in Copper Homeostasis. The Journal of Biological Chemistry **272(14)**: 9221-9226 (published).

1.2 Data protection

No
(indicate if data protection is claimed)

1.2.1 Data owner

Give name of company

Public domain

1.2.2 Criteria for data protection

Choose one of the following criteria (see also TNsG on Product Evaluation) and delete the others: No data protection claimed

110 GUIDELINES AND QUALITY ASSURANCE

110.1 Guideline study

No. This was a non-regulatory study to search for an homologue of Atx1p (a copper-binding protein in *Saccharomyces cerevisiae* encoded by ATX1) and to elucidate any functional role for such a protein in antioxidant defence and copper homeostasis. No guidelines are available to address this objective.

(If yes, give guidelines; if no, give justification, e.g. "no guidelines available" or "methods used comparable to guidelines xy")

110.2 GLP

No. This was a non-regulatory study.

(If no, give justification, e.g. state that GLP was not compulsory at the time the study was performed)

110.3 Deviations

Yes. Refer to section 5.3.2 for a general discussion of deviations and deficiencies.

(If yes, describe deviations from test guidelines or refer to respective field numbers where these are described, e.g. "see 3.x.y")

111 MATERIALS AND METHODS

In some fields the values indicated in the EC or OECD test guidelines are given as default values. Adopt, change or delete these default values as appropriate.

111.1 Test material

Refer to section 3.3

111.1.1 Lot/Batch number

Not applicable

111.1.2 Specification

Deviating from specification given in section 2 as follows
(describe specification under separate subheadings, such as the following; additional subheadings may be appropriate):

111.1.2.1	Description	*If appropriate, give e.g. colour, physical form (e.g. powder, grain size, particle size/distribution)* Not applicable
111.1.2.2	Purity	*Give purity in % of active substance* [redacted]
111.1.2.3	Stability	*Describe stability of test material* Not applicable
111.1.2.4	Radiolabelling	*give structural location of radio labelling, give reason if not labelled* [^{32}P]CTP; [^{32}P]dCTP; ^{64}Cu (600 Ci/mmol).
111.2 Test Animals		*Non*-entry *field*
111.2.1 Species		Not applicable
111.2.2 Strain		Not applicable
111.2.3 Source		Not applicable
111.2.4 Sex		Not applicable
111.2.5 Age		Not applicable
111.3 Procedures		Non-entry field
111.3.1 cDNA and genomic library screening		A GenBank search for sequences homologous to yeast *ATX1* identified a partial cDNA sequence from a porcine small intestine cDNA library. To identify a human homologue of *ATX1*, 250,000 recombinant clones from a human liver λgt11 cDNA library were transferred to nitrocellulose membranes and hybridised using a ^{32}P-labelled cDNA probe derived from the porcine clone. Hybridised filters were washed, and positive clones were purified by subsequent rounds of screening. Phage DNA was isolated from positive clones by liquid lysis, and inserts were analysed by agarose gel electrophoresis following restriction digestion with *Eco*RI. The largest size inserts were subcloned and the nucleotide sequence determined by dideoxy chain termination. To isolate genomic clones encoding HAH1 (human ATX homologue 1), a ^{32}P-labelled full-length *HAH1* cDNA was used to screen 800,000 recombinants of a human genomic library in λFixII (Stratagene). Isolated phage DNA was characterised by restriction enzyme digestion and nucleotide sequence determination.
111.3.2 RNA, Southern Blot Analysis and Chromosomal Localisation		RNA blot analysis was performed using nitrocellulose membranes containing poly(A)$^+$ RNA from different human tissues. RNA was isolated by dissolution of human tissues and cell lines in guanidinium isothiocyanate followed by CsCl gradient centrifugation. RNA samples were subjected to agarose-formaldehyde gel electrophoresis, transferred to nylon membranes, and analysed using a ^{32}P-labelled HAH1 cRNA. Human genomic DNA was isolated from peripheral blood leucocytes, digested with restriction enzymes overnight, electrophoresed on 0.8% agarose gels, transferred to nylon membranes and analysed using a ^{32}P-labelled *HAH1* cDNA probe. A bacteriophage clone encompassing the *HAH1* gene was labelled with digoxygenin dUTP by nick translation. Labelled probe was hybridised to normal metaphase chromosomes from phytohemagglutinin-stimulated peripheral blood lymphocytes in 50% formamide, 10% dextran sulphate, and 2 x SSC. Specific hybridisation signals were detected by incubation with fluorescein-conjugated anti-

	digoxygenin antibodies, followed by counterstaining of the slides with 4'6-diaminidino-2-phenylindole. A total of 57 specifically labelled metaphase cells were analysed, and localisation was confirmed using a probe known to localise to 5q21.
111.3.3 Complementation Experiments	To express *HAH1* in *S. cerevisiae*, the coding region encompassing nucleotides 114-318 (**Figure A6.2(21)-1A**) was amplified by polymerase chain reaction and directionally subcloned into the *Eco*RI and *Bam*HI sites of pSM703. The resulting construct pHAH703 was verified by nucleotide sequencing and transformed into KS107 (*sod1*~) and SL215 (*atx1***A**) strains. The empty CEN pRS413 and 2μ pSM703 vectors, and the CEN p413-A1 and 2μ pRS-A1 plasmids containing a functional copy of the *ATX1* gene were transformed into these same strains. To test for reversal of lysine auxotrophy, cells were grown in air on synthetic dextrose (SD) plates with or without lysine for 3 days at 30°C. Iron-dependent growth was determined on SD complete media buffered with 50 mM Na-2-(N-morpholino)ethanesulphonic acid (MES), pH 6.1, and 3 μM ferrozine with or without 350 μM ferrous ammonium sulphate for 5 days at 30°C.
111.3.4 HoloFet3p Biosynthesis	To examine the biosynthesis of holoFet3p (copper incorporation into Fet3p), saturated cultures were used to inoculate 100 ml of yeast nitrogen base culture medium without copper, iron, and dextrose, supplemented with amino acids, 2% glucose, 50 mM Na-MES, pH 6.1, and 100 μM ferrozine. All stock solutions were treated with Chelex100. After growth to $_{A600}$ of 0.4, cells were labelled for 2 h with 2.5 μCi/ml ^{64}Cu. Cells were washed extensively in 150 mM NaCl, 25 mM Tris-HCl pH 7.5, and an aliquot of cells was used to determine cell-associated radioactivity. Cells were lysed by vigorous shaking with glass beads for 1 h, and protein extracts of crude membrane fractions were prepared. Samples (100 μg) were analyzed on 7.5% nonreducing SDS-PAGE without heat denaturation followed by direct autoradiography of the gels. For Western blot analysis of Fet3p, crude membrane extracts were separated by SDS-PAGE and transferred to nitrocellulose by semidry transfer. Following blocking in 5% nonfat dry milk, 0.1% Tween 20, 0.02% Nonidet P-40 in phosphate-buffered saline, membranes were incubated for 1 h with a 1:1000 dilution of an anti-peptide antiserum specific for Fet3p. Membranes were subsequently washed in phosphate-buffered saline containing 0.1% Tween 20 and incubated for 1 h with horseradish peroxidase-conjugated secondary antibody, and the antibody-antigen complex was detected using enhanced chemiluminescence.
	112 RESULTS AND DISCUSSION *Describe findings. If appropriate, include table. Sample tables are given below.*
112.1 Results	Non-entry field

112.1.1 cDNA and genomic library screening	To search for a mammalian Atxlp homologue, an *ATX1* genomic DNA fragment was used to screen a human liver cDNA library by colony hybridization at low stringency and by polymerase chain reaction using degenerate oligonucleotides corresponding to the conserved amino- and carboxyl-terminal domains of *ATX1* (**Figure A6.2(21)-1B**). This approach did not result in isolation of full-length clones, and thus a partial porcine cDNA with homology to the 3' region of *ATX1* was used to rescreen this human liver cDNA library. Seven clones were isolated by this method, and the largest size insert was characterized by nucleotide sequencing. This clone, termed *HAH1*, encompassed 113 bp of 5' untranslated region, a 204-bp open reading frame, and 185 bp of 3' untranslated sequence (**Figure A6.2(21)-1A**). A polyadenylation consensus sequence was identified 18 bp from the poly(A) tail. The open reading frame of *HAH1* encoded a protein of 68 amino acids with 47% identity and 58% similarity to Atxlp including conservation of both the copper-binding domain (MTCXGC) and the lysine-rich carboxyl terminus (**Figure A6.2(21)-1B**). A GenBank search identified homologous open reading frames with these consensus regions in other eukaryotic species including plants and worms, supporting the concept that Atxlp has been phylogenetically conserved (**Figure A6.2(21)-1B**).
112.1.2 RNA, Southern Blot Analysis and Chromosomal Localisation	To determine the tissue-specific expression of *HAH1*, RNA blot analysis was performed using a *HAH1* cDNA probe. This analysis revealed a single transcript of 0.5 kilobases in agreement with the size of the HAH1 cDNA isolated by library screening. *HAH1* mRNA was abundant in all tissues examined both in the peripheral tissues and in the central nervous system (**Figure A6.2(21)-2A and B**). These experiments suggested that the *HAH1* gene is widely expressed under normal conditions, and, consistent with this concept, a *HAH1*-specific transcript was also detected in RNA isolated from a variety of human tissue-derived cell lines (**Figure A6.2(21)-2C**). To characterize the gene encoding *HAHl*, the full-length cDNA clone was used as a probe to analyze human genomic DNA by Southern blot analysis. As shown in **Figure A6.2(21)-3**, hybridization of restriction endonuclease-digested genomic DNA revealed a simple pattern consistent with the presence of single copy gene in the haploid genome. Three independent clones encompassing the *HAH1* gene were then isolated from a genomic library and characterized using Southern blot analysis and sequencing. The largest of these clones was used to determine the chromosomal localization of the *HAH1* gene. **Figure A6.2(21)-4A** shows fluorescent *in situ* hybridization analysis of normal metaphase chromosomes derived from peripheral blood lymphocytes utilizing this 15-kilobase genomic fragment as a probe. Consistent with the Southern blot experiments, this analysis revealed specific labeling of a single locus on the distal long arm of chromosome 5 in a total of 57 metaphase cells. Cohybridization of the *HAH1* probe with a probe that precisely mapped to 5q21 resulted in double-labeling of the long arm of chromosome 5. Measurements of 10 specifically labeled chromosome 5 preparations demonstrated that the *HAH1* gene is located at a position that is 75% of the distance from the centromere to the telomere at an area that corresponds to the interface between bands 5q32 and 5q33 (**Figure A6.2(21)-4B**).
112.1.3 Complementation Experiments	The *ATX1* gene was isolated by virtue of its ability to reverse the aerobic lysine auxotrophy observed in *sod1***ls** strains. To ascertain the function of *HAHl*, the coding region of the *HAH1* cDNA was placed

under control of the *S. cerevisiae* phosphoglycerate kinase promoter and introduced into the *sod1***A** null mutant. This strain was subsequently analyzed for its ability to grow aerobically on plates without lysine. As can be seen in **Figure A6.2(21)-5A**, yeast strains transformed with either *ATX1* or *HAH1* were able to suppress the lysine auxotrophy of a *sod1***lS** mutant strain. Since complementation in these experiments is accomplished by over expression of these proteins, the slight difference in growth rate between the *ATX1* and the *HAH1* transformants (**Figure A6.2(21)-5A, b versus c**) may reflect a difference in the amount of protein expressed under these circumstances.

112.1.4 HoloFet3p Biosynthesis

Atxlp is essential for efficient high affinity iron uptake in *S. cerevisiae*. As shown in **Figure A6.2(21)-5B**, an *atxl***lS** null strain is dependent upon high concentrations of exogenous iron for growth, but will grow on iron-depleted media after reintroduction of the *ATX1* gene. Transformation of the *atxl***lS** strain with *HAH1* also suppressed this irondependent phenotype, as evidenced by support of growth on low iron medium (**Figure A6.2(21)-5B, c**). Cells transformed with vector alone failed to grow under these conditions (**Figure A6.2(21)-5B, b and d**), indicating that the observed effect is specific for *HAH1*.

The role of copper in high affinity iron uptake in *S. cerevisiae* is due to the plasma membrane multicopper oxidase Fet3p, and the iron deficiency in the *atxl***lS** strain is considered to result from a failure of copper incorporation into Fet3p. To directly test this hypothesis and to obtain functional data on the role of *HAH1* in copper metabolism, yeast strains were cultured in copper-free medium, pulse-labeled with ^{64}Cu, and then newly synthesized holoFet3p was detected in membrane fractions. When membrane fractions were analyzed, a protein with the molecular mass of Fet3p was detected in wild type (**FigureA6.2(21)-6A, lane 1**) but not in a *ccc2***lS** mutant strain (**Figure 6.2(20)-6A, lane 2**) previously shown to have Fet3p oxidase activity. Consistent with the partial iron deficiency in *atxl***ls** null mutants, a marked reduction, but not complete impairment of copper incorporation into Fet3p was observed in the *atxl***ls** strains transformed with either the pRS413 or pSM703 vectors alone (**Figure 6.2(20)-6A, lanes 3 and 5**). However, radiolabeled Fet3p equivalent in amount to that observed in the wild type strain was detected in the *atxl***ls** mutant following introduction of *ATX*1 on an episomal plasmid (**Figure A6.2(21)-6, lane 4**). Furthermore, introduction of *HAH1* also resulted in restoration of holoFet3p biosynthesis to amounts observed in the wild-type strain, indicating that *HAH1* can function to facilitate copper incorporation in an analogous fashion to Atxlp (**Figure A6.2(21)-6A, lane 6**). These same membrane samples were examined for immunoreactive Fet3p by Western blotting using a polyclonal antiserum to Fet3p. As can be seen in Figure **A6.2(21)-6B**, the amount of Fet3p detected by this technique was equivalent in each of the *atxl***lS** strains, thus confirming that the changes in holoFet3p biosynthesis observed in the copper-labeling experiment were not due to an effect of Atxlp on the amount of Fet3p present in these strains. The mobility of Fet3p under these circumstances was lower than that observed for holoFet3p analyzed in nonreducing SDS-PAGE gels (**Figure A6.2(21)-6, A versus B**).

112.2 Discussion

The sequence data reported in this study suggest that *HAH1* is a human homologue of the *S. cerevisiae* copper-binding protein Atxlp. The considerable amino acid identity between these two proteins, including

conservation of the MTCXGC copper binding motif, as well as the occurrence of homologous sequences as open reading frames in the DNA of other diverse eukaryotic organisms, supports this concept. Perhaps most importantly, the expression of *HAH1* in *sodl***A** and *atxl***A** null yeast strains reconstitutes the defects in antioxidant defense and iron homeostasis in these mutants, indicating that the *HAH1* open reading frame encodes a functional protein.

RNA blot analysis of *HAH1* expression identified a single 0.5-kilobase transcript in all tissues and cell lines examined, with no evidence of qualitative differences in gene expression among tissues. These data are consistent with the size of the isolated full-length cDNA (**Figure A6.2(21)-lA**). The observation that *HAH1* is ubiquitously and abundantly expressed supports the concept that this protein plays an important role in cellular copper homeostasis.

Based upon the complementation of atx1A null strains by *HAH1* and the role of Atxlp in iron metabolism in *S. cerevisiae*, it is reasonable to assume that *HAH1* functions in an analogous fashion in mammalian cells. In this context, *HAH1* would be responsible for the delivery of cytosolic copper to the Menkes and Wilson disease proteins in the trans-Golgi network prior to transport of this metal by these ATPases into the secretory pathway. This model is consistent with the known intracellular localization of these copper transport ATPases in mammalian cells, as well as the clearly defined role of the Wilson disease ATPase in providing copper for the biosynthesis of the Fet3p multicopper oxidase homologue ceruloplasmin.

In addition to, and independent of, its role in iron homeostasis, Atxlp functions as an antioxidant protecting yeast from the toxic effects of superoxide and hydrogen peroxide. As Atxlp itself does not appear to have antioxidant properties, the most likely explanation for these observations is that Atxlp and *HAH1* deliver copper to an as yet uncharacterized protein, which functions in cellular antioxidant defense.

Collectively, the data presented here suggest that *HAH1* is a novel human copper-binding protein, which is abundantly and ubiquitously expressed and which functions in copper homeostasis and antioxidant defense.

113 APPLICANT'S SUMMARY AND CONCLUSION

113.1 Materials and methods

Give concise description of method; give test guidelines no. and discuss relevant deviations from test guidelines

A study was carried out to search for a mammalian homologue of Atx1p (a copper-binding protein in *Saccharomyces cerevisiae* encoded by ATX1) and to elucidate any functional role for such a protein in antioxidant defence and copper homeostasis. The study was not designed to follow internationally accepted guidelines, and was not carried out or reported in compliance with GLP.

cDNA and genomic library screening: A partial cDNA sequence homologous to yeast ATX1 was identified from a porcine small intestine cDNA library. To identify a human homologue, recombinant clones from a human liver cDNA library were transferred to nitrocellulose membranes and hybridised using a ^{32}P-labelled cDNA probe derived from the porcine clone. Hybridised filters were washed, and subsequent rounds of screening purified positive clones. Phage DNA was isolated from positive clones by liquid lysis, and inserts were

	analysed by agarose gel electrophoresis following restriction digestion with *Eco*RI. The largest inserts were subcloned and the nucleotide sequence determined by dideoxy chain termination. To isolate genomic clones encoding HAH1 (human ATX homologue 1), a ^{32}P-labelled full-length *HAH1* cDNA was used to screen 800,000 recombinants of a human genomic library. Isolated phage DNA was characterised by restriction enzyme digestion and nucleotide sequence determination. *RNA, Southern Blot Analysis and Chromosomal Localisation*: RNA blot analysis was performed using nitrocellulose membranes containing poly(A)$^+$ RNA from different human tissues. RNA was isolated by dissolution of human tissues in guanidinium isothiocyanate, followed by CsCl gradient centrifugation. RNA samples were subjected to agarose-formaldehyde gel electrophoresis, transferred to nylon membranes, and analysed using a ^{32}P-labelled HAH1 cRNA. Human genomic DNA was isolated from peripheral blood leucocytes, digested with restriction enzymes, electrophoresed on 0.8% agarose gels, transferred to nylon membranes and analysed using a ^{32}P-labelled HAH1 cDNA probe. A bacteriophage clone encompassing the HAH1 gene was labelled with digoxygenin dUTP by nick translation. Labelled probe was hybridised to normal metaphase chromosomes from phytohemagglutininstimulated lymphocytes in 50% formamide, 10% dextran sulphate, and 2 x SSC. Specific hybridisation signals were detected by incubation with fluorescein-conjugated anti-digoxygenin antibodies, followed by counterstaining of slides with 4'6-diaminidino-2-phenylindole. A total of 57 specifically labelled metaphase cells were analysed, and localisation was confirmed using a probe known to localise to 5q21. *Complementation experiments:* To express *HAH1* in *S. cerevisiae*, the coding region encompassing nucleotides 114-318 was amplified by polymerase chain reaction and directionally subcloned into the *Eco*RI and *Bam*HI sites of pSM703. The resulting construct pHAH703 was verified by nucleotide sequencing and transformed into KS107 (*sod1~*) and SL215 (*atx1***A**) strains. The empty CEN pRS413 and 2μ pSM703 vectors, and the CEN p413-A1 and 2μ pRS-A1 plasmids containing a functional copy of the *ATX1* gene were transformed into these same strains. To test for reversal of lysine auxotrophy, cells were grown in air on synthetic dextrose (SD) plates with or without lysine for 3 days at 30°C. Iron-dependent growth was determined on SD complete media buffered with 50 mM Na-2-(N-morpholino)ethanesulphonic acid (MES), pH 6.1, and 3 μM ferrozine with or without 350 μM ferrous ammonium sulphate for 5 days at 30°C. *HoloFet3p Biosynthesis:* To examine the biosynthesis of holoFet3p (copper incorporation into Fet3p), saturated cultures were used to inoculate 100 ml of yeast nitrogen base culture medium without copper, iron, and dextrose, supplemented with amino acids, 2% glucose, 50 mM Na-MES, pH 6.1, and 100 μM ferrozine. All stock solutions were treated with Chelex-100. After growth to $_{A600}$ of 0.4, cells were labelled for 2 h with 2.5 μCi/ml ^{64}Cu. Cells were washed extensively in 150 mM NaCl, 25 mM Tris-HCl pH 7.5, and an aliquot of cells was used to determine cell-associated radioactivity. Vigorous shaking with glass beads for 1 hour lysed cells, and protein extracts of crude membrane fractions were prepared. Samples (100 μg) were analyzed on 7.5% nonreducing SDS-PAGE without heat denaturation followed by direct autoradiography of the gels. For Western blot analysis of Fet3p, crude membrane extracts were separated by SDS-PAGE and transferred to nitrocellulose by semidry transfer. Following blocking in 5% non-fat	X

	dry milk, 0.1% Tween 20, 0.02% Nonidet P-40 in phosphate-buffered saline, membranes were incubated for 1 h with a 1:1000 dilution of an anti-peptide antiserum specific for Fet3p. Membranes were subsequently washed in phosphate-buffered saline containing 0.1% Tween 20 and incubated for 1 h with horseradish peroxidase-conjugated secondary antibody, and the antibody-antigen complex was detected using enhanced chemiluminescence.
113.2 Results and discussion	*Summarize relevant results; discuss dose-response relationship.* To search for a mammalian homologue of *ATX1*, a human liver cDNA library was screened and a cDNA clone was isolated, which encodes a protein with 47% amino acid identity to Atxlp including conservation of the MTCXGC copper-binding domain. RNA blot analysis using this cDNA identified an abundant 0.5-kilobase mRNA in all human tissues and cell lines examined. Southern blot analysis using this same clone indicated that the corresponding gene exists as a single copy in the haploid genome, and chromosomal localization by fluorescence *in situ* hybridization detected this locus at the interface between bands 5q32 and 5q33. Yeast strains lacking copper/zinc superoxide dismutase (*SOD1*) are sensitive to redox cycling agents and diogygen and are auxotrophic for lysine when grown in air, and expression of this human *ATX1* homologue (*HAH1*) in these strains restored growth on lysinedeficient media. Yeast strains lacking *ATX1* are deficient in high affinity iron uptake and expression of *HAH1* in these strains permits growth on iron-depleted media and results in restoration of copper incorporation into newly synthesized Fet3p. These results identify *HAH1* as a novel ubiquitously expressed protein, which may play an essential role in antioxidant defense and copper homeostasis in humans.
113.3 Conclusion	It has been demonstrated that *HAH1* is one of a series of human copper chaperone proteins involved in the transfer of copper from the cell surface to the intracellular targets. Specifically, *HAH1* is thought to deliver copper to a Cu-ATPase in the Golgi apparatus.
113.3.1 Reliability	*Based on the assessment of materials and methods include appropriate reliability indicator 0, 1, 2, 3, or 4* *2*
113.3.2 Deficiencies	Yes This study was not conducted and/or reported in strict compliance with the principles of GLP. However, this does not compromise the validity of the data generated, or the author's interpretation of that data, given that the study was not carried out for regulatory purposes. Furthermore, the research was published in a peer-reviewed journal, and has therefore been subject to the prior scrutiny of experts in the field. No internationally accepted guidelines are available that address the objective of the research presented in this summary. *(If yes, discuss the impact of deficiencies and implications on results. If relevant, justify acceptability of study.)*

Evaluation by Competent Authorities

Section A6.2	**Metabolism in mammals**
Annex Point IIA6.2	*Specify section no., heading and species as appropriate*
IUCLID 5.0/21	**A6.2(21), Cellular and molecular metabolism of copper**

	Use separate "evaluation boxes" to provide transparency as to the comments and views submitted
	EVALUATION BY RAPPORTEUR MEMBER STATE
Date	[redacted]
Materials and Methods	• [redacted]
Results and discussion	[redacted]
Conclusion	[redacted]
Reliability	[redacted]
Acceptability	[redacted]
Remarks	

	COMMENTS FROM ...
Date	*Give date of comments submitted*

Figure A6.2(21)-1

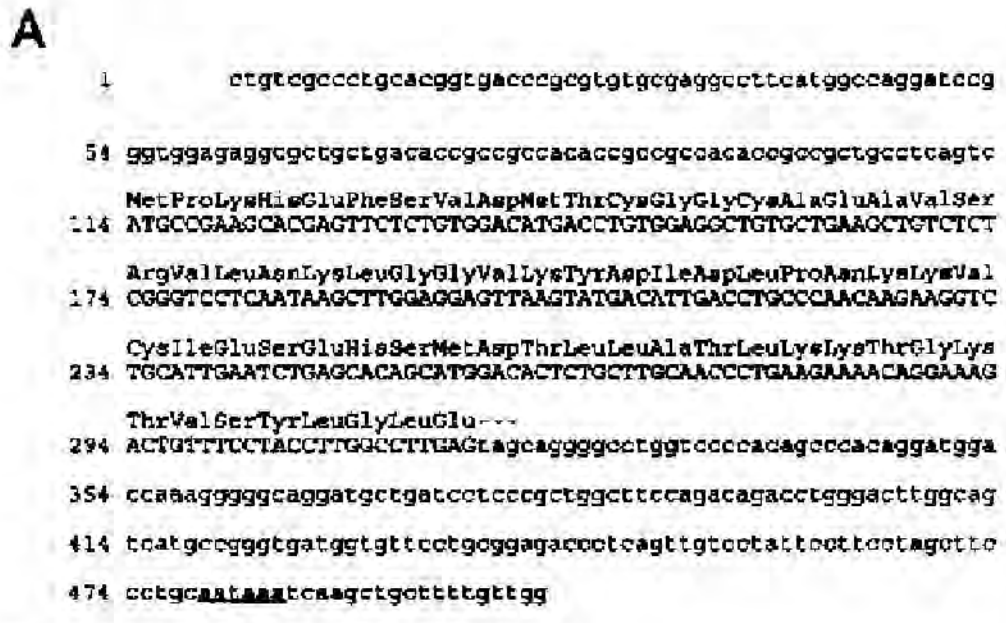

FIG. 1. *A*, nucleotide sequence of *HAH1* cDNA clone and derived amino acid sequence of HAH1 (nucleotides 114–318); polyadenylation consensus sequence is *underlined*. *B*, derived amino acid sequence of HAH1 (*H. sap*) aligned with homologues identified in *S. cerevisiae* (*ATX1*, *S. cer.*), *Caenorhabditis elegans* (*C. ele.*), and *Arabidopsis thaliana* (*A. tha.*). Amino acids identical to HAH1 are shown in *bold*. The copper-binding motif (MTCXGC) and the carboxyl-terminal lysine rich region (****) are indicated.

Figure A6.2(21)-2

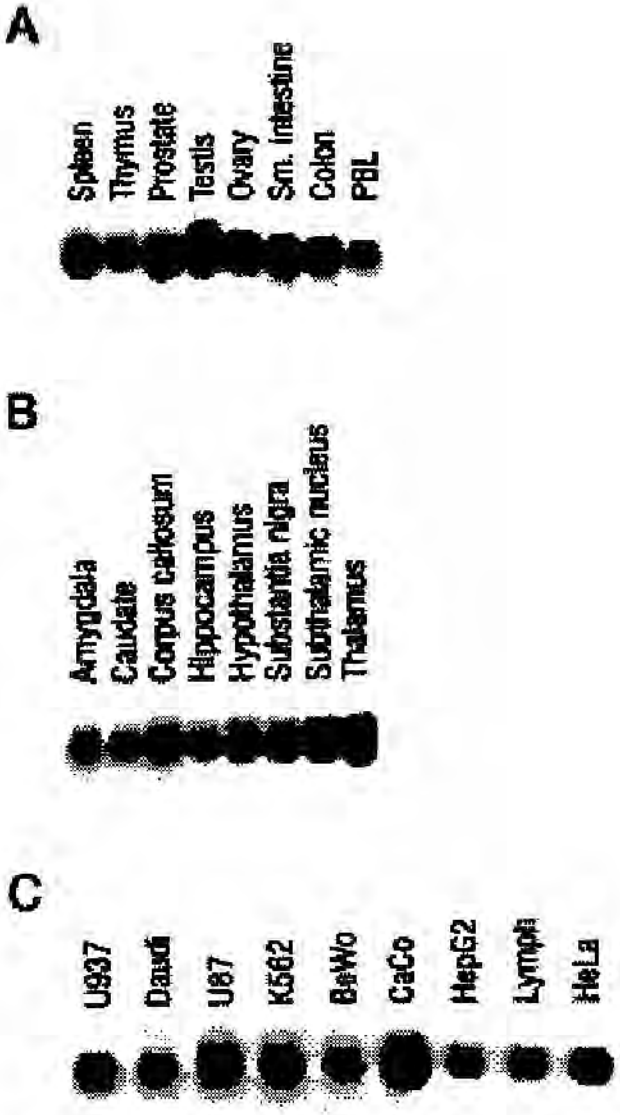

FIG. 2. **Expression of the *HAH1* gene in human tissues and cell lines.** RNA blot analysis of poly(A)$^+$ RNA from human tissues (*A*), regions of the central nervous system (*B*), and human tissue-derived cell lines (*C*). 2 μg of poly(A)$^+$ RNA (*A* and *B*) or 15 μg of total RNA (*C*) were subjected to electrophoresis, transferred to membranes, and hybridized with a ^{32}P-labeled HAH1-specific cRNA probe as described under "Experimental Procedures." Blots were exposed to film for 1 h at −70 °C.

Figure A6.2(21)-3

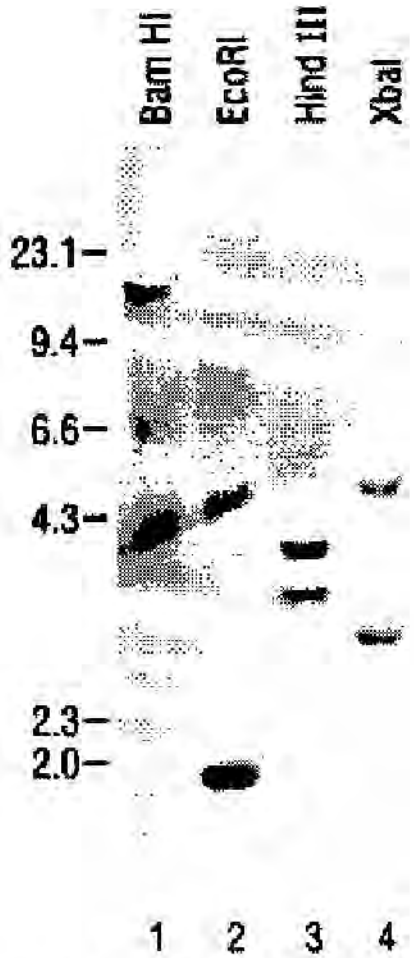

FIG. 3. **Southern blot analysis of the *HAH1* gene.** Human genomic DNA (10 μg/lane) was digested with the restriction enzymes shown, subjected to electrophoresis, transferred to membranes, and hybridized with a ^{32}P-labeled HAH1-specific cDNA probe as described under "Experimental Procedures." Molecular size markers are shown on the left in kilobases. The blot was exposed to film at −70 °C for 22 h.

Figure A6.2(21)-4

Figure A6.2(21)-5

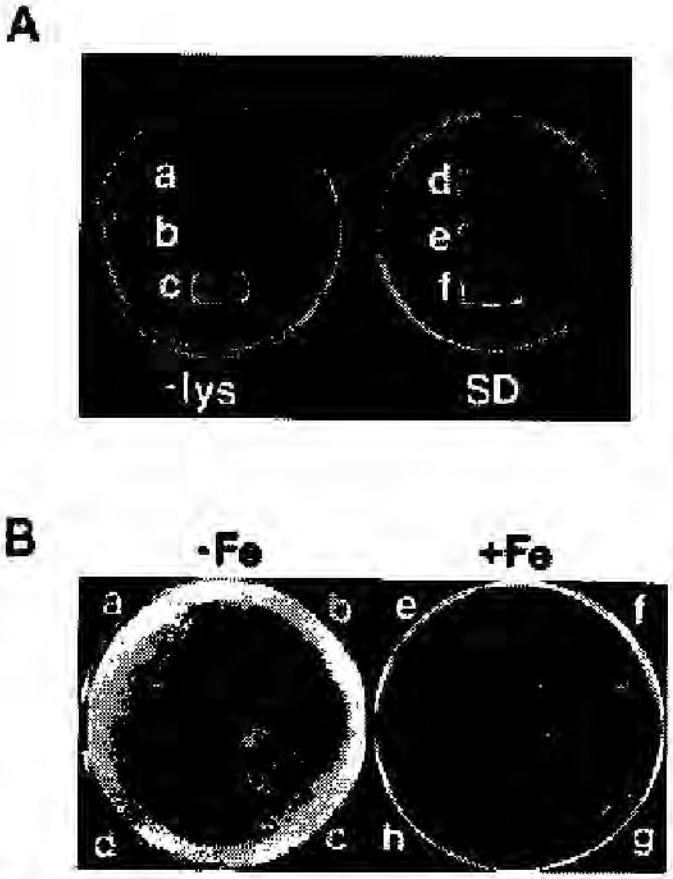

FIG. 5. *A*, complementation of aerobic lysine auxotrophy in *sod1Δ* strain KS107 grown on lysine-deficient (*a–c*) or SD complete media containing lysine (*d–f*) following transformation with pHAH-703 (*b* and *e*) or pRS-A1 (*c* and *f*). *B*, complementation of iron-deficient growth in *atx1Δ* strain SL215 grown on 3 μM ferrozine (*a–d*) or 3 μM ferrozine plus 350 μM ferrous ammonium sulfate (*e–h*) following transformation with *ATX1* containing p413-A1 (*a* and *e*), control vector pRS413 (*b* and *f*), HAH1 containing pHAH 703 (*c* and *g*), or control vector pSM703 (*d* and *h*).

Figure A6.2(21)-6

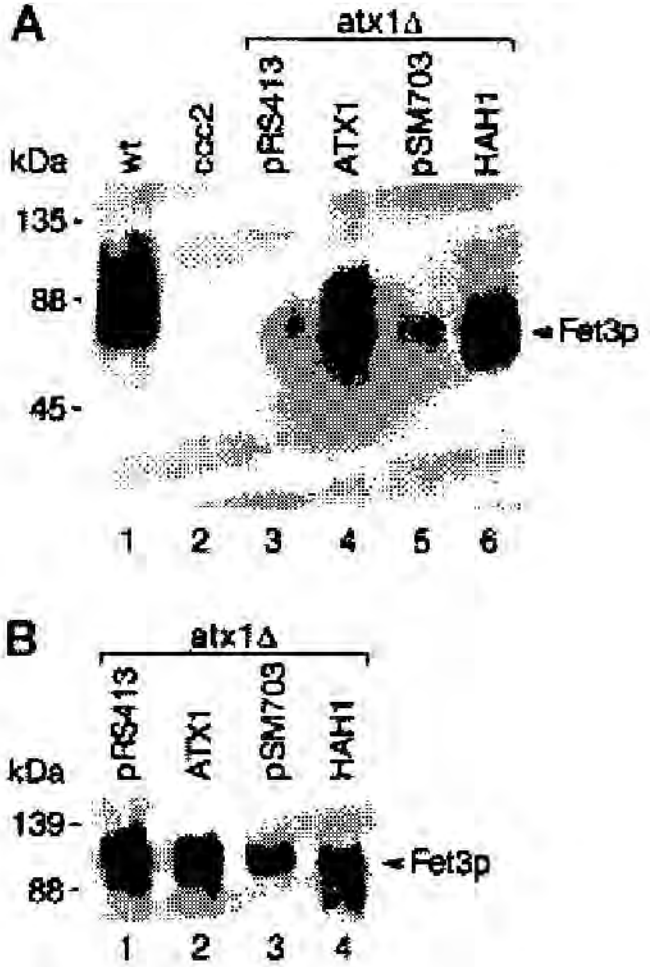

FIG. 6. *A*, biosynthesis of holoFet3p in wild type (*lane 1*), *ccc2Δ* mutant (*lane 2*), and *atx1Δ* null mutant (*lanes 3–6*) *S. cerevisiae* stra *atx1Δ* strains were transformed with the indicated control vec (*lanes 3* and *5*), p413-A1 (Atx1) (*lane 4*), or pHAH-703 (HAH1) (*lan* prior to analysis as described under "Experimental Procedures." identify holoFet3p, cells were pulse-labeled with ^{64}Cu, and membr fractions analyzed by nonreducing SDS-PAGE, followed by copper toradiography of gels as described under "Experimental Procedur ^{64}Cu-labeled Fet3p is indicated by the *arrow*. *B*, Western blot anal of Fet3p in *atx1Δ* strains transformed with control vectors (*lanes 1* 3), *ATX1* (*lane 2*), or *HAH1* (*lane 4*). Identical membrane fractions a *A* were electrophoresed in 7.5% SDS-PAGE, transferred to nitroce lose, incubated with a polyclonal antiserum to Fet3p, and developed chemiluminescence as described under "Experimental Procedures."

			Official use only
		114 REFERENCE	
1.1	**Reference**	*Author(s), year, title, laboratory name, laboratory report number, report date (if published, list journal name, volume: pages) If necessary, copy field and enter other reference(s).* Amaravadi, R., Glerum, D.M. and Tzagoloff, A. (1997). Isolation of a cDNA encoding the human homolog of *COX17*, a yeast gene essential for mitochondrial copper recruitment. Hum Genet. **99:** 329-333 (published).	
1.2	**Data protection**	No *(indicate if data protection is claimed)*	
1.2.1	Data owner	*Give name of company* Public domain	
1.2.2	Criteria for data protection	Choose one of the following criteria (see also TNsG on Product Evaluation) and delete the others: No data protection claimed	
		115 GUIDELINES AND QUALITY ASSURANCE	
115.1	**Guideline study**	No. This was a non-regulatory study that describes the use of functional complementation to clone the human homolog of yeast *COX17*. *COX17* codes for a 69 amino acid cytosolic protein involved in the recruitment of Cu to mitochondria (null mutations in *COX17* elicit a loss of cytochrome oxidase due to a failure of mutants to complete assembly of the complex). No guidelines are available to address this objective. *(If yes, give guidelines; if no, give justification, e.g. "no guidelines available" or "methods used comparable to guidelines xy")*	
115.2	**GLP**	No. This was a non-regulatory study. *(If no, give justification, e.g. state that GLP was not compulsory at the time the study was performed)*	
115.3	**Deviations**	Yes. Refer to section 5.3.2 for a general discussion of deviations and deficiencies. *(If yes, describe deviations from test guidelines or refer to respective field numbers where these are described, e.g. "see 3.x.y")*	
		116 MATERIALS AND METHODS	
		In some fields the values indicated in the EC or OECD test guidelines are given as default values. Adopt, change or delete these default values as appropriate.	
116.1	**Test material**	Refer to section 2.3	X
116.1.1	Lot/Batch number	Not applicable	
116.1.2	Specification	Deviating from specification given in section 2 as follows *(describe specification under separate subheadings, such as the following; additional subheadings may be appropriate):*	

116.1.2.1	Description	*If appropriate, give e.g. colour, physical form (e.g. powder, grain size, particle size/distribution)* Not applicable
116.1.2.2	Purity	*Give purity in % of active substance* [redacted]
116.1.2.3	Stability	*Describe stability of test material* Not applicable
116.1.2.4	Radiolabelling	*give structural location of radio labelling, give reason if not labelled* Not applicable
116.2 Test Animals		*Non-*entry *field*
116.2.1 Species		*Saccharomyces cerevisiae*
116.2.2 Strain		*cox 17* null mutant.
116.2.3 Source		Not applicable
116.2.4 Sex		Not applicable
116.2.5 Age		Not applicable
116.3 Procedures		Non-entry field
116.3.1 Strains, transformation conditions and screen for functional complementation		The *cox17* null mutant (W303**A**COX17) was transformed with a human cDNA expression library consisting of HeLa cell cDNA cloned into the *ADH1* expression cassette of the *Escherichia coli*/yeast shuttle vector pDB20. This vector also carries the URA3 gene for selection of transformants. Transformation mixtures were plated on minimal glucose medium containing all auxotrophic requirements of W303**A**COX17 except uracil. Plates generally containing 1.0×10^4 – 1.5×10^4 uracil-independent transformants were replicated into YEPG media (3% glycerol, 2% ethanol, 1% yeast extract) and incubated at 30°C for up to 1 week.
116.3.2 Miscellaneous methods		Isolation of plasmid DNA from yeast, transformation of E. coli with recombinant plasmids, restriction enzyme mapping, and isolation and ligation of restriction fragments were all performed by standard methods. DNA sequencing was done using 5' end-labelled single-stranded restriction fragments.

117 RESULTS AND DISCUSSION

Describe findings. If appropriate, include table. Sample tables are given below.

117.1 Results		Non-entry field
117.1.1 Complementation of a *cox17* null mutant by recombinant plasmids with human cDNAs		W303**A**COX17 is a respiratory deficient mutant carrying a disrupted allele of *COX17*. Several large-scale transformations of this mutant with a yeast expression library constructed from HeLa cell cDNA yielded approximately 8×10^5 uracil-independent clones. Further screens revealed that 40 transformants had acquired the ability to grow on the nonfermentable substrate glycerol. In each case, the respiratory competent phenotype co-segregated with the uracil prototrophy, confirming that the transformed phenotype was plasmid-dependent. Plasmid DNA was isolated from 20 respiratory competent clones and

	amplified in *E. coui*. Most of the complementing plasmids had cDNA inserts of a size (450 bp) identical to that of pG74H/T1 (**Figure A6.2(22)-1A**). Two plasmids (pG74H/T4 and pG74H/T11) had larger inserts of 1.1 kb and 0.85 kb. The latter two contain chimeric cDNAs, only part of which are related to the insert of pG74H/T1.
117.1.2 The presence of a common sequence in plasmids capable of complementing the yeast *cox17* mutant	Based on its sequence, the cDNA insert recovered from pG74H/T1 had a length of 443 nucleotides (**Figure A6.2(22)-2**). Analysis of the DNA sequence revealed a single open reading frame. The predicted protein consisted of 62 amino acids with a calculated M_r of 6916. The primary structure of the protein predicted from the DNA sequence was homologous to yeast Cox17p, suggesting that the cloned cDNA codes for the human homolog. Partial sequence analysis of the 850 bp fragment cloned in pG74H/T11 indicated the presence of the sequence from nt –53 to 292 reported in **Figure A.2(21)-2**, and another fragment with part of the cDNA for human reticulocalbin . The fusion of the two different sequences occurred at nt 292 of the inert pG74H/T1. The insert in pG74H/T4 was more complex, having been produced by the fusion of the cDNA present in pG74H/T1 to two other fragments, one originating from human mitochondrial DNA and the other coding for the ribosomal protein L32. In the three plasmids studied, the presence of an idential reading frame whose encoded product is homologous to Cox17p, provided strong evidence that the restoration of respiration in the *cox17* mutant is due to complementation by the human equivalent of the yeast protein.
117.1.3 Growth properties of the *cox17* null mutant transformed with yeast and human *COX17*	The *cox17* mutant transformed with pG74H/T1 has a slower growth rate on YEPG than either wild-type yeast or the mutant transformed with the yeast COX17 gene (**Figure A6.2(22)-3**). The failure of the cDNA fragment in pG74H/T1, removed from the *ADH1* cassette and integrated in single copy (pG74H/ST7 in **Figure A6.2(22) -1B**) into the chromosomal DNA of the mutant, to confer growth on the respiratory substrate also argues that the human cDNA only partially complements the mutant. This could be due to less efficient expression of the human gene or because the human protein is only partially functional in the yeast. To distinguish between these two possibilities, a new plasmid was constructed in which the regions 5' and 3' of the coding sequence in pG74H/T1 were replaced by the sequences flanking the yeast gene (pG74H/ST5 in **Figure A6.2(22)-1B**). This construct is identical to pG74/ST8 (see **Figure A6.2(22)-1B**), except for the presence of the human coding sequence. Introduction of the plasmid into the cox17 null mutant did not result in any noticeable improvement in growth on YPEG over that conferred by pG74H/T1 (not shown). The lack of effect of the yeast flanking sequences on complementation suggests that the explanation for the partial restoration of respiration lies in the properties of the protein itself. This interpretation is supported by the failure of the human cDNA (pG74H/T1) to complement the *cox17* mutant when integrated in single copy at the *LEU2* locus. In contrast to pG74H/T1 and pG74H/T4, growth on YEPG of the transformant harbouring pG74H/T11 was almost as good as wild-type (**Figure A6.2(22)-3**). Since the inserts in pG74H/T1 and pG74H/T11 have different 5' and 3' flanking sequences, either sequence could affect expression of the human *COX17* gene. The 3' flanking region in pG74H/T11 containing the recombinant sequence coding for part of reticulocalbin was excluded from being important since its removal

	(pG74H/ST6 in **Figure A6.2(22)-1B**) did not alter the growth properties of the transformant. Replacement of the 3' flanking region of pG74H/T1 with the 3' region of pG74H/ST6 also did not affect growth of the transformant on glycerol (see pG74H/ST11 in **Figure A6.2(22)- 1B**). To exclude an effect of plasmid copy number, pG74H/T11 was integrated at the *URA3* locus. The transformant harbouring the human gene with the shorter 5'leader in single copy was complemented for its respiratory defect, but grew more slowly than wild type or transformants containing the plasmid in multicopy. These results indicate that the absence of 33 nucleotides in the upstream region of pG74H/T11 is responsible for the improved growth in glycerol, probably as a result of more efficient expression of the protein.
117.1.4 Human and yeast Cox17p are highly homologous and contain a cysteine-rich domain also present in metallothioneins	Human and yeast Cox17p share 22 identities and 8 conservative substitutions (**Figure A6.2(22)-4**). A comparison of the Cox17p to human and mouse metallothionein reveals a short common domain. Two other conserved cysteines in Cox17p can be aligned with cysteines in the mammalian metallothioneins if two short gaps are allowed in the sequences. All five of the cysteines that are conserved between the metallothioneines and the Cox17ps are involved in binding Cu.
117.2 Discussion	Evidence is presented for the existence of a human gene whose encoded product functions in cytochrome oxidase assembly. This protein is homologous to a cytoplasmic protein of yeast that functions in delivery of Cu to mitochondria. A HeLa cell cDNA encoding the human Cox17p homolog was selected from an expression library by functional complemetation of a yeast *cox17* null mutant. The protein's primary structure, deduced from the nucleotide sequence of the cDNA clone, displayed a high degree of sequence similarity to yeast Cox17p. The existence of a human Cox17p homolog, and its ability to substitute *in vivo* for the yeast protein, supports the idea that Cox17p is likely to be present in all mammalian cells in which cytochrome oxidase is the terminal oxidase of the respiratory chain. Even though human Cox17p is capable of complementing the defect in the yeast *cox17* null mutant, the growth properties of transformants harbouring different constructs suggest that the human Cox17p is less efficient than the yeast protein in the heterologous environment. This is supported by 1) the slow growth rate on glycerol transformants harbouring pG74H/T1 (single or multi-copy) and 2) a similar slow growth on glycerol of the *cox17* mutant transformed with a plasmid containing the human coding sequence flanked by the yeast 5' and 3' untranslated regions (UTRs). The same plasmid with the yeast coding sequence elicits wild-type growth on glycerol. In addition, growth differences of transformants harbouring two complementing plasmids with the same coding region but different flanking regions (pG74H/T1 and pG74H/ST6) demonstrate that noncoding human sequences, particularly in the 5'UTR, can affect expression of the human protein, and hence may also contribute to the observed growth phenotypes. The human and yeast Cox17ps share features with metallothioneins. Both Cox17p and metallothionein are low-molecular-weight proteins with a high molar content of cysteine residues. Both also contain a short conserved domain with the sequence KxCCxC. Metallothioneins protect cells from toxic metals by means of their high binding potential for Cu, Cd and other heavy metals. The ability of high exogenous Cu to rescue *cox17* null mutants argues against a metal-scavenging role for

Cox17p, but favours a role in the delivery of Cu to mitochondria.

118 APPLICANT'S SUMMARY AND CONCLUSION

118.1 Materials and methods

Give concise description of method; give test guidelines no. and discuss relevant deviations from test guidelines

A study that describes the use of functional complementation to clone the human homolog of yeast COX17 was carried out. COX17 codes for a 69 amino acid cytosolic protein involved in the recruitment of Cu to mitochondria (null mutations in COX17 elicit a loss of cytochrome oxidase due to a failure of mutants to complete assembly of the complex). The study was not designed to follow internationally accepted guidelines, and was not carried out or reported in compliance with GLP. The following techniques were used:

Strains, transformation conditions and screen for functional complementation: The *cox17* null mutant (W303**A**COX17) was transformed with a human cDNA expression library consisting of HeLa cell cDNA cloned into the *ADH1* expression cassette of the *Escherichia coli*/yeast shuttle vector pDB20. This vector also carries the *URA3* gene for selection of transformants. Transformation mixtures were plated on minimal glucose medium containing all auxotrophic requirements of W303**A**COX17 except uracil. Plates generally containing $1.0 \times 10^4 - 1.5 \times 10^4$ uracil-independent transformants were replicated into YEPG media and incubated at 30°C for up to 1 week.

Miscellaneous methods: Isolation of plasmid DNA from yeast, transformation of E. coli with recombinant plasmids, restriction enzyme mapping, and isolation and ligation of restriction fragments were all performed by standard methods. DNA sequencing was done using 5' end-labelled single-stranded restriction fragments.

118.2 Results and discussion

Summarize relevant results; discuss dose-response relationship.

Complementation of a cox17 *null mutant by recombinant plasmids with human cDNAs :* W303**A**COX17 is a respiratory deficient mutant carrying a disrupted allele of *COX17*. Large-scale transformations of this mutant with a yeast expression library constructed from HeLa cell cDNA yielded approximately 8×10^5 uracil-independent clones. Further screens revealed that 40 transformants had acquired the ability to grow on nonfermentable substrate. In each case, the respiratory competent phenotype co-segregated with the uracil prototrophy, confirming that the transformed phenotype was plasmid-dependent.

Plasmid DNA was isolated from 20 respiratory competent clones and was amplified in *E. coli*. Most of the complementing plasmids had cDNA inserts of a size (450 bp) identical to that of pG74H/T1. Two other plasmids (pG74H/T4 and pG74H/T11) had larger inserts of 1.1 kb and 0.85 kb, respectively. These contained chimeric cDNAs, only part of which are related to the insert of pG74H/T1.

The presence of a common sequence in plasmids capable of complementing the yeast cox17 *mutant:* The cDNA insert recovered from pG74H/T1 had a length of 443 nucleotides. Analysis of the DNA sequence revealed a single open reading frame. The predicted protein consisted of 62 amino acids with an M_r of 6916. The predicted structure of the protein was homologous to yeast Cox17p, suggesting that the cloned cDNA coded for the human homolog. Partial analysis of the

fragments cloned in pG74H/T11 and pG74H/T1 also revealed the presence of this sequence. An idential reading frame in all 3 plasmids, whose encoded product was homologous to Cox17p, provided evidence that restoration of respiration in the *cox17* mutant was due to complementation by the human equivalent of the yeast protein.

Growth properties of the cox17 *null mutant transformed with yeast and human* COX17: The *cox17* mutant transformed with pG74H/T1 had a slower growth rate on YEPG than either wild-type yeast or the mutant transformed with the yeast COX17 gene. Failure of the cDNA fragment in pG74H/T1 to confer growth when integrated into chromosomal DNA of the mutant also argues that the human cDNA only partially complements the mutant. To invesigate this, a new plasmid was constructed in which the 5' and 3' regions of the coding sequence in pG74H/T1 were replaced by the sequences flanking the yeast gene. Introduction of this plasmid into the cox17 null mutant did not result in any noticeable improvement in growth on YPEG. This lack of effect suggests that the explanation for the partial restoration of respiration lies in the properties of the protein itself. This interpretation is supported by the failure of the human cDNA to complement the *cox17* mutant when integrated in single copy at the *LEU2* locus.

In contrast to pG74H/T1 and pG74H/T4, growth on YEPG of the transformant harbouring pG74H/T11 was almost as good as wild-type. Since the inserts in pG74H/T1 and pG74H/T11 have different 5' and 3' flanking sequences, either sequence could affect expression of the human *COX17* gene. The 3' flanking region in pG74H/T11 (pG74H/ST6) was excluded from being important, since removal did not alter the growth properties of the transformant. Replacement of the 3' flanking region of pG74H/T1 with the 3' region of pG74H/ST6 also did not affect growth on glycerol. To exclude an effect of plasmid copy number, pG74H/T11 was integrated at the *URA3* locus. The transformant harbouring the human gene with the shorter 5'leader in single copy was complemented for its respiratory defect, but grew more slowly than wild type or transformants containing multiple copies of the plasmid. These results indicate that the absence of 33 nucleotides in the upstream region of pG74H/T11 is responsible for the improved growth in glycerol, probably as a result of more efficient protein expression.

Human and yeast Cox17p are highly homologous and contain a cysteine-rich domain also present in metallothioneins: Human and yeast Cox17p share 22 identities and 8 conservative substitutions. A comparison of Cox17p to human metallothionein reveals a short common domain. Two other conserved cysteines in Cox17p can be aligned with cysteines in the mammalian metallothioneins if two short gaps are allowed in the sequences. All 5 of the cysteines that are conserved between the metallothioneines and the Cox17ps are involved in binding Cu. Metallothioneins protect cells from toxic metals by means of their high binding potential for Cu, Cd and other heavy metals. The ability of high exogenous Cu to rescue *cox17* null mutants argues against a metal-scavenging role for Cox17p, but favours a role in the delivery of Cu to mitochondria.

118.3 Conclusion

The *COX17* gene of *S. cerevisiae* codes for a cytoplasmic protein essential for the expression of functional cytochrome oxidase. To determine if Cox17p is present in human cells, a yeast strain carrying a null mutation of *COX17* was transformed with a human cDNA expression library. All the respiratory competent clones obtained from

	the transformations carried a common cDNA sequence with a reading frame predicting a product homologous to yeast Cox17p. The cloning of a mammalian *COX17* homolog suggests that the encoded product is likely to funtion in copper recruitment in eucaryotic cells in general.
118.3.1 Reliability	*Based on the assessment of materials and methods include appropriate reliability indicator 0, 1, 2, 3, or 4* 2
118.3.2 Deficiencies	Yes This study was not conducted and/or reported in strict compliance with the principles of GLP, and experimental details have been omitted on a number of occasions. However, this does not necessarily compromise the validity of the data presented, or the author's interpretation of those data, given that the study was not carried out for regulatory purposes. Furthermore, the research was published in a peer-reviewed publication, and has therefore been subject to the prior scrutiny of experts in the field. In addition, this report has been included in a number of expert reviews of copper toxicokinetics. No internationally accepted guidelines are available that specifically address the objective of the research presented in this summary. Overall, this is an adequately-presented study, and its findings are considered to make a valuable contribution to the 'weight of evidence' approach that has been adopted for the purposes of the current review of copper toxicokinetics. A reliability indicator of 2 has been assigned on this basis. *(If yes, discuss the impact of deficiencies and implications on results. If relevant, justify acceptability of study.)*

Evaluation by Competent Authorities	
	Use separate "evaluation boxes" to provide transparency as to the comments and views submitted
	EVALUATION BY RAPPORTEUR MEMBER STATE
Date	[redacted]
Materials and Methods	• [redacted]
Results and discussion	[redacted]
Conclusion	[redacted]
Reliability	[redacted]
Acceptability	[redacted]
Remarks	

	COMMENTS FROM ...
Date	*Give date of comments submitted*

Figure A6.2(22)-1

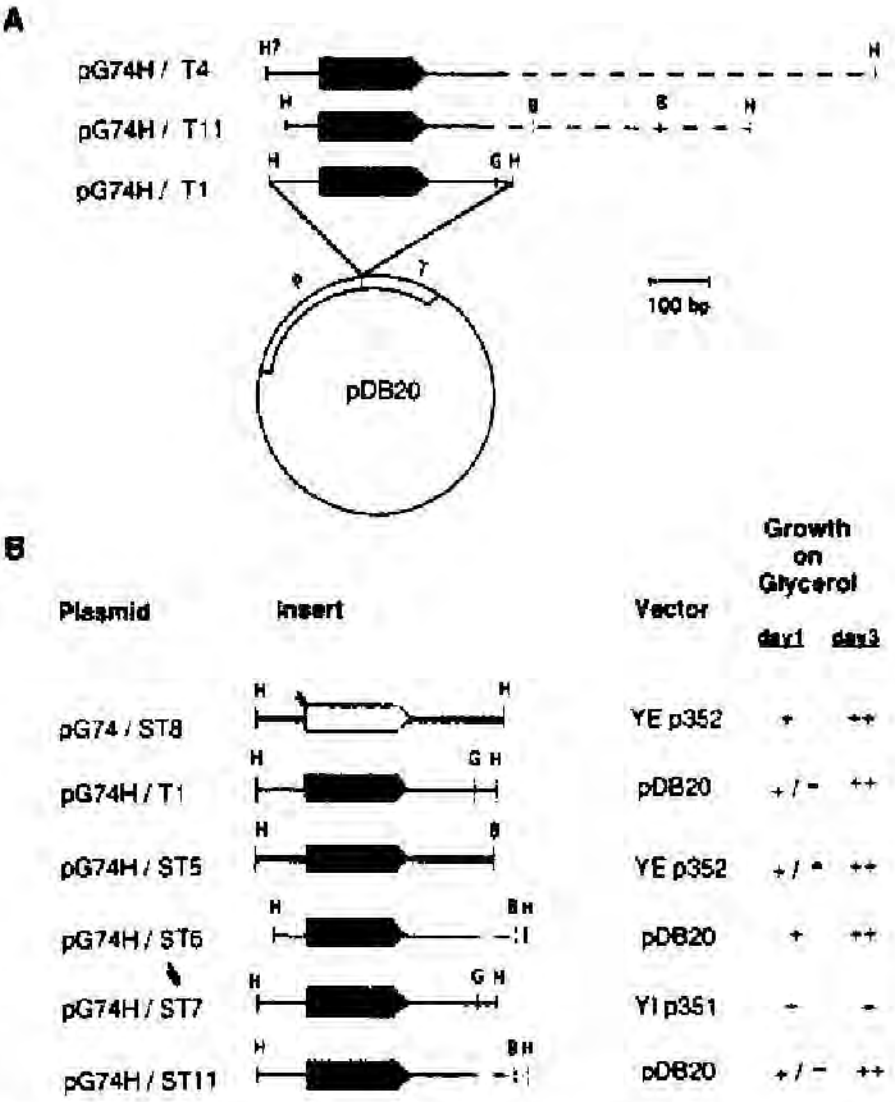

Fig. 1A,B Restriction maps of human cDNA clones and of derivative plasmids. **A** The locations of the *Hind*III (*H*), *Bam*H1 (*B*), and *Bgl*II (*G*) sites in the cDNA inserts of pG74H/T1, T4, and T11 are shown above the pDB20 vector. The *dashed lines* in the inserts of pG74H/T4 and T11 correspond to sequences derived from other cDNAs. The *question mark* denotes an approximate location of the upstream *Hind*III site in pG74H/T4. The reading frame coding for the human Cox17p is indicated by the *solid arrow*. *Open arcs* in pDB20 represent the promoter (*P*) and terminator (*T*) regions of *ADH1*. **B** Complementation of the *cox17* null mutant by different constructs containing human and yeast sequences. YEp352 is a multicopy plasmid with *URA3* as the selective marker and YIp351 is an integrative plasmid with the yeast *LEU2* gene (Hill et al. 1986). *Minus signs* indicate absence of visible growth on YEPG, +/- indicate poor growth, and ++ indicate good growth. The *open bar* and *arrow* denote yeast coding and flanking regions, and the *solid line* and *arrow* represent the corresponding human sequences

Figure A6.2(22)-2

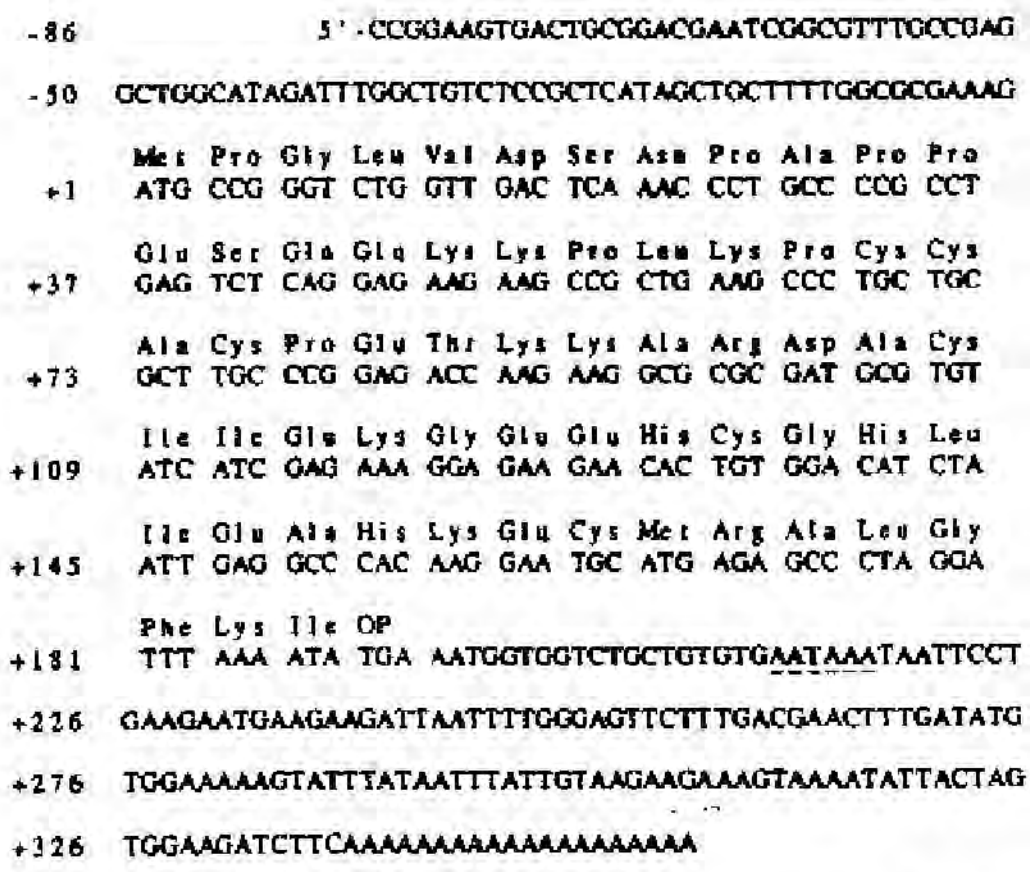

Fig. 2 Nucleotide sequence of the cDNA insert of pG74H/T1. Only the sequence of the coding strand is shown. The open reading frame proposed to code for human Cox17p is translated and is shown above the DNA sequence. A possible polyadenylation signal has been *underlined*. The sequence has been deposited in GenBank under accession number L77701

Figure A6.2(22)-3

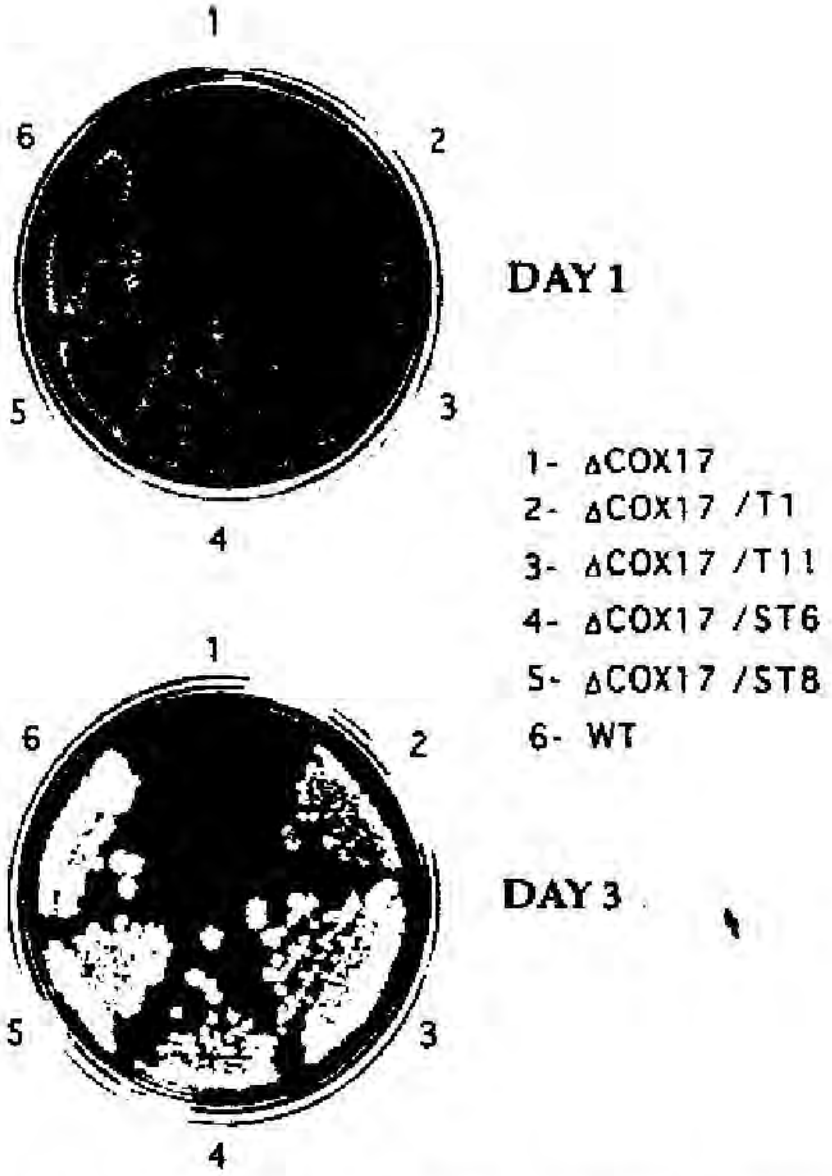

Fig. 3 Growth of the *cox17* null mutant harboring plasmids coding for the yeast and human Cox17p. The mutant, wild-type, and transformant strains were replica-plated from rich glucose medium (YPD) to rich glycerol medium (YEPG). Growth on the YEPG plate was scored after incubation at 30° C for 1 day (*upper*) and 3 days (*lower*). The following strains were streaked on: *sectors 1* the *cox17* null mutant W303DCOX17. *2* mutant transformed with pG74H/T1; *3* mutant transformed with pG74H/T11; *4* mutant transformed with pG74H/ST6; *5* mutant transformed with pG74/ST8; and 6 wild-type W303-1B

Figure A6.2(22)-4

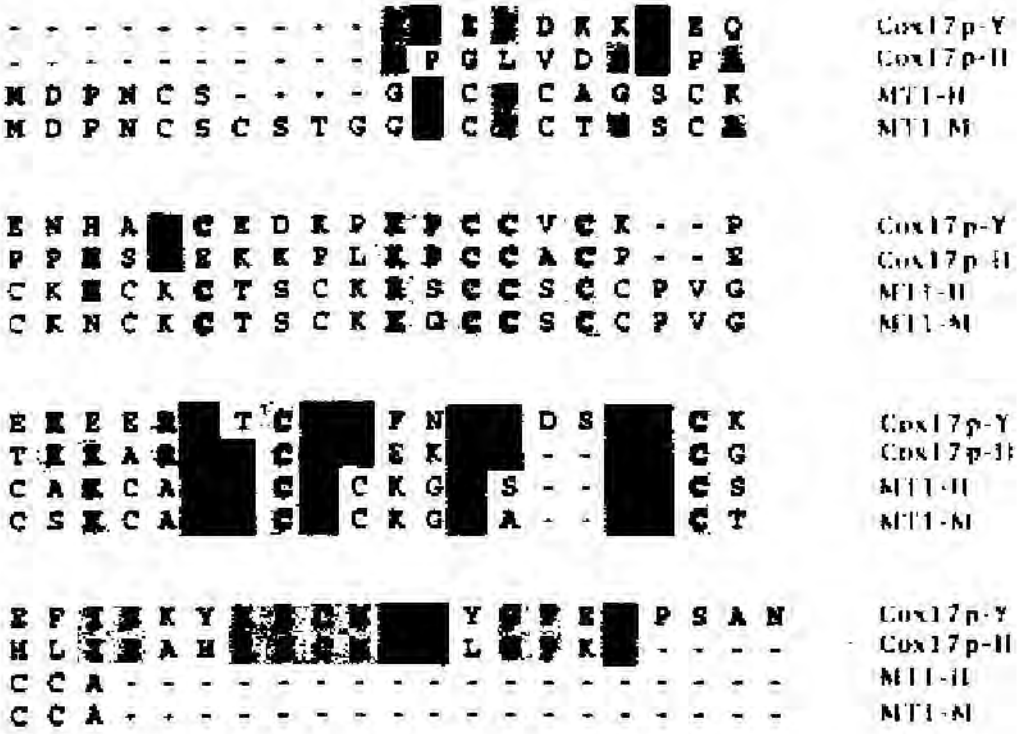

Fig. 4 Homology of human and yeast Cox17p. Human (*H*) and yeast (*Y*; Glerum et al. 1996) Cox17p's, and the human (MT1-H; Schmidt et al. 1985) and mouse (MT1-M; Glanville et al. 1981) metallothionein sequences were aligned by the motif recognition algorithm of Vingron and Argos (1991). Identical residues and conserved substitutions present only in the two Cox17p sequences are highlighted by the *lighter* and *darker boxes*, respectively. Also highlighted are identical and conserved residues present in at least one Cox17p and one of the metallothionein sequences. Wherever possible, identical or conserved residues across all four species have been marked

			Official use only
		119 REFERENCE	
1.1	**Reference**	*Author(s), year, title, laboratory name, laboratory report number, report date (if published, list journal name, volume: pages) If necessary, copy field and enter other reference(s).*	
		Culotta, V.C., Klomp, J.S., Casareno, R.L.B., Krems, B. And Gitlin, J.D. (1997). The Copper Chaperone for Superoxide Dismutase. The Journal of Biological chemistry. **272 (38)**: 23469 - 23472 (published).	X
1.2	**Data protection**	No *(indicate if data protection is claimed)*	
1.2.1	Data owner	*Give name of company* Public domain	
1.2.2	Criteria for data protection	Choose one of the following criteria (see also TNsG on Product Evaluation) and delete the others: No data protection claimed	
		120 GUIDELINES AND QUALITY ASSURANCE	
120.1	**Guideline study**	No. This was a non-regulatory study to confirm the insertion of copper into superoxide dismutase 1 (SOD1) by a specific metal carrier or "copper chaperone" identified as *Saccharomyces cerevisiae* LYS7 and human CCS (copper chaperone for SOD). No guidelines are available to address this objective. *(If yes, give guidelines; if no, give justification, e.g. "no guidelines available" or "methods used comparable to guidelines xy")*	
120.2	**GLP**	No. This was a non-regulatory study. *(If no, give justification, e.g. state that GLP was not compulsory at the time the study was performed)*	
120.3	**Deviations**	Yes. Refer to section 5.3.2 for a general discussion of deviations and deficiencies. *(If yes, describe deviations from test guidelines or refer to respective field numbers where these are described, e.g. "see 3.x.y")*	
		121 MATERIALS AND METHODS	
		In some fields the values indicated in the EC or OECD test guidelines are given as default values. Adopt, change or delete these default values as appropriate.	
121.1	**Test material**	Refer to section 2.3	X
121.1.1	Lot/Batch number	Not applicable	
121.1.2	Specification	Deviating from specification given in section 2 as follows *(describe specification under separate subheadings, such as the following; additional subheadings may be appropriate):*	

Section A6.2		**Metabolism in mammals**
Annex Point IIA6.2		*Specify section no., heading and species as appropriate*
IUCLID: 5.0/23		**A6.2(23), Cellular and molecular metabolism of copper**
121.1.2.1	Description	*If appropriate, give e.g. colour, physical form (e.g. powder, grain size, particle size/distribution)* Not applicable
121.1.2.2	Purity	*Give purity in % of active substance* [redacted]
121.1.2.3	Stability	*Describe stability of test material* Not applicable
121.1.2.4	Radiolabelling	*give structural location of radio labelling, give reason if not labelled* ^{64}Cu
121.2 Test Animals		*Non-entry field*
121.2.1 Species		Not applicable
121.2.2 Strain		Not applicable
121.2.3 Source		Not applicable
121.2.4 Sex		Not applicable
121.2.5 Age		Not applicable
121.3 Procedures		Non-entry field
121.3.1 Cloning and RNA Analysis		Overlapping cDNA clones corresponding to expressed sequence tags (ESTs) homologous to LYS7 were sequenced using a fluorescent dye terminator cycle sequencing kit (Perkin-Elmer), followed by analysis on a Perkin-Elmer ABI 373A XL sequencer. A 1068 bp cDNA sequence was identified containing an 822-base pair open reading frame, which was termed Copper Chaperone for SOD (CCS). RNA blot analysis was performed using membranes containing poly(A)$^+$ RNA from different human and foetal tissues or isolated from human cell lines. To construct the CCS expressing plasmid pSMCCS, the coding region of human CCS was amplified by PCR and inserted at the *Eco*RI and *Bam*HI sites of pSM703, placing CCS under the control of *S. cerevisiae PGK1* (phosphoglycerol kinase) promoter. The pHAL7 plasmid expressing the epitope-tagged LYS7-HA protein was obtained by first amplifying LYS7 sequences –440 to the stop codon by PCR using a downstream primer that converted the termination codon to a *Nde*I site. This modified LYS7 fragment was then inserted at the *Apa*I and *Nde*I sites of the LEU2 CEN vector, pA2HA-cen-resulting in the in-frame fusion of LYS7 to two copies of the HA epitope from influenza virus. Construction of the *sod2***ls***::URA3* plasmid pGSOD2 was as follows: S. cerevisiae SOD2 sequences –680 to –80 with respect to the start codon were amplified by PCR and directionally inserted at the *Bam*HI and *Hind*III sites of pRS306, an *URA*3 integrating vector. *SOD2* sequences +560 to +1700 were then directionally inserted in this plasmid at *Spe*I and *Bam*HI sites. The resultant pGSOD2 plasmid was linearised by digestion with *Bam*HI and used to delete the chromosomal *SOD2* gene of strain 1783 by a one-step gene deletion, creating strain JS002.